

REVIEW

Green's functions for geophysics: a review

To cite this article: Ernian Pan 2019 *Rep. Prog. Phys.* **82** 106801

View the [article online](#) for updates and enhancements.

You may also like

- [Rate-programming of nano-particulate delivery systems for smart bioactive scaffolds in tissue engineering](#)
Mohammad Izadifar, Azita Haddadi, Xiongbiao Chen et al.
- [High surface area graphene foams by chemical vapor deposition](#)
Simon Drieschner, Michael Weber, Jörg Wohlketter et al.
- [Graphene-based fibers for supercapacitor applications](#)
Lianlian Chen, Yu Liu, Yang Zhao et al.

Review

Green's functions for geophysics: a review

Ernian Pan 

University of Akron, Akron, OH 44325, United States of America

E-mail: ernian.pan@gmail.com

Received 9 November 2018, revised 16 March 2019

Accepted for publication 11 April 2019

Published 4 September 2019



Recommended Professor Michael Bevis

Abstract

The Green's function (GF) method, which makes use of GFs, is an important and elegant tool for solving a given boundary-value problem for the differential equation from a real engineering or physical field. Under a concentrated source, the solution of a differential equation is called a GF, which is singular at the source location, yet is very fundamental and powerful. When looking at the GFs from different physical and/or engineering fields, i.e. assigning the involved functions to real physical/engineering quantities, the GFs can be scaled and applied to large-scale problems such as those involved in Earth sciences as well as to nano-scale problems associated with quantum nanostructures. GFs are ubiquitous and everywhere: they can describe heat, water pressure, fluid flow potential, electromagnetic (EM) and gravitational potentials, and the surface tension of soap film. In the undergraduate courses Mechanics of Solids and Structural Analysis, a GF is the simple influence line or singular function. Dropping a pebble in the pond, it is the circular ripple traveling on and on. It is the wave generated by a moving ship in the opening ocean or the atom vibrating on a nanoscale sheet induced by the atomic force microscopy. In Earth science, while various GFs have been derived, a comprehensive review is missing. Thus, this article provides a relatively complete review on GFs for geophysics. In section 1, the George Green's potential functions, GF definition, as well as related theorems and basic relations are briefly presented. In section 2, the boundary-value problems for elastic and viscoelastic materials are provided. Section 3 is on the GFs in full- and half-spaces (planes). The GFs of concentrated forces and dislocations in horizontally layered half-spaces (planes) are derived in section 4 in terms of both Cartesian and cylindrical systems of vector functions. The corresponding GFs in a self-gravitating and layered spherical Earth are presented in section 5 in terms of the spherical system of vector functions. The singularity and infinity associated with GFs in layered systems are analyzed in section 6 along with a brief review of various layer matrix methods. Various associated mathematical preliminaries are listed in appendix, along with the three sets of vector function systems. It should be further emphasized that, while this review is targeted at geophysics, most of the GFs and solution methods can be equally applied to other engineering and science fields. Actually, many GFs and solutions methods reviewed in this article are derived by engineers and scientists from allied fields besides geophysics. As such, the updated approaches of constructing and deriving the GFs reviewed here should be very beneficial to any reader.

Keywords: dislocation, Love number, layered sphere, layered half-space, Green's function, elasticity, viscoelasticity

(Some figures may appear in colour only in the online journal)

List of main symbols

L, M, N	Vector functions
$\delta(\mathbf{r}), \delta_{ij}$	Dirac delta function of \mathbf{r} and Kronecker delta (scalar and tensor)
∇	Gradient operator vector
$\nabla^2 = \partial_{ii}$	2D or 3D Laplacian operator
∂f	Partial derivative of f with respect to coordinate x_i
$\partial_n f = n_i \partial_i f$	Partial derivative along normal direction n_i
c_{ij}	Elastic (or viscoelastic) coefficients
\mathbf{x}^s	(or \mathbf{x}_s) Source point coordinates
\mathbf{x}^f	Field point coordinates
$(x, y, z) = (x_1, x_2, x_3)$	Cartesian coordinates
$[A]$	matrix with elements as A_{ij}
ν_j	Dislocation (or displacement discontinuity) components
n_j	Normal directions of the dislocation (or fault) plane
ξ_j	Tangential of dislocation line
dA	Dislocation element
$c_{\text{iner}} = 0$ for elastostatic $= \rho\omega^2$ for time-harmonic $= -\rho s^2$ for viscoelastic in Laplace-transform domain (related to the inertia term)	
λ	Horizontal transform variable; also for one of the elastic Lamé constants
λ, μ or λ_e, μ_e	Elastic Lamé constants
λ_v, μ_v or $(\lambda(s), \mu(s))$	Viscoelastic Lamé constants
ρ	Material density; also for the source function
g	Gravity
u_i	Elastic (or viscoelastic) displacements
σ_{ij}	Elastic (or viscoelastic) stresses
ε_{ij}	Elastic (or viscoelastic) strains
ϕ	Perturbed potential
s	Laplace variable
t	Time variable
ω	Angular frequency
2D	Two-dimensional
3D	Three-dimensional
G	Scalar Green's function; also for the universal gravitational constant
GF	Green's function or Green function
ELLN	Elastic load Love number
DLN	Dislocation Love number
GIA	Glacial isostatic adjustment
DDM	Displacement discontinuity method
BEM	boundary element method
FEM	Finite element method
NME	Normal mode expansion or normal mode summation
SMM	Stiffness matrix method
PMM	Propagator matrix method

DVP

VSH

TI

Dual variable and position

Vector spherical harmonics; also the spherical system of vector functions

Transversely isotropic or transverse isotropy; For spherical geometry, TI denotes spherically isotropic, or spherical isotropy

1. Introduction

'In the other class of methods the quantities to be determined are expressed by definite integrals, the elements of the integrals representing the effects of *singularities* distributed over the surface or through the volume. This class of solutions constitutes an extension of the methods introduced by Green in the Theory of the Potential.'

... A. E. H. Love, 1944

In this section, using potential theory as an example, we introduce the concept of Green's function (GF) and related fundamental theorems. These include the GF definition, basic features of the GFs, Green's theorems, the representative relation, and the corresponding boundary integral equations. We neglect the detailed derivation of most of the formulae since this would be beyond the scope of the article. We also assume that all the functions and their derivatives discussed in this paper satisfy the necessary smoothness/continuity conditions and that the involved integrations are bounded, unless specified otherwise. For readers who are interested in more details on the theory of potential and potential GFs, the following references are recommended: Books and reviews concentrated on potential theory only (Kellogg 1953, Helms 2009, Freeden and Gerhards 2013, Gerhards 2018), textbooks on partial differential equations or mathematical methods where GFs of potential were presented more rigorously as a tool to solve the differential equations (Folland 1976, Roach 1982, Riley *et al* 2002, Greenberg 2015), and books where GFs of elasticity as well as potentials were discussed (Butkovskiy 1982, Seremet 2003, Melnikov and Melnikov 2012, Bona and Slawinski 2015, Duffy 2015, Pan and Chen 2015). The historical development of GFs in general can be found in Duffy (2015).

The GF is named after George Green for his seminal contributions in physics and mathematics (Green 1828, Dyson 1993, Schwinger 1993, Cannell 2001, Challis and Sheard 2003). Below we use the three-dimensional (3D) potential problem as an example to introduce the fundamental concepts and relations. Even for this simple potential problem, the GF has applications in nearly every science and engineering field when assigning the potential function to the related real physical or engineering quantity. In geophysics, the potential function describes the gravitational potential.

1.1. Green's function (GF)

We assume that ρ is the 'source' function given in a bounded domain V in 3D space (figure 1(a)) and that the boundary of V is S . The potential function ϕ in V is the solution of the

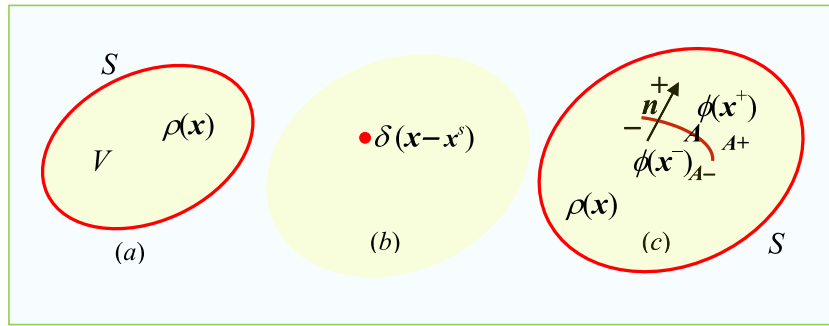


Figure 1. A distributed source ρ within a domain V bounded by S in (a), a concentrated source at \mathbf{x}^s in the corresponding infinite space in (b), and an arbitrarily oriented internal surface A (with its normal direction \mathbf{n}) over which the field quantity ϕ is discontinuous in (c).

following Poisson's equation, subjected to proper boundary conditions for ϕ and/or its derivative on the boundary S .

$$\nabla^2 \phi(\mathbf{x}) = \rho(\mathbf{x}); \quad \mathbf{x} \in V \quad (1.1)$$

where ∇^2 is the 3D Laplace differential operator and \mathbf{x} is any field point within the problem domain V . It should be pointed out that the potential ϕ and source function ρ are quite general in mathematical point of view, and as such, are applicable to many different engineering and physical fields when associating them with the corresponding field quantities. For instance in Earth science, equation (1.1) will be the governing equation for the gravitational potential with the source function ρ being proportional to the mass density (Dahlen and Tromp 1998, Gerhards 2018). Furthermore, if $\rho = 0$ in (1.1), we then have the Laplace equation with its solutions being generally called harmonic functions (Helms 2009). The Laplace equation is the mathematical key and describes phenomena that are everywhere in our daily life (Cole 2016).

The corresponding free-space GF G in the entire 3D space is defined as (figure 1(b))

$$\nabla^2 G(\mathbf{x}; \mathbf{x}^s) = \delta(\mathbf{x} - \mathbf{x}^s) \quad (1.2)$$

where \mathbf{x}^s is the source point at which a concentrated source of unit magnitude is applied, and δ is the Dirac delta function 'distribution' (Zemanian 1987). The GF solution (also called singular or fundamental solution) of equation (1.2) is (Pan and Chen 2015)

$$G(\mathbf{x} - \mathbf{x}^s) = \frac{-1}{4\pi |\mathbf{x} - \mathbf{x}^s|} \equiv -1/(4\pi r) \quad (1.3)$$

where r is the distance between the field and source points.

1.2. Basic features of GF

- Uniqueness: The GF solution (1.3) is the unique solution of (1.2) upon making use of the integration property of the Dirac delta function, as elaborated below.
- Singularity: The GF solution (1.3) is singular at the source point $\mathbf{x} = \mathbf{x}^s$ (in the order of $1/r$) and decays to zero with increasing relative distance between the source and field points (also in the order of $1/r$).
- Integration around the source point: The volumetric integration of the GF (1.3) over any domain including the source point should equal to one (i.e. the unit magnitude on the right-hand side of equation (1.2)). This is actually

the integration condition which makes the GF solution (1.3) unique.

- Reciprocity between the source and field points of the GF (1.3): $G(\mathbf{x} - \mathbf{x}^s) = G(\mathbf{x}^s - \mathbf{x})$, or in more general notation, $G(\mathbf{x}; \mathbf{x}^s) = G(\mathbf{x}^s; \mathbf{x})$. Furthermore, $\partial G(\mathbf{x}; \mathbf{x}^s)/\partial x_i = -\partial G(\mathbf{x}; \mathbf{x}^s)/\partial x_i^s$. Note that these relations only hold for GFs in an infinite homogeneous space without any boundary!

1.3. Green's representative theorem

The Green's theorem presented below is also called the divergence theorem, Gaussian theorem, or Green's second identity. It states that for any two functions which are twice differentiable with respect to the 3D coordinate $(x, y, z) = (x_1, x_2, x_3)$, the following identity holds (similar to the well-known Maxwell reciprocity or Betti's reciprocity).

$$\int_S [\phi \nabla \psi - \psi \nabla \phi] \cdot d\mathbf{S} = \int_V [\phi \nabla^2 \psi - \psi \nabla^2 \phi] dV \quad (1.4)$$

where the gradient ∇ (a vector!) is with respect to the vector variable \mathbf{x} (i.e. ∂_i). Notice that a relation similar to equation (1.4) is the Stokes' theorem/relation, where the area integral is connected to the line integral along the contour (or loop) of the area. Stokes' theorem is very useful in analyzing a 3D fault/dislocation loop (Hirth and Lothe 1982), where one can convert the area integral over the fault to the line integral along its contour (or loop).

We now apply (1.4) to the following two different sets: one is the real problem associated with ϕ (governed by (1.1) in V and bounded by S , with also suitable boundary conditions on S), and the other is the GF, governed by (1.2) and defined by G . In other words, we let ϕ be the solution of the real problem of (1.1) with given boundary conditions and G the solution of (1.2) for the entire space. Then, upon substituting these solutions into equation (1.4), we arrive at, for any point \mathbf{x}^s within the problem domain V ,

$$\begin{aligned} \phi(\mathbf{x}^s) &= \int_S [\phi(\mathbf{x}) \nabla G(\mathbf{x}; \mathbf{x}^s) - G(\mathbf{x}; \mathbf{x}^s) \nabla \phi(\mathbf{x})] \cdot d\mathbf{S}(\mathbf{x}) \\ &+ \int_V G(\mathbf{x}; \mathbf{x}^s) \rho(\mathbf{x}) dV(\mathbf{x}) \end{aligned} \quad (1.5)$$

Equation (1.5) expresses the unknown function ϕ in the problem domain in terms of the given inhomogeneous 'source' ρ ,

and the given ϕ and/or its derivative on the problem boundary. This is the well-known representative theorem derived first by Green (1828) for the general potential problem. It is suited for a very general problem where the source ρ can be arbitrary and ϕ and/or its derivative is described on the problem boundary.

Important applications of representative theorem (1.5):

- (1) We assume that the potential function ϕ and GF G in equation (1.5) satisfy the same homogeneous boundary conditions on S (Burridge and Knopoff 1964, Pan 1991). Then equation (1.5) is reduced to

$$\phi(\mathbf{x}^s) = \int_V G(\mathbf{x}; \mathbf{x}^s) \rho(\mathbf{x}) dV(\mathbf{x}). \quad (1.6)$$

Examples of equation (1.6) are: (1) the homogeneous half-space (plane) or spherical (circular) domain where its boundary is either traction-free (i.e. the normal derivative of both $\partial_n G$ and $\partial_n \phi$ are zero on the boundary) or rigid (i.e. both G and ϕ are zero on the boundary); and (2) the homogeneous and infinite space where both G and ϕ and their first derivatives decay in such a way that the boundary integral on a very large sphere (a very large circle) in equation (1.5) is zero.

It is noted that, in general, the locations of the two coordinate variables \mathbf{x} and \mathbf{x}^s in the GF G in equation (1.6) cannot be exchanged. They are exchangeable only when G in equation (1.6) is the GF in the corresponding infinite and homogeneous space. For this case, equation (1.6) can be alternatively written as

$$\phi(\mathbf{x}) = \int_V G(\mathbf{x}; \mathbf{x}^s) \rho(\mathbf{x}^s) dV(\mathbf{x}^s). \quad (1.7)$$

Both equations (1.6) and (1.7) simply imply that the potential ϕ induced by a given source ρ can be obtained by the method of superposition, i.e. by integrating the GF over the source domain V . Furthermore, by substituting GF expression (1.3) into equation (1.7), we then have the well-known solution for the (gravitational) potential due to a given distributed (mass) density.

- (2) The opposite case of (1), where the body source ρ is zero but there are applied boundary conditions over S . Then, the solution at any point \mathbf{x}^s of the problem domain can be represented in terms of the given boundary values as the following boundary integration

$$\phi(\mathbf{x}^s) = \int_S [\phi(\mathbf{x}) \nabla G(\mathbf{x}; \mathbf{x}^s) - G(\mathbf{x}; \mathbf{x}^s) \nabla \phi(\mathbf{x})] \cdot d\mathbf{S}(\mathbf{x}). \quad (1.8)$$

Three special cases of (2):

- (a) ϕ is given on the entire boundary (i.e. the type I, or Dirichlet boundary-value problem). Then, the solution can be simply expressed as (by choosing the ‘rigid’ GF G^{rigid} which is zero on the problem boundary S)

$$\phi(\mathbf{x}^s) = \int_S [\phi(\mathbf{x}) \nabla G^{\text{rigid}}(\mathbf{x}; \mathbf{x}^s)] \cdot d\mathbf{S}(\mathbf{x}). \quad (1.9)$$

- (b) $\partial_n \phi$ ($\equiv \mathbf{n} \cdot \nabla \phi$ where \mathbf{n} is the outward normal of the boundary S) is given on the entire boundary (i.e. the type II or Neumann boundary-value problem). Then, the solution can be simply expressed as (by choosing the flux ‘free’ GF G^{free} such that its normal derivative $\partial_n G^{\text{free}}$ on the problem boundary S is zero)

$$\phi(\mathbf{x}^s) = - \int_S [G^{\text{free}}(\mathbf{x}; \mathbf{x}^s) \nabla \phi(\mathbf{x})] \cdot d\mathbf{S}(\mathbf{x}). \quad (1.10)$$

- (c) The integral representative expression (1.8) is the fundamental relation in deriving the boundary integral equation and the corresponding well-known boundary element method (BEM). To achieve the boundary integral equation, we only need to let \mathbf{x}^s approach any smooth boundary point $\mathbf{x}^b \in S$ (at which its tangential derivative is continuous). This gives us

$$0.5\phi(\mathbf{x}^b) = \int_S [\phi(\mathbf{x}) \nabla G(\mathbf{x}; \mathbf{x}^b) - G(\mathbf{x}; \mathbf{x}^b) \nabla \phi(\mathbf{x})] \cdot d\mathbf{S}(\mathbf{x}). \quad (1.11)$$

In equation (1.11), both the field and source points are on the problem boundary. Therefore, the boundary can be discretized and the resulting equation can be solved for the involved unknowns (at discretized collocation points). This is the essential formulation used in the BEM (i.e. Liu *et al* (2011)), as applied to various engineering material fields (Qin 2007) and also extended to wave propagation with cracks (Zhang and Gross 1998). A brief history on BEM can be found in Cheng and Cheng (2005).

- (3) A final application of equation (1.5): we let ϕ be the particular solution of equation (1.1), as shown in figure 1(c). We assume now that there exists an internal surface A with normal \mathbf{n} , across which ϕ is discontinuous (with its normal derivative $\partial_n \phi$ being continuous). By applying this problem to (1.5), and assuming the potential function ϕ and GF G in equation (1.5) satisfy the same homogeneous boundary conditions on S (Burridge and Knopoff 1964 Pan 1991), we then have

$$\phi(\mathbf{x}^s) = \int_A [\phi(\mathbf{x})] \nabla G(\mathbf{x}; \mathbf{x}^s) \cdot d\mathbf{A}(\mathbf{x}) + \int_V G(\mathbf{x}; \mathbf{x}^s) \rho(\mathbf{x}) dV(\mathbf{x}) \quad (1.12)$$

where $[f] = f(\mathbf{A}+) - f(\mathbf{A}-)$ denotes the jump of the function across the internal interface A , with its normal being defined as $\mathbf{n} = \mathbf{n}^- = -\mathbf{n}^+$ and its two sides being $A+$ and $A-$, as in figure 1(c)).

Furthermore, if there is no body source ρ , then we arrive at another representative expression where the potential at any location induced by a given internal discontinuity of itself can be simply expressed in terms of an area integral over the internal surface (with the point-source GF gradient and the given internal discontinuity being the integrand).

Actually, the corresponding elastic formulation of (1.12) forms the displacement-discontinuity method (DDM)

(Crouch 1976). The DDM formulation is very convenient in analyzing fracture problems where the crack could experience a displacement discontinuity (or relative displacement) over its two surfaces (Weertman 2008). They are potential applications for equation (1.12) in ground movement due to mining (Berry 1960, Berry and Sales 1961, 1962), as well as in rock breakage and mine excavation (Tan *et al* 1998, Yacoub 1999).

By introducing the delta function ‘distribution’ property, as well as the GF properties (i.e. Burridge and Knopoff (1964) and Aki and Richards (1980)), equation (1.12) can be rewritten as

$$\begin{aligned} \phi(\mathbf{x}^s) = & \int_V G(\mathbf{x}; \mathbf{x}^s) \left[- \int_A [\phi(\boldsymbol{\xi})] n_i \partial_{x_i} \delta(\mathbf{x} - \boldsymbol{\xi}) dA(\boldsymbol{\xi}) \right] dV(\mathbf{x}) \\ & + \int_V G(\mathbf{x}; \mathbf{x}^s) \rho(\mathbf{x}) dV(\mathbf{x}). \end{aligned} \quad (1.13)$$

Comparing the first and second terms on the right-hand side of equation (1.13), one immediately concludes that the internal discontinuity $[\phi]$ over A (or dislocation) can be equivalently expressed in terms of a body-source (or body-force) function as

$$\rho(\mathbf{x}) = - \int_A [\phi(\boldsymbol{\xi})] n_i \partial_{x_i} \delta(\mathbf{x} - \boldsymbol{\xi}) dA(\boldsymbol{\xi}). \quad (1.14)$$

The body-force equivalent expression (1.14) has many applications when it is extended to different fields, e.g. poroelasticity (i.e. Pan (1991)) and magnetoelasticity (Zhao *et al* 2015). We will revisit the equivalent body-force expression for the dislocation or displacement discontinuity over a fault surface later on.

1.4. Summary of section 1

Using the 3D potential problem as an example, we have introduced the GF or GF solution of equations (1.1) and (1.2), along with various useful features. Based on the Green’s theorem (1.4), we have derived the important representative expression (1.5). This expression (1.5) is then applied to the point source (or source as force) as well as the discontinuity source (or dislocation) cases. These two types of sources can be further connected by introducing the so-called equivalent body-force concept of the concentrated ‘dislocation’ (or displacement discontinuity), which will be used later when deriving the GF solutions due to dislocations. Equation (1.5) is further the essential expression for the boundary integral equation and thus the corresponding numerical methods, like the BEM.

While the GF of the potential problem can find various direct applications in fluid mechanics, this review emphasizes only on the elastic and/or viscoelastic media. Readers who are interested in GFs in fluid mechanics with applications can refer to the following typical and related works by the GF researchers in fluid mechanics (Dorning, 1981, Telste and Noblesse 1986, Chen *et al* 2001, Jensen *et al* 2011). For GFs in solid-state physics, readers may refer to the review article

by Tewary (1973) and the book by Doniach and Sondheimer (1999). GFs for nanoscale device applications can be found in Datta (2000).

2. Elasticity and viscoelasticity

In this section, we review the basic equations associated with elastostatic, viscoelastic, and time-harmonic elastic deformations. While we derive only 3D equations, they can be simply reduced to the corresponding 2D (x, y) (or x_1, x_2) plane-strain deformation (u_x, u_y) (or u_1, u_2) plus the anti-plane deformation (u_z) (or u_3) by assuming that all the physical quantities including the boundary conditions are independent of the third coordinate z (or x_3) and that the involved material properties satisfy certain symmetric conditions (Ting 1996). The Cartesian coordinate system is used; however, the corresponding governing equations in other systems, particularly in the cylindrical and spherical coordinate systems, can be easily derived. We present the formulation for general anisotropy, but when applying to geophysics, we only concentrate on the isotropic or transversely isotropic (TI) case with its axisymmetry along the given normal direction of the plane (for 2D half-plane and 3D half-space deformation) or along the radial direction of the sphere (for spherical Earth deformation). In geophysics, depending upon the time-scale, our Earth could deform elastically or viscoelastically.

2.1. Elasticity

In terms of the displacement gradient $u_{k,l}$, the symmetric strain tensor can be expressed as $\varepsilon_{ij} = 0.5(u_{ij} + u_{ji})$. Then, the constitutive relation and equations of motion are, respectively,

$$\sigma_{ij} = c_{ijkl} u_{k,l} \quad (2.1)$$

$$\sigma_{ji,j} + f_i = \rho \partial_{tt} u_i. \quad (2.2)$$

For an orthotropic elastic material (with TI and isotropy being its special cases), the constitutive relation in terms of the Cartesian system and the Voigt notation, from 4 indices in c_{ijkl} (varying from 1 to 3) to 2 indices in c_{ij} (varying from 1 to 6), using the correspondence between their indices $11 \leftrightarrow 1, 22 \leftrightarrow 2, 33 \leftrightarrow 3, 23 \leftrightarrow 4, 13 \leftrightarrow 5, 12 \leftrightarrow 6$, can be written as

$$\begin{aligned} \sigma_{xx} &= c_{11} u_{x,x} + c_{12} u_{y,y} + c_{13} u_{z,z} \\ \sigma_{yy} &= c_{12} u_{x,x} + c_{22} u_{y,y} + c_{23} u_{z,z} \\ \sigma_{zz} &= c_{13} u_{x,x} + c_{23} u_{y,y} + c_{33} u_{z,z} \\ \sigma_{yz} &= c_{44} (u_{y,z} + u_{z,y}); \sigma_{xz} = c_{55} (u_{x,z} + u_{z,x}); \sigma_{xy} = c_{66} (u_{x,y} + u_{y,x}). \end{aligned} \quad (2.3)$$

In general, for the orthotropic material, there are nine independent constants. For the TI material with z -axis being its axis of symmetry, there are only five independent constants (since $c_{11} = c_{22}$, $c_{13} = c_{23}$, $c_{44} = c_{55}$, and $c_{66} = (c_{11} - c_{12})/2$). Furthermore, for the isotropic elastic material, there are only two independent constants, say the two Lamé elastic constants, related to c_{ij} as

$$\begin{aligned} c_{11} &= c_{33} = \lambda_e + 2\mu_e \\ c_{12} &= c_{13} = \lambda_e; \quad c_{44} = c_{66} = \mu_e \end{aligned} \quad (2.4)$$

where the subscript e to the two Lamé constants is used to distinguish the elastic one from the viscoelastic one (with subscript v and depending on the Laplace variable s) to be discussed later. For the elastostatic case, the inertial term on the right-hand side of equation (2.2) is zero.

For many elastodynamic problems, a typical approach is to first solve the governing equations in the frequency domain and then transform them back to the time domain. The Fourier-transform pair for any function $f(t)$ is defined as

$$f(x_i; \omega) = \int_{-\infty}^{\infty} f(x_i; t) e^{i\omega t} dt \quad (2.5a)$$

$$f(x_i; t) = \frac{1}{2\pi} \int_{-\infty}^{\infty} f(x_i; \omega) e^{-i\omega t} d\omega. \quad (2.5b)$$

Notice that, to distinguish if the solution is in the frequency or time domain, if needed, we add the function's dependence as $f(\omega)$ or $f(t)$. Thus, for solving the dynamic problem, finding the corresponding *time-harmonic solution* is sufficient. Note that for the Fourier-transform pair, people may also switch the positive and negative signs in the exponential terms on the right-hand sides of equations (2.5a) and (2.5b). In so doing, the results in the transformed frequency domain would be different, although the final time-domain solutions are the same.

Considering only the time-harmonic problem, equation (2.2) is then replaced by its Fourier-transformed (frequency) domain one as (time-domain solution is proportional to $e^{-i\omega t}$)

$$c_{ijkl} u_{k,lj} + \rho \omega^2 u_i + f_i = 0. \quad (2.6)$$

Notice that the constitutive relation (2.1) is the same in Fourier-transformed domain if we assume that the material properties are independent of frequency. After the problem is solved in the frequency domain, the fast Fourier transform (FFT) is usually applied to find the time-domain solution. Therefore, to treat the transient dynamic deformation, we only need to solve and discuss the Fourier-transformed amplitudes of the physical quantities, say the displacement $u_j(x_i; \omega)$ (since the time-domain solution is proportional to $e^{-i\omega t}$).

2.2. Viscoelasticity

In most viscoelastic problems in Earth science, we assume that the time-scale is very large and the response is extremely slow. Therefore, the inertia term in the dynamic equation (2.2) can be assumed to be zero. For the viscoelastic problem, it is the Laplace transform pairs, instead of the Fourier transform ones, which are applied to solve the problem. While for the elastodynamic case, we have the same constitutive relations, for the viscoelastic case, the explicit time-dependent constitutive relations are used as briefly reviewed below.

For the given viscoelastic problem, one first solves the problem in the Laplace-transformed domain; then, the transformed domain solution is inverted (usually numerically) back to the time domain. Based on the viscoelastic correspondence principle (Lee 1955, 1962, Radok 1957, Christensen 1982),

under the condition that all the quantities and their derivatives are zero for time $t < 0$, the formulation of the viscoelastic problem will be equal to the corresponding elastic problem in the Laplace domain with Laplace-transformed complex material properties. The Laplace transform pairs of a real function f with $f(t) = 0$ for $t < 0$ and its inverse are defined as (we further assume that all the physical quantities and their different orders of time-derivatives are also zero when $t < 0$)

$$\begin{aligned} f(s) &= \int_0^{\infty} e^{-st} f(t) dt \\ f(t) &= \frac{1}{2\pi i} \int_{\gamma-i\infty}^{\gamma+i\infty} e^{st} f(s) ds \end{aligned} \quad (2.7)$$

where the integration path is chosen along the vertical line $\gamma = \text{Re}(s)$ in the complex plane such that γ is greater than the real part of all singularities of $f(s)$.

In Earth science, the initial and final values of $f(t)$ (i.e. the deformation field) are very important and they can be found by taking the limit of its Laplace transform $f(s)$, as

$$\lim_{t \rightarrow 0^+} f(t) = \lim_{s \rightarrow \infty} [sf(s)]; \quad \lim_{t \rightarrow \infty} f(t) = \lim_{s \rightarrow 0} [sf(s)]. \quad (2.8)$$

Notice that while the initial value for a viscoelastic problem corresponds to the elastic solution, the final value is useful because it gives the long-term behavior without having to perform partial decompositions or other difficult algebra. The second expression holds under the assumption that $f(s)$ has no pole in the right-hand plane nor on the imaginary axis.

Then, in the Laplace-transformed domain, the equilibrium equation can be expressed as

$$\sigma_{ji,j} - \rho s^2 u_i + f_i = 0 \quad (2.9)$$

where we have assumed that the initial values of u_i and its derivatives are all zero. Comparing equation (2.9) to the frequency-domain equation (2.6), we immediately obtain the simple relation between the two transformed systems of equations, i.e. simply substituting their variables using $s = -i\omega$. This can be also observed by comparing the definition of the two transforms defined above.

What is left is the constitutive relation in the Laplace-transformed domain. This is discussed based on the work by Carcione (1990). In a given orthonormal coordinate system, the general constitutive relation for a linear anisotropic viscoelastic medium, in both time and Laplace domains, can be expressed as (Christensen 1982),

$$\sigma_{ij}(\mathbf{x}; t) = J_{ijkl}(\mathbf{x}; t) * \partial_i \varepsilon_{kl}(\mathbf{x}; t) \quad (2.10a)$$

$$\sigma_{ij}(\mathbf{x}; s) = s J_{ijkl}(\mathbf{x}; s) \varepsilon_{kl}(\mathbf{x}; s) = c_{ijkl}(\mathbf{x}, s) \varepsilon_{kl}(\mathbf{x}; s) \quad (2.10b)$$

while equation (2.10b) defines the fourth-order viscoelastic tensor in the Laplace-transformed domain, the right-hand side in equation (2.10a) is the convolution integral, defined as (for a strain history from time $t = -\infty$ to t)

$$J_{ijkl}(\mathbf{x}; t) * \dot{\varepsilon}_{kl}(\mathbf{x}; t) = \int_{-\infty}^t J_{ijkl}(\mathbf{x}; t - \tau) \partial_\tau \varepsilon_{kl}(\mathbf{x}; \tau) d\tau \quad (2.11)$$

with $J_{ijkl}(t)$ ($=0$ for $-\infty < t < 0$) being the fourth-order relaxation function tensor (Carcione 1990). It is noted that this tensor has the same symmetry properties as the stiffness tensor in the purely elastic case.

Following Carcione (1990) and also Molavi Tabrizi and Pan (2015), the Laplace-transformed $J_{ijkl}(s)$ (with $c_{ijkl}(s) = sJ_{ijkl}(s)$) can be expressed (in the reduced Voigt notation and for general viscoelasticity) as

$$[\mathbf{J}(s)] = \begin{bmatrix} J_{11}(s) & J_{12}(s) & J_{13}(s) & c_{14}/s & c_{15}/s & c_{16}/s \\ & J_{22}(s) & J_{23}(s) & c_{24}/s & c_{25}/s & c_{26}/s \\ & & J_{33}(s) & c_{34}/s & c_{35}/s & c_{36}/s \\ & & & c_{44}\chi_2(s) & c_{45}\chi_2(s) & c_{46}\chi_2(s) \\ \text{Sym} & & & c_{55}\chi_2(s) & c_{56}\chi_2(s) & \\ & & & & & c_{66}\chi_2(s) \end{bmatrix} \quad (2.12)$$

where c_{ij} are the time-independent elastic moduli at $t = 0$ of the general anisotropic material. For the TI case with z -axis (or x_3 -axis) being its axis symmetry, we have only five independent elastic moduli (Molavi Tabrizi and Pan 2015) as discussed above (c_{11} , c_{12} , c_{13} , c_{33} , and c_{44} , with $c_{66} = 0.5(c_{11} - c_{12})$).

In equation (2.12), the elements of the relaxation matrix are defined as,

$$\begin{cases} J_{ij}(s) = [c_{ij} - D]/s + (D - 4\mu_e/3)\chi_1(s) + 4\chi_2(s)\mu_e/3 & \text{if } i = j \\ J_{ij}(s) = [c_{ij} - D + 2\mu_e]/s + (D - 4\mu_e/3)\chi_1(s) - 2\chi_2(s)\mu_e/3 & \text{if } i \neq j \end{cases} \quad (2.13)$$

with

$$D = (c_{11} + c_{22} + c_{33})/3; \mu_e = (c_{44} + c_{55} + c_{66})/3. \quad (2.14)$$

Furthermore in equations (2.12) and (2.13), the two relaxation functions are defined as

$$\chi_\nu(s) = 1/s - \sum_{l=1}^{L_\nu} (1 - \tau_{el}^\nu/\tau_{\sigma l}^\nu) [1/s - 1/(s + 1/\tau_{\sigma l}^\nu)] \quad \nu = 1, 2 \quad (2.15)$$

where τ_{el}^ν and $\tau_{\sigma l}^\nu$ are the material relaxation times for the l th mechanism and L_ν is the total number of relaxation mechanisms. It is noted that the relaxation matrix $[\mathbf{J}]$ is formed in such a way that the trace and deviatoric components of the stress tensor depend on the time variable through the kernels χ_1 and χ_2 , respectively. The trace of the stress tensor is an invariant upon the transformation of the coordinate system, implying that the hydrostatic stress (one third of the trace) is only related to function χ_1 . Hence, function χ_1 describes the dilatational deformation whereas χ_2 represents the shear deformation (Carcione *et al* 1988 and Carcione 1990). We should point out that the relaxation functions presented in equation (2.15) are similar to, but different from, those in Carcione (1990). The difference is that in Carcione (1990), time $t = \infty$ (0) corresponds to the elastic (relaxation) limit whilst in equations (2.13) and (2.15), $t = 0$ (∞) corresponds to the elastic (relaxation) limit.

The constitutive relations in the Laplace domain presented above are for the general anisotropic viscoelastic media. They can be reduced to the TI viscoelastic case (Molavi Tabrizi and Pan 2015), and particularly to the isotropic viscoelastic case. The most commonly studied Maxwell viscoelastic model (Peltier 1974) can be reduced from equations (2.10)–(2.15) and expressed as (with $L_\nu = 1$, $\chi_1 = \chi_2$, $\tau_{el}^\nu = 0$, and $\tau_{\sigma l}^\nu = \nu_t/\mu_e$)

$$c_{ijkl}(s) = \lambda(s)\delta_{ij}\delta_{kl} + \mu(s)(\delta_{ik}\delta_{jl} + \delta_{il}\delta_{jk}) \quad (2.16)$$

with

$$\lambda_\nu \equiv \lambda(s) = \frac{\lambda_e s + \mu_e B/\nu_t}{s + \mu_e/\nu_t}; \quad \mu_\nu \equiv \mu(s) = \frac{\mu_e s}{s + \mu_e/\nu_t}; \quad B = \lambda_e + 2\mu_e/3 \quad (2.17)$$

where ν_t is the shear viscosity. It is noted that this Maxwell material behaves as fluid when time t approaches infinity, or s approaches zero. It is further noted that the purely elastic constitutive relation can be simply obtained from (2.16) and (2.17) by letting s approach infinity (i.e. the values at the initial time $t = 0$). For Kelvin-Voigt model and other linear viscoelastic models with multiple elements, one is referred to Spada (2008).

In summary, the elastostatic deformation, time-harmonic deformation (its proportional amplitude in the frequency domain), and the viscoelastic deformation (in the Laplace domain) problems can all be discussed uniformly by solving their equilibrium/motion equations in the transformed domain. We now derive the important reciprocity theorem, which has been very useful in obtaining the GF solution.

2.3. Betti's reciprocity

We first derive the Betti's reciprocity theorem for the elastostatic deformation, for the time-harmonic deformation in the transformed domain (in terms of their amplitude, proportional to $e^{-i\omega t}$), and the viscoelastic deformation in the Laplace-transformed domain (in terms of their amplitude, proportional to e^{st}).

We assume that there are two sets of the boundary-value problem (with superscripts (1) and (2)) associated with the same material system. Then the following reciprocity theorem holds for the stresses and strains in the two sets of the system:

$$\sigma_{ij}^{(1)} u_{i,j}^{(2)} = \sigma_{ij}^{(2)} u_{i,j}^{(1)}. \quad (2.18)$$

This important relation can be easily proved by making use of the constitutive relation (with the same material property) and noticing the symmetric conditions of the stresses, strains, and material properties.

We now integrate equation (2.18) over the problem domain by parts, and making use of the Green's theorem (1.4) to arrive at

$$\int_{\partial V} \sigma_{ij}^{(1)} u_i^{(2)} n_j dS - \int_V \sigma_{ij,j}^{(1)} u_i^{(2)} dV = \int_{\partial V} \sigma_{ij}^{(2)} u_i^{(1)} n_j dS - \int_V \sigma_{ij,j}^{(2)} u_i^{(1)} dV. \quad (2.19)$$

Furthermore, making use of the equilibrium equations (or the equations in the Fourier-/Laplace-transformed domain), we have

$$\int_{\partial V} \sigma_{ji}^{(1)} n_j u_i^{(2)} dS + \int_V [f_i^{(1)} + c_{\text{iner}} u_i^{(1)}] u_i^{(2)} dV = \int_{\partial V} \sigma_{ji}^{(2)} n_j u_i^{(1)} dS + \int_V [f_i^{(2)} + c_{\text{iner}} u_i^{(2)}] u_i^{(1)} dV. \quad (2.20)$$

where

$$c_{\text{iner}} = \begin{cases} 0 & \text{Elastostatic} \\ \rho\omega^2 & \text{Time-harmonic} \\ -\rho s^2 & \text{Viscoelastic} \end{cases} \quad (2.21)$$

Equation (2.20) is the well-known Betti's reciprocity, which was originally derived by Love (1944). It states that the work done by the forces of the first set (including kinetic reaction), acting over the displacements produced by the second set, is equal to the work done by the second set, acting over the displacements produced by the first.

As indicated clearly by equations (2.20) and (2.21), this Betti's reciprocity contains the following three deformation cases: elastostatic ($c_{\text{iner}} = 0$), time-harmonic ($c_{\text{iner}} = \rho\omega^2$), and viscoelastic in the Laplace-transformed domain ($c_{\text{iner}} = -\rho s^2$). It is further noted that the reciprocity (2.20) holds also for the self-gravitating elastostatic (viscoelastic or time-harmonic) deformation of the Earth, provided that we have (along the interface and also on the surface)

$$[\psi_i^{(1)} + 4\pi G\rho u_i^{(1)}]_{\pm}^{\pm} = [\psi_i^{(2)} + 4\pi G\rho u_i^{(2)}]_{\pm}^{\pm} = 0 \quad (2.22)$$

where ψ is the perturbed gravitational potential, and G is the universal gravitational constant. For detailed discussion on this relation, readers are referred to the works by Smylie and Mansinha (1971), Dahlen (1972) and Boschi (1973). An interesting application to the relation between the body and surface Love numbers can be found in Pan and Ding (1986).

2.4. Representative theorem and relation between force and dislocation GFs

The most important application of the Betti's reciprocity relation (2.20) is the reduced representative theorem presented below. This can be obtained by letting set (1) be the real problem of the given material domain V (bounded by ∂V) and set (2) the corresponding GF domain of the concentrated force in the same material.

$$\begin{aligned} u_k(\mathbf{y}) = & \int_{\partial V} \sigma_{ij}(\mathbf{x}) u_i^k(\mathbf{x}; \mathbf{y}) n_j(\mathbf{x}) dS(\mathbf{x}) \\ & - \int_{\partial V} c_{ijml} u_{m,x_l}^k(\mathbf{x}, \mathbf{y}) u_i(\mathbf{x}) n_j(\mathbf{x}) dS(\mathbf{x}) \\ & + \int_V f_i(\mathbf{x}) u_i^k(\mathbf{x}; \mathbf{y}) dV(\mathbf{x}) \end{aligned} \quad (2.23)$$

where the displacement GF u_i^k is the solution of the following governing equations (in the full-space, or in the given special spaces to be discussed later)

$$c_{ijlm} u_{l,mi}^k + c_{\text{iner}} u_j^k = -\delta_{jk}(\mathbf{x} - \mathbf{y}) \quad (2.24)$$

where c_{iner} is defined by (2.21), and c_{ijlm} is either the elastic stiffness (for time-harmonic deformation) or the viscoelastic stiffness (for viscoelastic deformation in the Laplace domain). The superscript k in the displacement GF denotes the applied point-force direction, and the subscript l (or i, j) the displacement component. The concentrated unit force is applied at \mathbf{y} , and the derivative in the second term on the right-hand side of equation (2.23) is with respect to the field point of the displacement GF. It is very important that in writing this Green's representative theorem, one should be very careful on the point-force source point \mathbf{y} and the field point \mathbf{x} since their translational symmetry only holds in an infinite and homogeneous space.

We now assume that the real problem is the one associated with an internal dislocation in a given bounded domain

V similar to that in figure 1(c) without body force f_i . In other words, we let n_i ($= n_i^- = -n_i^+$) be the unit normal to the internal surface A , and $b_j = u_j^+ - u_j^-$ be the dislocation on the plane with normal n_i . This dislocation over A may have any form provided that the following traction-continuity condition holds:

$$\sigma_{ij}^+ n_i^+ + \sigma_{ij}^- n_i^- = 0. \quad (2.25)$$

Applying the representative expression (2.23) to this case by further assuming that the field quantities in both sets satisfy the homogeneous boundary conditions on ∂V , we then have (Pan and Chen 2015).

$$u_k(\mathbf{y}) = \int_A \sigma_{ij}^k(\mathbf{x}; \mathbf{y}) b_j(\mathbf{x}) n_i(\mathbf{x}) dA(\mathbf{x}). \quad (2.26)$$

It is noted that the kernel function in equation (2.26) is the Green's stress with component (ij) at the field point \mathbf{x} due to a point force at \mathbf{y} applied in the k -direction. Alternatively and in terms of definition, the displacements u_k^{ij} at \mathbf{x} due to the point dislocation 'tensor' $b_j n_i$ at \mathbf{y} can be expressed by the point-dislocation kernel function as,

$$u_k(\mathbf{x}) = \int_A u_k^{ij}(\mathbf{y}; \mathbf{x}) b_j(\mathbf{y}) n_i(\mathbf{y}) dA(\mathbf{y}) \quad (2.27)$$

where u_k^{ij} represents the induced displacement in k -direction due to a point dislocation with its plane normal in the i -direction and its Burgers vector component in the j -direction.

Comparing equation (2.27) to (2.26) and also noticing that $b_j n_i$ is an arbitrary dislocation density tensor, we immediately obtain the following important equivalence between the stress due to a point force and the displacement due to a point dislocation (the first relation below)

$$u_k^{ij}(\mathbf{y}; \mathbf{x}) = \sigma_{ij}^k(\mathbf{x}; \mathbf{y}) = c_{ijml}(\mathbf{x}) u_{m,x_l}^k(\mathbf{x}; \mathbf{y}) \quad (2.28)$$

where the second relation is from the constitutive relation. It is noted that the locations of the source and field points in the point-force Green's stresses need to be switched in order to obtain the point-dislocation Green's displacements. This relation has to be very carefully executed particularly when the material is heterogeneous, as in a layered material system. If the system under consideration is a full-plane or full-space, the field and source points can be switched in equation (2.28); If the problem domain is a half-plane or half-space, then only the components of the field and source points parallel to the surface of the half-plane or half-space can be exchanged.

One can define the moment density 'tensor' (moment 'tensor' per unit area) as

$$m_{lq}(\mathbf{x}) = c_{ijlq}(\mathbf{x}) b_j(\mathbf{x}) n_i(\mathbf{x}). \quad (2.29)$$

Then, in terms of the moment tensor, equation (2.26) can be expressed as

$$u_k(\mathbf{y}) = \int_A m_{lq}(\mathbf{x}) u_{l,x_q}^k(\mathbf{x}; \mathbf{y}) dA(\mathbf{x}). \quad (2.30)$$

Since u_i^k are the displacement solutions due to the point force, $u_{i,q}^k$ can be considered as the solutions corresponding

to the couple force (point force in k -direction with a force arm in q -direction, Bacon *et al* 1979). In other words, the moment tensor and the dislocation pair ($b_j n_i$) are equivalent to each other. Furthermore, since the indices i and j in c_{ijkl} are exchangeable, the responses from pairs ($b_j n_i$) and ($b_i n_j$) are undistinguishable.

Finally, the surface integration over the dislocation can be changed using the delta function properties (Aki and Richards 1980, Pan and Chen 2015), and by doing so, one can find the following important representation of the equivalent body-force density of a given dislocation over the area A

$$f_i(\boldsymbol{\eta}) = - \int_A c_{ijlp} b_j(\boldsymbol{\xi}) n_i(\boldsymbol{\xi}) \frac{\partial}{\partial \eta_p} \delta(\boldsymbol{\eta} - \boldsymbol{\xi}) dA(\boldsymbol{\xi}). \quad (2.31)$$

This relation holds for the time-harmonic and viscoelastic deformations when reviewing them in the transformed domain. Notice further that a dislocation in material science and fault (or displacement discontinuity) in Earth science are the same in 3D deformation. In other words, the displacements due to a concentrated dislocation have a higher singularity than those due to a concentrated force. In the homogeneous full-space, to find the dislocation-induced displacement field, one just needs to take the derivative of the displacement GFs due to the point force and multiply the results by suitable coefficients, similar to the last term in equation (2.28). In the heterogeneous material, however, one needs to be very careful with the relation between \boldsymbol{x}^f and \boldsymbol{x}^s since they are no longer exchangeable. Besides the equivalent body-force expression of a dislocation ($b_j n_i$) (or seismic moment tensor), seismic moment tensors of different (higher) ranks can also be derived for static and dynamic deformations (Kagan 1987a, 1987b).

It should be noted, however, that a 2D fault in Earth science and a line dislocation in material science are completely different. A good reference for this is the review by Savage (1980). In the following sections, we will also illustrate their differences and furthermore, the interesting connections between them with examples.

2.5. Summary of section 2

For the elastostatic, time-harmonic, and viscoelastic (in the Laplace domain) deformations, we have derived the general Betti's reciprocity in equation (2.20), applicable also to the elastic-gravitational Earth medium. Based on it, the important representative expressions due to forces and dislocations are obtained, respectively, as in equations (2.23) and (2.27). The equivalence between the force and dislocation sources is presented in equation (2.28) and the equivalent body-force density is given in equation (2.31).

3. GFs in 2D/3D elastic and viscoelastic media

In this section, we present analytical GFs in 2D/3D full- and half-planes (spaces). For the 2D case, the deformation is located on the (x, y) -plane (for easy discussion using complex

variables). The source can be concentrated force or dislocation, and solutions to the corresponding finite source can be found by integrating the GF over the source domain. Traction-free boundary conditions are assumed on the surface of the half-plane (or half-space) for the internal source case. The materials are assumed to be isotropic or TI, with the GF solutions in the corresponding general anisotropic domain being further available in Pan and Chen (2015) for the static case and in Wang and Achenbach (1995) for the time-harmonic case. In 2D, we call the concentrated sources as the line forces and line dislocations (Nabarro 1967). An early brief history of dislocation can be found in Hirth (1985) and a brief review on 2D/3D faults in Earth science was given by van Zwieten *et al* (2013). The classic references on dislocations in 2D/3D from material point of view are the books by Hirth and Lothe (1982) and Hull and Bacon (2011). The two volumes, which comprise the proceedings of the conference on 'Fundamental Aspects of Dislocation Theory' edited by Simmons *et al* (1970), are also very important references. In this section, without loss of generality, for 2D deformation, we restrict ourselves to the plane-strain deformation, whilst the solution in the corresponding plane stress can be easily obtained by using the simple relation between plane-strain and plane-stress deformations. While we concentrate on the elastic solution, solutions of the corresponding viscoelastic deformation in the Laplace domain can be simply found by replacing the elastic moduli by the corresponding viscoelastic moduli (i.e. the ones depending on the Laplace variable s).

3.1. GFs in full- and half-planes by concentrated line forces and line dislocations

We start with the half-plane (in the (x, y) -plane) case with traction-free boundary condition on its surface. The solution for this case includes the reduced full-plane solution as the special case (by neglecting the complementary or image part of the solution). We first consider the anti-plane case where we have only the out-of-plane (or anti-plane) displacement u_z in z -direction and we further assume that the material is isotropic.

3.1.1. Anti-plane force. We assume that the half-plane ($-\infty < x < +\infty$ and $y > 0$) has a shear modulus μ (elastic or viscoelastic $\mu(s)$). We denote the anti-plane displacement by u ($\equiv u_z$). We further assume that an anti-plane line force of unit magnitude is applied at $(x, y) = (x_s, y_s)$. Therefore, the anti-plane governing equation of the GF in terms of the anti-plane displacement in the half-plane with shear modulus μ is

$$\nabla^2 u = -\delta(x - x_s)\delta(y - y_s)/\mu \quad (3.1)$$

where the Laplace differential operator ∇^2 is 2D in the (x, y) -plane. For the half-plane ($y > 0$) under the traction-free boundary condition ($\sigma_{zy} = 0$ on $y = 0$), the GF solution (Pan and Chen 2015) is

$$\begin{aligned} u(x, y; x_s, y_s) &= \frac{1}{2\pi\mu} \ln(1/r_1) + \frac{1}{2\pi\mu} \ln(1/r_2) \\ \sigma_{zx}(x, y; x_s, y_s) &= -\frac{x-x_s}{2\pi r_1^2} - \frac{x-x_s}{2\pi r_2^2} \\ \sigma_{zy}(x, y; x_s, y_s) &= -\frac{y-y_s}{2\pi r_1^2} - \frac{y+y_s}{2\pi r_2^2} \end{aligned} \quad (3.2)$$

where

$$r_1 = \sqrt{(x - x_s)^2 + (y - y_s)^2}; r_2 = \sqrt{(x - x_s)^2 + (y + y_s)^2}. \quad (3.3)$$

The first terms on the right-hand side of equation (3.2) are just the full-plane GFs, and the second part or the complementary (image) part is used to satisfy the traction-free boundary conditions.

3.1.2. Anti-plane dislocation. We assume that there is a uniformly distributed line (screw) dislocation (anti-plane dislocation, i.e. screw dislocation) with Burgers vector component b ($\equiv b_z$) in x_3 -direction located at z_s ($=x_s + iy_s$ with $y_s > 0$) in the half-plane ($y > 0$). More specifically, the dislocation is located on the horizontal semi-plane formed by $-\infty < x < x_s$, $y = y_s$, $-\infty < z < +\infty$. It is noted that hereafter the complex variable z simply denotes the (x, y) -plane coordinates, and it is different from the third axis coordinate z (i.e. x_3 that we also use in this article). We introduce the local polar coordinates (r, θ) originated at source location z_s , where r is the distance between the field point z ($=x + iy$) and source point z_s , and θ is the angle from the horizontal axis with the origin at z_s . Then the jump condition across the line dislocation is (in terms of the polar coordinates r and θ)

$$u(r, \pi) - u(r, -\pi) = b \quad (3.4)$$

where r is the distance measured relative to the source location z_s .

The dislocation-induced displacement and stresses can be found as

$$\begin{aligned} u(z; z_s) &= -\frac{b}{2\pi} \operatorname{Re}[\operatorname{iln}(z - z_s)] + \frac{b}{2\pi} \operatorname{Re}[\operatorname{iln}(z - \bar{z}_s)] \\ \sigma_{zx}(x, y; x_s, y_s) &= -\frac{\mu b}{2\pi} \frac{y - y_s}{r_1^2} + \frac{\mu b}{2\pi} \frac{y + y_s}{r_2^2} \\ \sigma_{zy}(x, y; x_s, y_s) &= \frac{\mu b}{2\pi} \frac{x - x_s}{r_1^2} - \frac{\mu b}{2\pi} \frac{x - x_s}{r_2^2} \end{aligned} \quad (3.5)$$

where the overbar denotes the complex conjugate. Similarly, the first term on the right-hand side is just the full-plane GF, and the second term, or the complementary (image) part is introduced to satisfy the traction-free boundary condition on the surface of the half-plane. Comparing the dislocation (3.5) and force (3.2) solutions, it is noted that their expressions are very similar to each other: displacements are in terms of logarithmic function and stresses are in terms of very simple rational functions.

3.1.3. Line force and line dislocation in plane-strain deformation. Under plane-strain deformation, the line-force and line-dislocation (or edge dislocation) induced displacement and stress fields can be expressed in a uniform format as in Pan and Chen (2015). We first define the following complex parameters.

— For line force (F_x, F_y) at $z = z_s$

$$A = -\frac{F_x + iF_y}{2\pi(1 + \kappa)}; B = \frac{\kappa(F_x - iF_y)}{2\pi(1 + \kappa)}. \quad (3.6a)$$

— For line (edge) dislocation (b_x, b_y) at $z = z_s$

$$A = -\frac{i\mu(b_x + ib_y)}{\pi(1 + \kappa)}; B = \frac{i\mu(b_x - ib_y)}{\pi(1 + \kappa)} \quad (3.6b)$$

where $\kappa = 3 - 4\nu$ with ν being the Poisson's ratio of the material.

In terms of complex variable z , the full-plane GFs of the line force and line dislocation can be expressed as

$$\begin{aligned} [2\mu(u_x + iu_y)]_f &= \kappa A \ln(z - z_s) - \bar{A}(z - z_s)/(\bar{z} - \bar{z}_s) - \bar{B} \ln(\bar{z} - \bar{z}_s) \\ [\sigma_{xx} + \sigma_{yy}]_f &= 2[A/(z - z_s) + \bar{A}/(\bar{z} - \bar{z}_s)] \\ [\sigma_{yy} - \sigma_{xx} + 2i\sigma_{xy}]_f &= 2[-A(\bar{z} - \bar{z}_s)/(z - z_s)^2 + B/(z - z_s)]. \end{aligned} \quad (3.7)$$

For the corresponding half-plane case under the traction-free boundary condition on the surface, we only need to add the following complementary (image) part to the full-plane solution (3.7)

$$\begin{aligned} [2\mu(u_x + iu_y)]_c &= -\kappa \left[\bar{A} \frac{z - z_s}{z - \bar{z}_s} + \bar{B} \ln(z - \bar{z}_s) \right] \\ &\quad + (A + B) \frac{z - \bar{z}}{\bar{z} - z_s} - A \frac{(z - \bar{z})(\bar{z} - \bar{z}_s)}{(z - z_s)^2} + A \ln(\bar{z} - z_s) \end{aligned} \quad (3.8)$$

$$\begin{aligned} [\sigma_{xx} + \sigma_{yy}]_c &= -2 \left[\frac{\bar{A} + \bar{B}}{z - \bar{z}_s} - \bar{A} \frac{z - z_s}{(z - \bar{z}_s)^2} + \frac{A + B}{\bar{z} - z_s} - A \frac{\bar{z} - \bar{z}_s}{(\bar{z} - z_s)^2} \right] \\ [\sigma_{yy} - \sigma_{xx} + 2i\sigma_{xy}]_c &= 2\bar{z} \left[\frac{\bar{B}}{(z - \bar{z}_s)^2} - 2\bar{A} \frac{\bar{z}_s - z_s}{(z - \bar{z}_s)^3} \right] \\ &\quad - \frac{2\bar{A}(z - z_s)}{(z - \bar{z}_s)^2} - \frac{4\bar{A}z(z - \bar{z}_s)}{(z - \bar{z}_s)^3} - \frac{2\bar{B}\bar{z}_s}{(z - \bar{z}_s)^2}. \end{aligned} \quad (3.9)$$

Again, comparing the line-force and line-dislocation solutions, it is noted that their expressions are the same, except for the fact that in order to find the solution due to the force and dislocation, one just needs to use the different parameters A and B defined by equations (3.6a) and (3.6b).

3.2. Solutions in full- and half-planes by line forces and line dislocations over finite region

It is observed from section 3.1 that the GFs due to concentrated forces and dislocations, in both anti-plane and in-plane deformations, and for both full- and half-planes, are in exact-closed forms and are in terms of very simple functions of the coordinates. Therefore, the solution corresponding to the finite force (or finite dislocation) over a finite line segment can be easily found by integrating the concentrated GF over the line segment. We select only the case of anti-plane (screw) dislocation-induced displacement to illustrate the process.

We assume that the Burgers vector component (screw dislocation) b in (3.5) is constant along the dislocation line segment from $A_1(x_{s1}, y_{s1})$ to $A_2(x_{s2}, y_{s2})$. To integrate over the line segment, we introduce the following parameter t which varies from 0 to 1 when the source point varies from A_1 to A_2 :

$$\begin{aligned} x_s &= x_{s1} + t(x_{s2} - x_{s1}); \quad y_s = y_{s1} + t(y_{s2} - y_{s1}) \\ L &= \sqrt{(x_{s2} - x_{s1})^2 + (y_{s2} - y_{s1})^2}. \end{aligned} \quad (3.10)$$

Then the total contribution at any field point z from the finite line segment can be found from the following line integration

$$u(z; L_{A_1-A_2}) = \frac{b}{2\pi} \text{Re} \int_{A_1}^{A_2} [i \ln(z - \bar{z}_s) - i \ln(z - z_s)] dL_s$$

$$= \frac{bL}{2\pi} \text{Re} \int_0^1 \{i \ln[z - \bar{z}_s(t)] - i \ln[z - z_s(t)]\} dt.$$

Making use of the following integral expression (3.11)

$$\int \ln(ax + c) dx = (x + c/a) \ln(ax + c) - x; \quad a \neq 0 \quad (3.12)$$

the integral in equation (3.11) can be carried out analytically so that we finally have

$$u(z; L_{A_1-A_2}) = \frac{bL}{2\pi} \text{Re} \left[\begin{aligned} & i[(a_1 + c_1) \ln(a_1 + c_1) - c_1 \text{In}c_1]/a_1 \\ & -i[(a_2 + c_2) \ln(a_2 + c_2) - c_2 \text{In}c_2]/a_2 \end{aligned} \right] \quad (3.13)$$

where

$$a_1 = -(x_{s2} - x_{s1}) + i(y_{s2} - y_{s1}); \quad c_1 = z - (x_{s1} - iy_{s1})$$

$$a_2 = -(x_{s2} - x_{s1}) - i(y_{s2} - y_{s1}); \quad c_2 = z - (x_{s1} + iy_{s1}). \quad (3.14)$$

Taking the derivative of equation (3.13) with respect to field point $z (=x + iy)$ of the displacement induced by the finite-length dislocation, one can find the strains and then the stresses using the constitutive relations (Molavi Tabrizi *et al* 2014). Similar analytical expressions can be obtained for non-uniform dislocation distributions (linear or quadratic), and for the corresponding in-plane deformation due to the finite edge dislocation (Molavi Tabrizi *et al* 2014).

3.3. Displacements in full- and half-planes by a 2D fault

It is noted from the solutions above for the concentrated line force and line dislocation that they both are in exactly the same form (with the same order of singularity). This is different from the corresponding 3D case where the point-force GF and the point-dislocation GF have different forms and thus different orders of singularity (e.g. equation (2.28)). This is due to the different definitions of the line dislocation and line force in 2D, as explained by Pan and Chen (2015). Therefore, the 2D line-dislocation solution (in material science) and the 2D fault solution (in Earth science) are different but can be connected via a special relation for many direct applications (Savage 1980). This is illustrated below.

We take a 2D line dislocation in the isotropic full-plane as example. Figure 2 shows an edge (line) dislocation with Burgers component b_y applied at the origin. The dislocation line vector ξ is along positive z -direction (i.e. x_3 -direction) (Hirth and Lothe 1982). Physically, it means that there is a cutting plane at $y = 0$ (with $x < 0$ and $-\infty < z < +\infty$) over which there exists the relative displacement on its top and bottom surfaces, or the displacement discontinuity $u_y(+)-u_y(-)$, is b_y . In other words, a line dislocation applied at origin of (x, y) -plane (in material science) is actually a semi-infinite fault on the $y = 0$ plane (in Earth science). This is the relation between the line dislocation and 2D fault.

Making use of the relation between GF solution by the line dislocation and that by the 2D fault, we can easily derive the GF solution due to a finite 2D fault using the exact-closed form expression of the line-dislocation GF. Let us assume that there

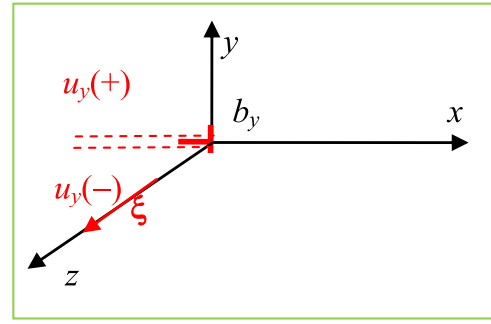


Figure 2. An edge dislocation with Burgers component b_y applied at $(x, y) = (0, 0)$ (i.e. the dislocation line direction vector ξ is along positive z -axis), reviewed equally as a semi-infinite fault on the $y = 0$ plane (with $x < 0$ and $-\infty < z < +\infty$) with the relative displacement $u_y(+)-u_y(-) = b_y$.

is finite 2D fault located on the $y = 0$ plane (infinitely long in z -direction), with a uniform relative displacement discontinuity Δu_y ($u_y(y = 0+) - u_y(y = 0-)$) over the width $2a$ (figure 3(b)). Then in order to find the GF solution of this 2D fault, we need only to superpose two GF solutions due to the line dislocations located at both ends of the 2D fault with Burgers components $b_y = \Delta u_y$ and $-b_y = -\Delta u_y$, respectively (figure 3(a)).

To further illustrate the process, we first write the line-dislocation solution equation (3.7) in a real form, for the stresses induced in the full-plane by Burgers component b_y only, as in figure 2. The stresses at (x, y) by the line dislocation located at (x_s, y_s) are

$$\sigma_{yy}(x, y; x_s, y_s) = \frac{\mu b_y}{2\pi(1-\nu)} \frac{(x-x_s)[(x-x_s)^2 + 3(y-y_s)^2]}{r^4}$$

$$\sigma_{xx}(x, y; x_s, y_s) = \frac{\mu b_y}{2\pi(1-\nu)} \frac{(x-x_s)[(x-x_s)^2 - (y-y_s)^2]}{r^4}$$

$$\sigma_{xy}(x, y; x_s, y_s) = \frac{\mu b_y}{2\pi(1-\nu)} \frac{(y-y_s)[(x-x_s)^2 - (y-y_s)^2]}{r^4} \quad (3.15)$$

where r is the distance between the field (x, y) and source (x_s, y_s) points.

Then, in order to find the stress field induced by a 2D fault with uniform displacement discontinuity $\Delta u_y (=u_y(y = 0+) - u_y(y = 0-))$ over the length $x \in [-a, a]$, we just need to superpose the solution (3.15) by the two Burgers components at $x_s = a$ and $x_s = -a$ ($b_y = \Delta u_y$ at $x_s = a$, and $b_y = -\Delta u_y$ at $x_s = -a$) (with $y_s = 0$). In so doing, we obtain the following relations

$$\sigma_{yy}(x, y) \Big|_{2a}^{\Delta u_y} = \sigma_{yy}(x, y; x_s, y_s) \Big|_{(x_s, y_s)=(a, 0)}^{b_y=\Delta u_y} + \sigma_{yy}(x, y; x_s, y_s) \Big|_{(x_s, y_s)=(-a, 0)}^{b_y=-\Delta u_y}$$

$$= \frac{\mu \Delta u_y}{2\pi(1-\nu)} \frac{(x-a)[(x-a)^2 + 3y^2]}{r_+^4} - \frac{\mu \Delta u_y}{2\pi(1-\nu)} \frac{(x+a)[(x+a)^2 + 3y^2]}{r_-^4}$$

$$\sigma_{xx}(x, y) \Big|_{2a}^{\Delta u_y} = \frac{\mu \Delta u_y}{2\pi(1-\nu)} \frac{(x-a)[(x-a)^2 - y^2]}{r_+^4} - \frac{\mu \Delta u_y}{2\pi(1-\nu)} \frac{(x+a)[(x+a)^2 - y^2]}{r_-^4}$$

$$\sigma_{xy}(x, y) \Big|_{2a}^{\Delta u_y} = \frac{\mu \Delta u_y}{2\pi(1-\nu)} \frac{y[(x-a)^2 - y^2]}{r_+^4} - \frac{\mu \Delta u_y}{2\pi(1-\nu)} \frac{y[(x+a)^2 - y^2]}{r_-^4}$$

$$r_+ = \sqrt{(x-a)^2 + y^2}; \quad r_- = \sqrt{(x+a)^2 + y^2}. \quad (3.16)$$

These are the exact-closed form GF stresses induced by a 2D finite fault located on the x -axis with $x \in [-a, a]$ in a full plane. It is noted that on the plane of $y = 0$, the stress expression σ_{yy} will be reduced to the one obtained by Crouch (1976) who solved this complicated boundary value problem using the Papkovitch functions. These and similar dislocation solutions are fundamental, and can be served as kernel functions in various crack/fracture analyses

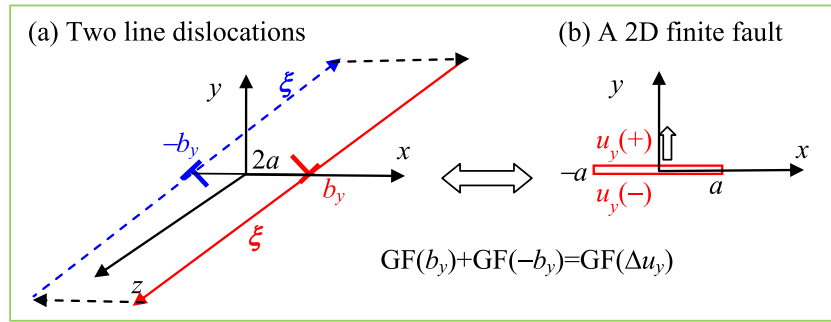


Figure 3. The GF relation between a 2D finite fault and two line-dislocations where the Burgers component b_y is related to the relative displacement discontinuity $\Delta u_y \equiv u_y(y=0+) - u_y(y=0-)$ with $b_y = \Delta u_y$. The field induced by the uniform displacement discontinuity $\Delta u_y (=u_y(y=0+) - u_y(y=0-))$ within the finite domain $x \in [-a, a]$ can be found by superposing the solutions by the two Burgers vector components at $x_s = a$ and $x_s = -a$ ($b_y = \Delta u_y$ at $x_s = a$ and $b_y = -\Delta u_y$ at $x_s = -a$) (with $y_s = 0$).

(e.g. Crouch and Starfield (1983), Hills *et al* (1996) and Weertman (2008)).

The GF solutions obtained so far are for the elastostatic deformation. They can be also regarded as the solutions for the corresponding viscoelastic deformation (in the Laplace-transformed domain, with material properties being functions of the Laplace variable s) without the inertia term (i.e. $c_{\text{iner}} = 0$) in equation (2.21). Since the line-dislocation GFs are also available in exact-closed form in the general anisotropic full-, half-, and bi-plane (Pan and Chen 2015, Vattre and Pan 2017), more complicated 2D fault solutions can be easily derived, including multiple 2D faults or dislocation arrays (Chu and Pan 2014, Vattre and Pan 2017), moving dislocation/fault (Wang and Pan 2007), and their important interactions (Savage 1980).

The corresponding strain GF due to the point force can be obtained by taking the derivatives of the displacement GF with respect to the field point \mathbf{x} . Namely, we have

$$\varepsilon_{lm}^k = \frac{1}{16\pi\mu(1-\nu)r^2} \left[\frac{\delta_{lm}(x_k - y_k) - (1-2\nu)[\delta_{mk}(x_l - y_l) + \delta_{kl}(x_m - y_m)]}{-3(x_k - y_k)(x_l - y_l)(x_m - y_m)/r^3} \right]. \quad (3.20)$$

Using the constitutive relation of the isotropic material, the stress GF can be expressed as:

$$\sigma_{lm}^k = \frac{1}{8\pi(1-\nu)r^2} \left[\frac{(1-2\nu)[\delta_{lm}(x_k - y_k) - \delta_{lk}(x_m - y_m) - \delta_{mk}(x_l - y_l)]}{-3(x_k - y_k)(x_l - y_l)(x_m - y_m)/r^3} \right]. \quad (3.21)$$

To find the displacement GF at \mathbf{y} due to a concentrated (point) dislocation at \mathbf{x} (with Burgers component b_i and unit normal n_j), we can simply make use of equation (2.28), which gives us

$$u_k(\mathbf{y}) = u_k^{lm}(\mathbf{y}; \mathbf{x}) b_l(\mathbf{x}) n_m(\mathbf{x}) = \frac{b_l(\mathbf{x}) n_m(\mathbf{x})}{8\pi(1-\nu)r^2} \left[\frac{(1-2\nu)[\delta_{lm}(x_k - y_k) - \delta_{lk}(x_m - y_m) - \delta_{mk}(x_l - y_l)]}{-3(x_k - y_k)(x_l - y_l)(x_m - y_m)/r^3} \right]. \quad (3.22)$$

By taking derivative with respect to \mathbf{y} in equation (3.22), we then find the concentrated dislocation-induced strains, and finally making use of the constitutive relation, we have the dislocation-induced stresses.

Remark 3.3. Since the solutions by a point force or a point dislocation are in terms of rational functions, finite forces and dislocations over a flat surface could be integrated out analytically. In material science, the area integral over the fault (or dislocation) surface is usually converted to a line (loop) integral using the Stokes' theorem (Hirth and Lothe 1982, Pan and Chen 2015), so that the loop integral can be integrated out for certain shapes of the fault plane, in the TI full-space (Yuan *et al* 2013a) and even the general anisotropic full-space (Chu *et al* 2011). The equivalent relation between the 3D fault and 3D dislocation loop as connected by the Stokes' theorem is particularly useful since it helps us reduce the area integral over the 3D fault plane into a simple line integral along the loop of the 3D dislocation (or boundary of the 3D fault).

3.4. GFs in a full-space by point forces and dislocations

The point-force GF in an isotropic elastic full space (with shear modulus μ and Poisson's ratio ν) is the famous Kelvin solution (Thompson 1848, Lord Kelvin). For a point force in k -direction applied at source point \mathbf{y} (y_1, y_2, y_3) of unit magnitude, the elastic displacement GF in j -direction at the field point \mathbf{x} (x_1, x_2, x_3) is

$$u_j^k(\mathbf{x}; \mathbf{y}) = \frac{1}{16\pi\mu(1-\nu)r} \left[(3-4\nu)\delta_{jk} + \frac{x_j - y_j}{r} \frac{x_k - y_k}{r} \right] \quad (3.17)$$

where r is the distance between the field and source points, i.e.

$$r = \sqrt{(x_1 - y_1)^2 + (x_2 - y_2)^2 + (x_3 - y_3)^2}. \quad (3.18)$$

Remark 3.1. The point-force induced elastic displacement GF is symmetric with respect to the direction of the point force and the direction of the displacement. In other words, the upper and lower indices k and j in equation (3.17) are exchangeable.

Remark 3.2. This GF is also symmetric with respect to the source and field positions. As such, the following relations hold

$$u_j^k(\mathbf{x}; \mathbf{y}) = u_k^j(\mathbf{x}; \mathbf{y}) = u_j^k(\mathbf{y}; \mathbf{x}). \quad (3.19)$$

3.5. GFs in a half-space by forces and dislocations

GFs by concentrated forces were, respectively, derived by Boussinesq (1885) and Cerruti (1888) for surface loading and by Mindlin (1936) for internal loading (commonly called Mindlin solution). The detailed formulation can be found in Pan and Chen (2015). These fundamental solutions can be integrated over a given domain to find the displacement and stress fields induced by the distributed loads. Various problems related to loading over a finite domain within an isotropic or TI half-space were also solved (i.e. Busby and Dydo (1995), Li and Berger (2001), Wang and Liao (2001, 2002a, 2002b), Becker and Bevis (2004), Yue *et al* (2005), Wang *et al* (2006a, 2009, 2013), Wang and Tzeng (2009), Lubarda (2013), Marmo and Rosati (2016) and Marmo *et al* (2016, 2018)). This topic is still an active research area in geomechanics and solid mechanics.

Making use of the relation between the point-force and point-dislocation solutions as discussed above, we can derive the corresponding point-dislocation GFs. Integrating over the finite fault (dislocation) surface, we then obtain the finite fault-induced fields in the elastic half-space. Notable contributions in faulting were made by Maruyama (1964, 1966) for both 2D/3D full and half-spaces. The most important and well-recognized works are those by Okada (1985, 1992) who also distributed his FORTRAN code for easy use by Earth scientists for a fault of rectangular shape. Faults are viewed in materials as dislocations and therefore, material scientists have also contributed to the topic, starting from the works by Steketee (1958) and Yoffe (1960, 1961).

The fault shape was extended to the more general case of triangle (Comninou and Dunders 1975, Jeyakumaran *et al* 1992, Meade 2007, Nikkhoo and Walter 2015). Maerten and colleagues took another step forward and developed a BEM code utilizing the triangular dislocation solution as the fundamental kernel function, which is now used intensively in Earth science (Maerten *et al* 2002, 2005, 2014). Most recently, the finite-dislocation solution in an isotropic elastic half-space was extended to the elastic TI (Yuan *et al* 2013b, Pan *et al* 2014) and general anisotropic (Chu *et al* 2012a, 2012b, Pan *et al* 2015a, Vattre and Pan 2018) half-spaces. In the viscoelastic case without the inertia term, the Laplace domain solution can be simply obtained by replacing the elastic coefficients with the Laplace variable-dependent coefficients, and then carrying out the inverse Laplace transform. These inverses were carried out numerically for the isotropic viscoelastic case (Singh and Rosenman 1974, Piombo *et al* 2007) and for the TI viscoelastic half-space case (Molavi Tabrizi and Pan 2015).

Besides the force- and dislocation-related GF solutions, various inclusion/inhomogeneity problems (Mura 1987, Li and Wang 2018) can be also solved and the corresponding GFs can be applied to different fields, including multi-phase coupled material solids (Liu *et al* 2001). An inclusion/inhomogeneity can be related either to an equivalent dislocation (Eshelby 1957, 1961, Mura 1987) or to an equivalent force (Pan 2004a, 2004b, Pan and Chen 2015). With the known fundamental solutions of the equivalent dislocation or equivalent force, the inclusion/inhomogeneity approach can be

applied to hydraulic fracture analysis (Chen *et al* 2018a), to finite 3D inhomogeneity in both elastic and viscoelastic half-spaces (Wu and Wang 1988, Bonafede 1990, Wu *et al* 1991, Bonafede and Ferrari 2009, Zhong *et al* 2019) and even to the current quantum-wire and quantum-dot nanotechnology (Pan 2004a, 2004b, Pan *et al* 2008, Zou and Pan 2012, Yue *et al* 2015, Lee *et al* 2015). Furthermore, the dislocation solutions can be directly or indirectly applied to solve various crack/fracture problems, as in Bonafede and Rivalta (1999a, 1999b) for the tensile dislocation/crack problems in a half-plane or a bimaterial plane. A brief review on elastic dislocation solutions in geophysics can be found in van Zwieten *et al* (2013). Fault rupture and ground motion were recently investigated by Meng (2017) and Meng and Wang (2018) using the FEM-related methods, with further open source codes available.

3.6. Time-harmonic GFs in full- and half-planes/spaces by forces

Under the action of a time-harmonic and concentrated line force in a full plane, the GFs for the anti-plane and in-plane deformation can be derived analytically (Achenbach 1973, Graff 1975, Kausel 2006). In a 3D full space, the transient GF in the time-domain can be found in Eringen and Suhubi (1974) and Aki and Richards (1980). Also in the 3D full-space case, the time-harmonic GF of the point force can be expressed in an exact-closed form (Kausel 2006). However, for the corresponding half-space, there is no closed-form solution. The corresponding time-harmonic GFs were derived numerically by Banerjee and Mamoon (1990) following the superposition method in Mindlin (1936) for the corresponding static case. Some of the functions involve line integral to infinity. While in principle, these GF expressions can be utilized to find the corresponding dislocation GFs, we will discuss the corresponding dislocation GF associated with horizontally layered half-space (plane) media later where the half-space or half-plane is the special case of the layered structure.

Below, we list only the 2D full-plane and 3D full-space solutions, derived by Dominguez and Abascal (1984) and Kausel (2006). While the 2D half-plane solution was presented by Rangelov and Manolis (2010), the 3D half-space solution by Banerjee and Mamoon (1990) may contain some errors (Yuan and Pan 2016). Again, since the half-plane and half-space solutions are the special cases of their corresponding layered systems, these will be discussed more in the next section.

First, it is noted that the GF for the time-harmonic wave case is governed by

$$c_p^2 \partial_i \partial_k u_k - c_s^2 \varepsilon_{ijk} \varepsilon_{klm} \partial_{jl} u_m + \omega^2 u_i = -\delta_{in}(\mathbf{x} - \mathbf{0})/\rho \quad (3.23)$$

where the force of unit magnitude is applied at the origin in the n -direction and the induced displacement GF is in i -direction at the field point \mathbf{x} ; ε_{ijk} is the permutation symbol; c_p and c_s are the longitudinal and shear wave velocity of the material, i.e. in terms of the two Lamé constants, $c_p = \sqrt{(\lambda + 2\mu)/\rho}$; $c_s = \sqrt{\mu/\rho}$. It should be noted that on

the right-hand side of (3.23), the delta function is divided by the material density ρ .

For an anti-plane (corresponding to the SH wave) line force (i.e. the force is in the z -direction) applied at $(x, y) = (0, 0)$ in the (x, y) -plane, the induced full-plane displacement GF in z -direction is

$$u_z^z(r) = \frac{-i}{4\mu} H_0^{(2)}(r\omega/c_s) \quad (3.24)$$

where r is the distance between the field and source points, and $H_n^{(2)}$ is the second Hankel function of order n , or Bessel function of the third kind.

For an in-plane line force (i.e. the P-SV wave) applied at the origin with force in α -direction ($\alpha = x, y$), the induced full-plane displacement GF in β -direction ($\beta = x, y$) at distance r from the origin is

$$u_\beta^\alpha(r) = (\psi\delta_{\alpha\beta} + \chi r_{,\alpha} r_{,\beta})/\mu \quad (3.25)$$

where $r_{,j}$ is the derivative of r with respect to x_j , and

$$\begin{aligned} \psi &= \frac{i}{4} \left[\frac{H_1^{(2)}(\omega r/c_s)}{\omega r/c_s} - \frac{c_s^2}{c_p^2} \frac{H_1^{(2)}(\omega r/c_p)}{\omega r/c_p} - H_0^{(2)}(\omega r/c_s) \right] \\ \chi &= \frac{i}{4} \left[\frac{c_s^2}{c_p^2} H_2^{(2)}(\omega r/c_p) - H_2^{(2)}(\omega r/c_s) \right]. \end{aligned} \quad (3.26)$$

Finally, for a concentrated point force in i -direction applied at the origin in 3D, the full-space displacement GF in j -direction at distance r from the origin is

$$u_j^i(r) = \frac{(\psi\delta_{ij} + \chi r_{,i} r_{,j})}{4\pi\mu r} \quad (3.27)$$

$$\begin{aligned} \psi &= e^{-i\omega r/c_p} \frac{c_s^2}{c_p^2} \left[\frac{i}{\omega r/c_p} + \frac{1}{(\omega r/c_p)^2} \right] + e^{-i\omega r/c_s} \left[1 - \frac{i}{\omega r/c_s} - \frac{1}{(\omega r/c_s)^2} \right] \\ \chi &= e^{-i\omega r/c_p} \frac{c_s^2}{c_p^2} \left[1 - \frac{3i}{\omega r/c_p} - \frac{3}{(\omega r/c_p)^2} \right] - e^{-i\omega r/c_s} \left[1 - \frac{3i}{\omega r/c_s} - \frac{3}{(\omega r/c_s)^2} \right]. \end{aligned} \quad (3.28)$$

It is noted that by replacing $-i\omega$ with s and the elastic moduli with the s -dependent ones, one then obtains the GFs in the corresponding Laplace domain (i.e. equation (2.21)).

3.7. Transient GFs in full- and half-planes/spaces by forces/dislocations

While transient GFs due to concentrated forces and dislocations are difficult to derive, some have been derived. These GFs should be particularly useful as benchmarks to verify the solutions based on the Fourier transform method presented above (i.e. first derive the GFs in the transformed-domain and then invert back them to the time-domain).

For the elastic isotropic case and under either impulsive source (i.e. $\delta(\mathbf{x} - \boldsymbol{\xi})\delta(t - \tau)$) or a given time history of the source (i.e. $\delta(\mathbf{x} - \boldsymbol{\xi})f(t)$), the full-space GFs of point forces and dipoles (and thus dislocations) can be found in Eringen and Suhubi (1974) and Aki and Richards (1980). Transient GFs in 2D and 3D full/half-planes and full/half-spaces due to forces and dipoles were collected and listed in details by Kausel (2006) with numerical examples.

For the general case of elastic anisotropy in a full domain (a full-plane or a full-space), Wang and Achenbach (1994)

derived both 2D and 3D transient GFs of a concentrated force under impulsive time variation by Radon transform. The solutions are in the form of a surface integral over a unit sphere for the 3D case and in the form of a contour integral over a unit circle for the 2D case. An interesting method was proposed by Yakhno and Cerdik Yaslan (2011) for deriving the 3D transient GFs. By this new method, the governing equations were first written in the form of the time-dependent first-order symmetric hyperbolic system with respect to the displacement velocity and stress components, and then solved as the summation of the Fourier-transformed images of the fundamental solution with respect to a space variable. The time-harmonic GFs in the full-plane/space domain were derived by Wang and Achenbach (1995). Tewary and Fortunko (1992) derived the retarded anisotropic GF in both full- and half-spaces where the source is delta function in space and delta or Heaviside function in time.

For the 3D half-space case, the Lamb's problem (Lamb 1904) is particularly useful. For the isotropic half-space with traction-free boundary conditions, Johnson (1974) derived the complete GFs using the Cagniard-de Hoop method. Feng and Zhang (2018) recently revisited the solution by Johnson (1974) and were able to obtain the exact closed-form GFs for the Lamb's problem using the superposition method where only elementary algebraic expressions and elliptic integrals were involved. For the corresponding anisotropic half-space (half-plane), Wang and Achenbach (1996) derived the GFs via superposition of the time-transient plane waves. When the concentrated forces are applied on the surface, the GF expression is given in terms of integrals defined in a finite domain, which has a simple structure for convenient computation. The computationally efficient half-space GF derived by Tewary and Fortunko (1992) should be also a good reference.

3.8. Summary of section 3

Since various line-dislocation solutions are available (Hirth and Lothe 1982) or can be derived, many 2D fault problems in geophysics can be solved by making use of the simple relation between the two as illustrated by figure 3. In other words, instead of carrying out the line integral of the concentrated GF solution along the 2D fault boundary, one just needs to superpose the two line-dislocation solutions correspondingly located at the ends of the 2D fault. Similarly and equally important is the relation between a 3D fault in geophysics and a (3D) dislocation loop in material science, where the area integral could be inverted into a simple line integral along the loop of the fault. Making use of it, one needs only to carry out the line integral along the loop of the dislocation (or the boundary of the fault), instead of the area integral over the 3D fault plane. Certain time-harmonic GFs in 2D and 3D domains are also briefly listed and/or discussed, involving both material isotropy and anisotropy. It is finally pointed out that while various analytical approaches with solutions in TI media can be found in Fabrikant (1989, 1991) and Ding *et al* (2006), many elastic GFs are listed in the handbook by Kachanov *et al* (2003).

4. GFs in layered half-spaces

In this section, we present the general formulation for the elastic and viscoelastic gravitational deformation in layered half-spaces, but concentrate on the elastostatic deformation and wave motion induced by concentrated forces and dislocations. Both 2D and 3D GFs in elastic (viscoelastic) and layered half-plane and layered half-space, with and without gravity, are considered. The sources will be concentrated forces and dislocations, or forces and dislocations applied over a given finite domain. Source functions and GF solutions are expressed in terms of both Cartesian and cylindrical systems of vector functions, with their expansion coefficients being derived via the dual variable and position (DVP) method. In geophysics, the regional structure of our Earth is a horizontally layered half-space.

4.1. General solutions with gravity

Considering the gravitational contribution, the general governing equation in terms of the cylindrical coordinate system can be written as

$$\begin{aligned} \sigma_{ji,j} + (\rho g u_z)_i - \rho \psi_{,i} - g(\rho u_j)_j \delta_{iz} + f_i + c_{\text{iner}} u_i &= 0 \\ \psi_{,jj} + 4\pi G(\rho u_j)_j &= 0 \end{aligned} \quad (4.1)$$

where c_{iner} is defined in equation (2.21) for the static, time-harmonic, and viscoelastic deformations. The sign convention used here is consistent with that in Farrell (1972) and Rundle (1980).

If we further assume that the material is TI with its symmetry axis along z -direction, then the constitutive relation between the stresses (σ_{ij}) and the deformation gradients ($u_{i,j}$) (in terms of the cylindrical coordinate system) is

$$\begin{aligned} \sigma_{rr} &= c_{11} u_{r,r} + c_{12} r^{-1} (u_{\theta,\theta} + u_r) + c_{13} u_{z,z} \\ \sigma_{\theta\theta} &= c_{12} u_{r,r} + c_{11} r^{-1} (u_{\theta,\theta} + u_r) + c_{13} u_{z,z} \\ \sigma_{zz} &= c_{13} u_{r,r} + c_{13} r^{-1} (u_{\theta,\theta} + u_r) + c_{33} u_{z,z} \\ \sigma_{\theta z} &= c_{44} (u_{\theta,z} + r^{-1} u_{z,\theta}); \sigma_{rz} = c_{44} (u_{z,r} + u_{r,z}) \\ \sigma_{r\theta} &= c_{66} (r^{-1} u_{r,\theta} + u_{\theta,r} - r^{-1} u_{\theta}) \end{aligned} \quad (4.2)$$

where c_{ij} are the elastic moduli (N/m²) with $c_{66} = 0.5(c_{11} - c_{12})$, which can be also regarded as the Laplace domain coefficients. This constitutive relation is similar to equation (2.3) in terms of the Cartesian coordinate system.

We define the flux component in z -direction, q_z , related to the perturbed potential ψ as

$$q_z = \psi_{,z} + 4\pi G \rho u_z. \quad (4.3)$$

For a given half-space (plane) problem with possible inhomogeneity in vertical z -direction, the general approach for solving the problem is to first apply an integral transform to suppress the horizontal variables. While the Fourier transform or the Cartesian system of vector functions (Pan 1989a) can be applied for the general deformation, axisymmetric problems are usually solved by applying the Hankel transform, or better the cylindrical system of vector functions (Pan 1989a). For the problem at hands where the governing equations are

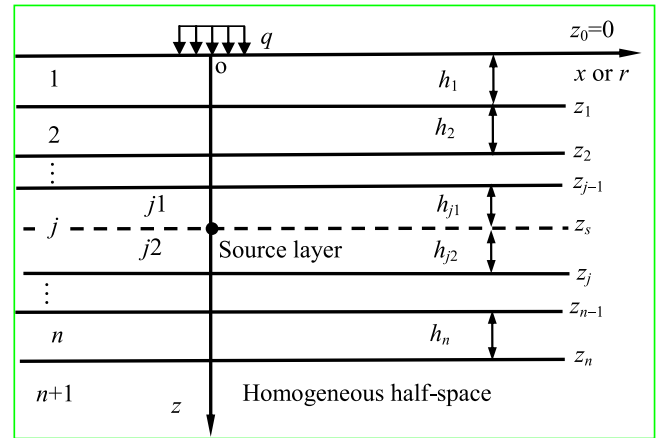


Figure 4. A layered structure over a homogeneous half-space with source located in layer j at $z = z_s$. The source layer is divided into two sublayers: sublayer $j1$ of thickness $z_s - z_{j-1}$, and sublayer $j2$ of thickness $z_j - z_s$. Concentrated or distributed loads can be also applied on the top surface (e.g. a uniform vertical load with load density q within a given surface region).

axisymmetric, we solve it in terms of the cylindrical system of vector functions ($\mathbf{L}, \mathbf{M}, \mathbf{N}$) (Pan 1989a, 1989b), as also listed in appendix where definition of the basis functions ($\mathbf{L}, \mathbf{M}, \mathbf{N}$) and their properties are discussed. In other words, we expand displacement and traction vectors as

$$\begin{aligned} \mathbf{u}(r, \theta, z) &\equiv u_r \mathbf{e}_r + u_\theta \mathbf{e}_\theta + u_z \mathbf{e}_z \\ &= \sum_m \int_0^{+\infty} [U_L(z) \mathbf{L}(r, \theta) + U_M(z) \mathbf{M}(r, \theta) + U_N(z) \mathbf{N}(r, \theta)] \lambda d\lambda \\ \mathbf{t}(r, \theta, z) &\equiv \sigma_{rz} \mathbf{e}_r + \sigma_{\theta z} \mathbf{e}_\theta + \sigma_{zz} \mathbf{e}_z \\ &= \sum_m \int_0^{+\infty} [T_L(z) \mathbf{L}(r, \theta) + T_M(z) \mathbf{M}(r, \theta) + T_N(z) \mathbf{N}(r, \theta)] \lambda d\lambda \end{aligned} \quad (4.4)$$

and the perturbed potential and flux z -component as

$$\begin{aligned} \psi &= \sum_m \int_0^{+\infty} [\Psi(z) S(r, \theta)] \lambda d\lambda \\ q_z &= \sum_m \int_0^{+\infty} [Q(z) S(r, \theta)] \lambda d\lambda. \end{aligned} \quad (4.5)$$

The body force (including the equivalent body force of dislocations) can be also expanded as

$$\mathbf{f}(r, \theta, z) = \sum_m \int_0^{+\infty} [F_L(z) \mathbf{L}(r, \theta) + F_M(z) \mathbf{M}(r, \theta) + F_N(z) \mathbf{N}(r, \theta)] \lambda d\lambda. \quad (4.6)$$

The surface boundary conditions can be also expressed in terms of them: a scalar function is expanded in terms of S , and a vector function in terms of ($\mathbf{L}, \mathbf{M}, \mathbf{N}$) vector system.

Substituting these into the governing equations, one obtains a linear system of ordinary differential equations with respect to z for the expansion coefficients. Since in general the elastic coefficients c_{ij} and density ρ (and gravity g) are functions of the depth-coordinate z , this system of differential equations needs to be solved numerically, using, for instance, the Runge–Kutta method (i.e. Abramowitz and Stegun (1970)).

On the other hand, if c_{ij} and ρ (and g) depend weakly (or piece-wisely) on z , which is true for the problem under consideration, one can then approximate them as piece-wise functions of z . In other words, we arrive at a layered half-space where c_{ij} and ρ (and g) in each layer are uniform as illustrated in figure 4. For this case, it can be shown that the N -type solution (the coefficients of

vector function N) is purely elastic, independent of the gravity effect. The associated deformation is torsional and is governed by the following ordinary differential equations in the given layer (with material properties c_{44} , c_{66} , and ρ)

$$\begin{aligned} U'_N &= T_N/c_{44} \\ T'_N &= \lambda^2 c_{66} U_N - F_N - c_{\text{iner}} U_N \end{aligned} \quad (4.7)$$

where the prime denotes the derivative with respect to z . As for the **LM**-type problem in any given layer (the coefficients of vector functions L , M , and of scalar function S), we have, from the constitutive and flux-potential relations,

$$\begin{aligned} T_L &= -\lambda^2 c_{13} U_M + c_{33} U'_L \\ T_M &= c_{44} (U_L + U'_M) \\ Q &= \Psi' + 4\pi G \rho U_L. \end{aligned} \quad (4.8)$$

The other three equations can be derived from the governing equation (4.1), which results, in the given layer,

$$\begin{aligned} -\lambda^2 c_{11} U_M(z) + c_{13} U'_L(z) + T'_M(z) + \rho g U_L - \rho \Psi + F_M(z) + c_{\text{iner}} U_M(z) &= 0 \\ -\lambda^2 T_M(z) + T'_L(z) - \rho \Psi' + \lambda^2 \rho g U_M + F_L(z) + c_{\text{iner}} U_L(z) &= 0 \\ (\Psi'' - \lambda^2 \Psi) + 4\pi G \rho (U'_L - \lambda^2 U_M) &= 0 \end{aligned} \quad (4.9)$$

where the material properties (c_{ij} , ρ , and g) are those related to each layer. Again, since the N -type problem equation (4.7) is related to the distortional deformation which is independent of

making certain reasonable assumptions, including the Adams–Williamson condition similar to that used by Longman (1963) for the corresponding layered spherical earth structure. This remedy method was discussed in details in the textbook by Segall (2010), and the corresponding formulation has been also implemented into the program PSGRN/PSCMP for studying the deformation and gravity change due to dislocations in a layered viscoelastic-gravitational half-space (Wang *et al* 2006b).

To illustrate the solution existence issue, we follow Wang (2005a, 2005b) and Segall (2010) by assuming that the problem is static (or quasi static, with $c_{\text{iner}} = 0$) and that only the constant gravity g is coupled to the elastic deformation. In other words, equation (4.10) is reduced to the following 4×4 system

$$\frac{d}{dz} \begin{bmatrix} U_L \\ U_M \\ T_L \\ T_M \end{bmatrix} = \begin{bmatrix} 0 & \lambda^2 c_{13}/c_{33} & 1/c_{33} & 0 \\ -1 & 0 & 0 & 1/c_{44} \\ 0 & -\rho g \lambda^2 & 0 & \lambda^2 \\ -\rho g & c_{11} \lambda^2 - (c_{13} c_{13}/c_{33}) \lambda^2 & -c_{13}/c_{33} & 0 \end{bmatrix} \begin{bmatrix} U_L \\ U_M \\ T_L \\ T_M \end{bmatrix}. \quad (4.11)$$

The general solutions of equation (4.11) can be derived by assuming the following type of solutions

$$(U_L, U_M, T_L, T_M) = (a_1, a_2, a_3, a_4) e^{\lambda p z} \quad (4.12)$$

which results in the following four eigenvalues

$$p_{1,2}^2 = \frac{(c_{11} c_{33} - 2c_{13} c_{44} - c_{13}^2) \pm \sqrt{(c_{11} c_{33} - 2c_{13} c_{44} - c_{13}^2)^2 - 4c_{33} c_{44} [c_{44} c_{11} - (\rho g/\lambda)^2]}}{2c_{33} c_{44}}. \quad (4.13)$$

the gravity effect, its solution is the same as that in the purely elastic system (Pan 1989a, 1989b). On the other hand, the **LM**-type deformation is coupled to the gravity, which is governed by the following set of first-order differential equations in each layer

$$\frac{d}{dz} \begin{bmatrix} U_L \\ U_M \\ \Psi \\ T_L \\ T_M \\ Q \end{bmatrix} = \begin{bmatrix} 0 & \lambda^2 c_{13}/c_{33} & 0 & 1/c_{33} & 0 & 0 \\ -1 & 0 & 0 & 0 & 1/c_{44} & 0 \\ -4\pi G \rho & 0 & 0 & 0 & 0 & 1 \\ -4\pi G \rho^2 - c_{\text{iner}} & -\rho g \lambda^2 & 0 & 0 & \lambda^2 & \rho \\ -\rho g & c_{11} \lambda^2 - (c_{13} c_{13}/c_{33}) \lambda^2 - c_{\text{iner}} & \rho & -c_{13}/c_{33} & 0 & 0 \\ 0 & \lambda^2 4\pi G \rho & \lambda^2 & 0 & 0 & 0 \end{bmatrix} \begin{bmatrix} U_L \\ U_M \\ \Psi \\ T_L \\ T_M \\ Q \end{bmatrix} - \begin{bmatrix} 0 \\ 0 \\ F_L \\ F_M \\ 0 \end{bmatrix}. \quad (4.10)$$

Equation (4.10) contains six equations for six unknown expansion coefficients. The general solution in each layer can be expressed in terms of the eigenvalues and eigenvectors of the coefficient matrix on the right-hand side of equation (4.10). However, since the eigenvalues and eigenvectors are also functions of the transformation variable (also called wavenumber) λ , physically sounded solution may not exist for all λ from zero to positive infinity. For the elastic isotropic, gravitational and layered half-space, Rundle (1980) found that depending on the λ value, the eigenvalues could be real, imaginary, or just zero.

This problem was studied by Wang (2005a, 2005b, 2007) and Wang *et al* (2006b) again, who has also provided a solution by

It is observed that in order to avoid the purely imaginary eigenvalue (i.e. to have the problem solvable), the wavenumber λ has to satisfy the following condition:

$$\lambda > \lambda_g \equiv \rho g / \sqrt{c_{11} c_{44}} \quad (4.14a)$$

$$\lambda > \lambda_g \equiv \rho g / \sqrt{\mu_e (\lambda_e + 2\mu_e)}. \quad (4.14b)$$

The first relation is for the TI material and the second for the isotropic material with subscript ‘ e ’ for elasticity. Equation (4.14) indicates that there will be no solution in the transformed domain if the wavenumber λ is less than the critical wavenumber λ_g . This is due to the fact that, in the perturbed half-space, the constant gravity g exists in the entire horizontal domain $-\infty < x, y < +\infty$ so that the solution there does not decay to zero (Amadei and Pan 1992).

Besides the remedy method by Wang (2005a, 2005b), the effect of gravity can be also considered by the following two simple/approximate approaches: (1) solving the problem numerically by introducing the gravity-related initial stress status (Aagaard *et al* 2013, 2017, Domez *et al* 2017); (2) including the gravity g by modifying the surface/interface condition, i.e. approximating the gravity contribution by the so-called ‘buoyancy restoring force’ (see, i.e. Pan (1990) and Barbot and Fialko (2010a)). Since locally the deformation would still be dominated by the elastic or visco-elastic nature,

a GF solution to the corresponding deformation without gravity g in a layered visco-elastic half-space is fundamental, as briefly reviewed and presented below.

4.2. General solutions in elastic or viscoelastic layered half-spaces

This subsection provides 2D/3D GFs in elastic (viscoelastic) and layered half-planes (2D) and layered half-spaces (3D). Surface loading cases have been extensively studied in geomechanics as well as in geophysics. Under internal loading, we constrain our discussion to the concentrated forces and dislocations, with traction-free boundary conditions on the surface of the half-space (plane). Before we present the GF solutions, we first provide a brief review on the related literature since scientists from different fields have made contributions in different ways.

As soil and/or rock foundation (and also pavement) is in general made of layered materials, surface (point and circular) and internal (concentrated and finite-size) loadings in the layered half-plane and half-space have been always active topics by researchers in different fields. In geomechanics, for surface loading over layered rock foundation, one may refer to the works by Wang and coworkers (see the review papers by Liao and Wang 1998, Wang *et al* 2003a). For both surface and internal loadings, and further from a more mathematical point of view with their applications to BEMs, one may refer to the works by Yue and colleagues (review papers by Yue (2015) along with many references, including Yue (1995, 1996) and a recent monography by Xiao and Yue (2014)). We should also mention an early contribution made by Chan *et al* (1974) where the generalized Mindlin solution (i.e. the elastic solution due to an internal point force in an elastic layered half-space) was derived. In layered pavements, important contributions were made by many, including the classic series of papers by Burmister (1945). It should be further mentioned that the approaches for solving the problems by these authors are semi-analytical and thus are very efficient (Chen *et al* 2009, 2011). Two other papers contributing to the geomechanics are the ones by Small and Booker (1984, 1986) where they proposed the finite layer analyses to the elastic layered structure modeling. The finite layer method is inspired from the finite element method (FEM), but in the former, one only needs to discretize along the thickness direction of the layered material and then to form the flexibility (or stiffness) matrix. Theory of an elastic layered system was also presented by Bufler (1971). An early brief review with the point-force GF solutions in a layered half-space can also be found in Pan (1997).

In Earth science and under surface loadings, early contributions were made by Kuo (1969) and Singh (1986). An interesting analytical solution was presented by Nakiboglu and Lambeck (1982) for predicting the deformation near Lake Bonneville of the flatly layered earth due to the time-dependent vertical load where the viscoelastic layer property was considered. Surface loading over TI and layered half-spaces was also solved with numerical examples (Pan 1989a). A fast algorithm was further developed for fast calculation where

the surface loads can involve many different stations on the surface (Pan *et al* 2007, Bevis *et al* 2015). A software product was published for predicting the elastic and viscoelastic deformation of the half-space under surface loading (Grapenthin 2014).

For 2D dislocation or 2D fault (or a general concentrated 2D source) in layered planes, scientists in solid mechanics contributed to this topic by studying the line dislocations as the GF sources. Wu and Chid (1995) derived the line-dislocation solution in an anisotropic strip; Kelly *et al* (1995) solved the stress field due to a line dislocation in layered isotropic media; Ma and Lee (2009) presented a theoretical analysis for dislocations in an anisotropic and magnetoelectroelastic layered half-plane where the purely elastic solution is a special case of their solution. More recent contributions on line dislocation-induced fields in layered elastic media are by Kuo (2014), Khanna and Kotousov (2015) and Xia *et al* (2016). In geophysics where the source is 2D fault, we refer to the works by Freund and Barnett (1976), Rybicki (1971, 1986) and Savage (1980, 1998). Xu and Mal (1987) derived the in-plane GFs for a layered viscoelastic solid (2D).

For the corresponding 3D dislocations (or concentrated sources) within the purely elastic or viscoelastic layered half-space, GF solutions for the static or quasi-static deformations were derived mostly in geophysics (Singh 1970, Ben-Menahem and Gillon 1970, Jovanovich *et al* 1974a, 1974b, Pan 1989b, Roth 1990, Hisada 1994, 1995, Zhu and Rivera 2002). Notice that once we have the point-dislocation GFs, solutions to the corresponding finite-dislocation source can be found by the simple method of superposition (Sato 1971, Sato and Matsu'ura 1973, Matsu'ura and Sato 1975, Ma and Kuszniir 1992, 1994, He *et al* 2003, Fukahata and Matsu'ura 2005). Finite faulting in the layered elastic half-space has also important applications on hydraulic fracture analyses as reported by Peirce and coworkers (Peirce and Siebrits 2001a, 2001b, Siebrits and Peirce 2002, Peirce *et al* 2009). For calculating the static deformation in a layered elastic half-space caused by finite dislocation, Wang *et al* (2003b) further published a FORTRAN code. By applying the Laplace transform, the corresponding viscoelastic deformation by finite dislocations can be also solved (Rundle 1978, Matsu'ura *et al* 1981, Folch *et al* 2000, Fukahata and Matsu'ura 2006, Hashima *et al* 2014), using the normal mode expansion (NME) approach (see, Schapery (1962)) for inverse Laplace transform. Deformation by a finite fault in the elastic and layered half-space with gravity was solved by Rundle (1981), and the corresponding deformation by a finite fault in a viscoelastic-gravity layered half-space was reported by Rundle (1982) and Wang *et al* (2006b) where the latter also published their FORTRAN code with the inverse Laplace transform being carried out by the FFT method. Viscoelastic (Maxwell) deformation by a finite fault in 3D layered half-spaces was also solved semi-analytically by Smith and Sandwell (2004) via the 3D Fourier transform method. The inverse Laplace transform issue will be discussed further in the next section.

Next, we present the GF solutions in horizontally layered system made of elastic media, in terms of the cylindrical (for 3D) and Cartesian (for both 2D and 3D) systems of vector

functions. The corresponding viscoelastic deformation can be obtained by applying the correspondence principle first and then carrying out the inverse Laplace transform. The time-harmonic deformation for general anisotropic and layered media will be also presented.

For the quasistatic deformation (purely elastic or viscoelastic without the inertia term), the eigenvalues p_i depend only on the material properties of the layer, independent of the wavenumber λ . In terms of both Cartesian and cylindrical systems of vector functions, the point source (point force and point dislocation) solutions can be derived (Pan 1997 for point force, and Pan 1989b for point dislocation). It is noted that, under the assumption of TI, the solution matrix in each layer as well as the propagator matrix are exactly the same in terms of both systems of vector functions so that both 2D and 3D deformations can be treated uniformly. Furthermore, in terms of the cylindrical system of vector functions, the axisymmetric deformation (and the deformation associated with volumetric change) is related to the **LM**-type only and torsional deformation to the **N**-type only. In the time-harmonic case, the **LM**-type is associated with Rayleigh (P and SV) wave and the **N**-type the Love (SH) wave. In terms of the Cartesian system of vector functions, the **LM**-type is associated with the in-plane deformation/wave (Rayleigh), and the **N**-type with the anti-plane or out-of-plane deformation/wave (Love).

By letting $\rho g = 0$ in equation (4.11), we then have four eigenvalues for the purely elastic (or viscoelastic) case (depending on the layer material properties only, but independent of the wavenumber λ), and their corresponding eigenvectors (**LM**-type). As such, the general solution in each homogenous (TI) layer ($z_{j-1} < z < z_j$) can be expressed as, including also the **N**-type, (Pan 1989a, 1989b, Liu *et al* 2018):

$$\begin{bmatrix} \mathbf{U}(z) \\ \mathbf{T}(z) \end{bmatrix} = \begin{bmatrix} \mathbf{E}_{11} & \mathbf{E}_{12} \\ \mathbf{E}_{21} & \mathbf{E}_{22} \end{bmatrix} \begin{bmatrix} \langle e^{\lambda p_{12}^* z} \rangle & \mathbf{0} \\ \mathbf{0} & \langle e^{\lambda p_{34}^* (z-z_{j-1})} \rangle \end{bmatrix} \begin{bmatrix} \mathbf{c}_+ \\ \mathbf{c}_- \end{bmatrix} \quad (4.15a)$$

$$\langle e^{\lambda p_{12}^* z} \rangle = \begin{bmatrix} e^{\lambda p_1 z} & 0 \\ 0 & e^{\lambda p_2 z} \end{bmatrix}; \quad \langle e^{\lambda p_{34}^* z} \rangle = \begin{bmatrix} e^{\lambda p_3 z} & 0 \\ 0 & e^{\lambda p_4 z} \end{bmatrix}$$

with $\text{Re}(p_1) \geq \text{Re}(p_2) \geq \text{Re}(p_3) \geq \text{Re}(p_4)$

(4.15b)

$$\begin{bmatrix} U_N(z) \\ T_N(z)/\lambda \end{bmatrix} = \begin{bmatrix} E_{11}^N & E_{12}^N \\ E_{21}^N & E_{22}^N \end{bmatrix} \begin{bmatrix} e^{\lambda p_1^N (z-z_j)} & 0 \\ 0 & e^{\lambda p_2^N (z-z_{j-1})} \end{bmatrix} \begin{bmatrix} c_+^N \\ c_-^N \end{bmatrix}$$

$p_1^N = \sqrt{c_{66}/c_{44}}; \quad p_2^N = -\sqrt{c_{66}/c_{44}}$

(4.15c)

where $[\mathbf{E}_{ij}]$ are the submatrices of the eigenvectors of **LM**-type and E_{ij}^N are the elements of the eigenvectors of **N**-type. Also in equation (4.15a),

$$\mathbf{U} = [U_L, \lambda U_M]^t; \quad \mathbf{T} = [T_L/\lambda, T_M]^t. \quad (4.16)$$

By eliminating coefficients \mathbf{c}_+ , \mathbf{c}_- , c_+^N , and c_-^N in equations (4.15a) and (4.15c), one can find the following propagating relations for both **LM**- and **N**-types between the upper ($z = z_{j-1}$) and lower ($z = z_j$) interfaces of any layer j (which is assumed to be source free, Liu *et al* 2018)

$$\begin{bmatrix} \mathbf{U}(z_{j-1}) \\ \mathbf{T}(z_j) \end{bmatrix} = \begin{bmatrix} \mathbf{S}_{11}^j & \mathbf{S}_{12}^j \\ \mathbf{S}_{21}^j & \mathbf{S}_{22}^j \end{bmatrix} \begin{bmatrix} \mathbf{U}(z_j) \\ \mathbf{T}(z_{j-1}) \end{bmatrix}$$

$$\begin{bmatrix} U_N(z_{j-1}) \\ T_N(z_j)/\lambda \end{bmatrix} = \begin{bmatrix} N_{11}^j & N_{12}^j \\ N_{21}^j & N_{22}^j \end{bmatrix} \begin{bmatrix} U_N(z_j) \\ T_N(z_{j-1})/\lambda \end{bmatrix} \quad (4.17)$$

where the submatrices and matrix elements are

$$[\mathbf{S}^j] \equiv \begin{bmatrix} \mathbf{S}_{11}^j & \mathbf{S}_{12}^j \\ \mathbf{S}_{21}^j & \mathbf{S}_{22}^j \end{bmatrix} = \begin{bmatrix} \mathbf{E}_{11} \langle e^{-\lambda p_{12}^* h_j} \rangle & \mathbf{E}_{12} \\ \mathbf{E}_{21} & \mathbf{E}_{22} \langle e^{\lambda p_{34}^* h_j} \rangle \end{bmatrix}$$

$$\times \begin{bmatrix} \mathbf{E}_{11} & \mathbf{E}_{12} \langle e^{\lambda p_{34}^* h_j} \rangle \\ \mathbf{E}_{21} \langle e^{-\lambda p_{12}^* h_j} \rangle & \mathbf{E}_{22} \end{bmatrix}^{-1} \quad (4.18)$$

$$[\mathbf{N}^j] \equiv \begin{bmatrix} N_{11}^j & N_{12}^j \\ N_{21}^j & N_{22}^j \end{bmatrix} = \begin{bmatrix} E_{11}^N e^{-\lambda p_1^N h_j} & E_{12}^N \\ E_{21}^N & E_{22}^N e^{\lambda p_2^N h_j} \end{bmatrix}$$

$$\times \begin{bmatrix} E_{11}^N & E_{12}^N e^{\lambda p_2^N h_j} \\ E_{21}^N e^{-\lambda p_1^N h_j} & E_{22}^N \end{bmatrix}^{-1} \quad (4.19)$$

where $h_j = z_j - z_{j-1}$ is the thickness of layer j . Similar propagating relation as equation (4.17) can be written for its adjacent layer $j + 1$ (Liu *et al* 2018).

Assuming that the interface z_j between the two layers are well-bonded (i.e. the displacements and tractions are continuous at $z = z_j$), and propagating the layer relation (similar to equation (4.17)) from layer j to layer $j + 1$, the following recursive relation is achieved

$$\begin{bmatrix} \mathbf{U}(z_{j-1}) \\ \mathbf{T}(z_{j+1}) \end{bmatrix} = \begin{bmatrix} \mathbf{S}_{11}^{jj+1} & \mathbf{S}_{12}^{jj+1} \\ \mathbf{S}_{21}^{jj+1} & \mathbf{S}_{22}^{jj+1} \end{bmatrix} \begin{bmatrix} \mathbf{U}(z_{j+1}) \\ \mathbf{T}(z_{j-1}) \end{bmatrix}$$

$$\begin{bmatrix} U_N(z_{j-1}) \\ T_N(z_{j+1})/\lambda \end{bmatrix} = \begin{bmatrix} N_{11}^{jj+1} & N_{12}^{jj+1} \\ N_{21}^{jj+1} & N_{22}^{jj+1} \end{bmatrix} \begin{bmatrix} U_N(z_{j+1}) \\ T_N(z_{j-1})/\lambda \end{bmatrix} \quad (4.20)$$

where the involved submatrices and elements are defined as

$$\mathbf{S}_{11}^{jj+1} = \mathbf{S}_{11}^j \mathbf{S}_{11}^{j+1} + \mathbf{S}_{11}^j \mathbf{S}_{12}^{j+1} [\mathbf{I} - \mathbf{S}_{21}^j \mathbf{S}_{12}^{j+1}]^{-1} \mathbf{S}_{21}^j \mathbf{S}_{11}^{j+1}$$

$$\mathbf{S}_{12}^{jj+1} = \mathbf{S}_{11}^j \mathbf{S}_{12}^{j+1} [\mathbf{I} - \mathbf{S}_{21}^j \mathbf{S}_{12}^{j+1}]^{-1} \mathbf{S}_{22}^j + \mathbf{S}_{12}^j$$

$$\mathbf{S}_{21}^{jj+1} = \mathbf{S}_{21}^{j+1} + \mathbf{S}_{22}^{j+1} [\mathbf{I} - \mathbf{S}_{21}^j \mathbf{S}_{12}^{j+1}]^{-1} \mathbf{S}_{21}^j \mathbf{S}_{11}^{j+1}$$

$$\mathbf{S}_{22}^{jj+1} = \mathbf{S}_{22}^{j+1} [\mathbf{I} - \mathbf{S}_{21}^j \mathbf{S}_{12}^{j+1}]^{-1} \mathbf{S}_{22}^j \quad (4.21a)$$

$$N_{11}^{jj+1} = N_{11}^j N_{11}^{j+1} + N_{11}^j N_{12}^{j+1} [1 - N_{21}^j N_{12}^{j+1}]^{-1} N_{21}^j N_{11}^{j+1}$$

$$N_{12}^{jj+1} = N_{12}^j + N_{11}^j N_{12}^{j+1} [1 - N_{21}^j N_{12}^{j+1}]^{-1} N_{22}^j$$

$$N_{21}^{jj+1} = N_{21}^{j+1} + N_{22}^{j+1} [1 - N_{21}^j N_{12}^{j+1}]^{-1} N_{21}^j N_{11}^{j+1}$$

$$N_{22}^{jj+1} = N_{22}^{j+1} [1 - N_{21}^j N_{12}^{j+1}]^{-1} N_{22}^j \quad (4.21b)$$

where $[\mathbf{I}]$ is a 2×2 identify matrix. This new recursive relation (4.21) can be propagated in the layered half-space involving multiple layers, as long as the interfaces are perfect, or well-bonded. As an example, we choose the **LM**-type to derive the transformed coefficients. We assume that the surface is traction-free and that at $z = z_s$ in layer j there is a given concentrated source (figure 4). We now propagate equation (4.20) from the surface $z = z_0$ to the upper side of the source z_{s-} ;

then from the lower side of the source z_{s+} to the last interface $z = z_n$ of the layered half-space. This gives us

$$\begin{aligned} \begin{bmatrix} \mathbf{U}(z_0) \\ \mathbf{T}(z_{s-}) \end{bmatrix} &= \begin{bmatrix} \mathbf{S}_{11}^{1:j1} & \mathbf{S}_{12}^{1:j1} \\ \mathbf{S}_{21}^{1:j1} & \mathbf{S}_{22}^{1:j1} \end{bmatrix} \begin{bmatrix} \mathbf{U}(z_{s-}) \\ \mathbf{T}(z_0) \end{bmatrix} \\ \begin{bmatrix} \mathbf{U}(z_{s+}) \\ \mathbf{T}(z_n) \end{bmatrix} &= \begin{bmatrix} \mathbf{S}_{11}^{j2:n} & \mathbf{S}_{12}^{j2:n} \\ \mathbf{S}_{21}^{j2:n} & \mathbf{S}_{22}^{j2:n} \end{bmatrix} \begin{bmatrix} \mathbf{U}(z_n) \\ \mathbf{T}(z_{s+}) \end{bmatrix}. \end{aligned} \quad (4.22)$$

Making use of the boundary conditions on the surface, the discontinuity conditions at the source level, and the conditions in the last homogeneous half-space, we can eventually solve analytically the expansion coefficients on the surface. After that, similar relations as equation (4.22) can be used to find the solutions at any z -level. It is noted that the new propagator matrix—the DVP method as introduced in equation (4.20)—is very stable at large/small λ and thin/thick layer, as has been demonstrated by many researchers (Zhong *et al* 2004, Cai and Pan 2018, Liu *et al* 2018).

As an example, we assume that the concentrated dislocation source is 3D with component $n_x v_y$ (or $v_x n_y$, noticing that the dislocation direction v_j and fault normal direction n_j are undistinguishable). Then, the displacements at any depth z can be expressed as (with the expansion coefficients U_L , U_M and U_N being solved from equation (4.22) using the DVP method)

$$\begin{aligned} u_r(r, \theta, z) &= -\sin(2\theta) \int_0^{+\infty} \left[\frac{U_M(z)}{i} \frac{\partial J_2(\lambda r)}{\partial r} + \frac{2U_N(z)J_2(\lambda r)}{r} \right] \lambda d\lambda \\ u_\theta(r, \theta, z) &= -\cos(2\theta) \int_0^{+\infty} \left[\frac{2U_M(z)J_2(\lambda r)}{ir} + \frac{U_N(z)\partial J_2(\lambda r)}{\partial r} \right] \lambda d\lambda \\ u_z(r, \theta, z) &= -\sin(2\theta) \int_0^{+\infty} \left[\frac{U_L(z)J_2(\lambda r)}{i} \right] \lambda d\lambda. \end{aligned} \quad (4.23)$$

Similar expressions can be derived for all the strains and stresses at the given z -level, with the final expression involving only simple line integration as in equation (4.23). The numerical integration involved can be carried out using the accurate Bessel function integral program (e.g. Lucas 1995, Ratnanather *et al* 2014) to find the physical-domain solutions (e.g. Pan 1997) and Pan and Han (2004)). These provides the displacements and strains/stresses at that depth of the given layered half-space due to the given dislocation sources (for both 2D line and 3D point faults). Therefore, the only left task is to derive the source functions corresponding to the concentrated force and dislocation, which are presented below.

4.3. Source functions of concentrated forces and dislocations

In terms of the Cartesian or cylindrical system of vector functions, the source functions U_s , T_s , U_{Ns} , and T_{Ns} (with subscript s for the source) are defined as the discontinuities at the source level $z = z_s$

$$\begin{aligned} U_{Ls} &= U_L(z_s + 0) - U_L(z_s - 0) \\ U_{Ms} &= U_M(z_s + 0) - U_M(z_s - 0) \\ U_{Ns} &= U_N(z_s + 0) - U_N(z_s - 0) \\ T_{Ls} &= T_L(z_s + 0) - T_L(z_s - 0) \\ T_{Ms} &= T_M(z_s + 0) - T_M(z_s - 0) \\ T_{Ns} &= T_N(z_s + 0) - T_N(z_s - 0). \end{aligned} \quad (4.24)$$

Notice that for the elastic-gravitational deformation, there is no discontinuity on the gravitational coefficients Ψ and Q if the source is the concentrated force or dislocation.

For a point force vector \mathbf{f} of unit amplitude applied at $(x, y, z) = (r, \theta, z) = (0, 0, z_s)$ with directional components n_j , we have (in terms of both Cartesian and cylindrical coordinate systems, respectively)

$$f_j(x, y, z) = \delta(x)\delta(y)\delta(z - z_s)n_j \quad (4.25a)$$

$$f_j(r, \theta, z) = \frac{\delta(r)\delta(\theta)\delta(z - z_s)}{r}n_j. \quad (4.25b)$$

Expanding (4.25a) and (4.25b) in terms of the Cartesian and cylindrical systems of vector functions, respectively, we find the corresponding expansion coefficients (Pan 1997). For the point force in terms of Cartesian vector system, we have

$$\begin{aligned} F_L(z) &= \delta(z - z_s)n_z/(2\pi) \\ F_M(z) &= -\delta(z - z_s)i(\alpha n_x + \beta n_y)/(2\pi\lambda^2) \\ F_N(z) &= -\delta(z - z_s)i(\beta n_x - \alpha n_y)/(2\pi\lambda^2) \end{aligned} \quad (4.26)$$

and in terms of the cylindrical system, we have

$$\begin{aligned} F_L(z) &= \delta(z - z_s)n_z/\sqrt{2\pi} \quad (m = 0) \\ F_M(z) &= -\delta(z - z_s)(\mp n_x + in_y)/(2\lambda\sqrt{2\pi}) \quad (m = \pm 1) \\ F_N(z) &= -\delta(z - z_s)(in_x \pm n_y)/(2\lambda\sqrt{2\pi}) \quad (m = \pm 1). \end{aligned} \quad (4.27)$$

This concentrated force causes the following nonzero discontinuities or the source functions as

$$\begin{aligned} T_{Ls} &= -n_z/(2\pi) \\ T_{Ms} &= i(\alpha n_x + \beta n_y)/(2\pi\lambda^2) \\ T_{Ns} &= i(\beta n_x - \alpha n_y)/(2\pi\lambda^2) \end{aligned} \quad (4.28)$$

in terms of the Cartesian vector system, and

$$\begin{aligned} T_{Ls} &= -n_z/\sqrt{2\pi} \quad (m = 0) \\ T_{Ms} &= (\mp n_x + in_y)/(2\lambda\sqrt{2\pi}) \quad (m = \pm 1) \\ T_{Ns} &= (in_x \pm n_y)/(2\lambda\sqrt{2\pi}) \quad (m = \pm 1) \end{aligned} \quad (4.29)$$

in terms of the cylindrical vector system.

Remark 4.1. For the axisymmetric deformation (i.e. the force component is in z -direction only), we have $m = 0$ in terms of the cylindrical system of vector functions. For 2D line forces in the (x, z) -plane, we have only 1D-type Fourier transform in the Cartesian system of vector functions (Pan 1989a, 1989b). As such, in order to reduce it to the 2D plane-strain (and anti-plane) deformation, we only need to replace 2π by $\sqrt{2\pi}$ and β by 0 (thus, $\lambda = |\alpha|$) in the expression of the 3D source functions, which gives the source functions corresponding to the 2D line forces.

For a point dislocation of magnitude Δu (i.e. $\Delta u_j = \Delta u v_j$, with v_j being the cosine of the dislocation magnitude, or the Burgers vector direction) located over a small element dA centered at $(x, y, z) = (0, 0, z_s)$ with its normal direction n_i , we have the equivalent body force (equation (2.31), or Aki and Richards 1980) in the Cartesian coordinate system as

$$f_i(\mathbf{x}) = -\Delta u dA c_{ijlp} n_j v_l \frac{\partial}{\partial x_p} [\delta(x)\delta(y)\delta(z - z_s)]. \quad (4.30)$$

If the source is described by $(r, \theta, z) = (0, 0, z_s)$, we have the equivalent body-force in the cylindrical coordinate system as

$$f_i(\mathbf{x}) = -\Delta u d A c_{ijp} n_j \nu_i \frac{\partial}{\partial \eta_p} \left[\frac{\delta(r) \delta(\theta) \delta(z - z_s)}{r} \right] \quad (4.31)$$

where $\partial \eta_1 = \partial r$, $\partial \eta_2 = r \partial \theta$, $\partial \eta_3 = \partial z$.

Expanding the equivalent body-force in terms of the Cartesian and cylindrical systems of vector functions, we find that the expansion coefficients of the equivalent body-force can be expressed as Pan (1989b)

$$\begin{aligned} F_L(z) &= F_L^\delta \delta(z - z_s) + F_L^d \delta'(z - z_s) \\ F_M(z) &= F_M^\delta \delta(z - z_s) + F_M^d \delta'(z - z_s) \\ F_N(z) &= F_N^\delta \delta(z - z_s) + F_N^d \delta'(z - z_s) \end{aligned} \quad (4.32)$$

where a prime indicates the derivative with respect to z . The quantities with superscripts δ and d are the proportional expansion coefficients, which can be derived easily. Thus, for the TI material and in terms of the reduced Voigt elastic constants (with isotropy being the special case), the source functions at the source point $z = z_s$ can be found in terms of both systems of vector functions (Takeuchi and Saito 1972, Kennett 1983, Pan 1989b). These important source functions are listed below.

For a point dislocation at $z = z_s$, the source functions in terms of the Cartesian system of vector functions are (omitting factor $\Delta u d A / (2\pi)$)

$$\begin{aligned} U_{Ls} &= (n_x \nu_x + n_y \nu_y) c_{13} / c_{33} + n_z \nu_z \\ U_{Ms} &= i[\alpha(n_x \nu_z + n_z \nu_x) + \beta(n_y \nu_z + n_z \nu_y)] / \lambda^2 \\ T_{Ms} &= -(n_x \nu_x + n_y \nu_y) c_{13}^2 / c_{33} \\ &\quad + [n_x \nu_x (\alpha^2 c_{11} + \beta^2 c_{12}) + n_y \nu_y (\alpha^2 c_{12} + \beta^2 c_{11}) \\ &\quad + 2(n_x \nu_y + n_y \nu_x) \alpha \beta c_{66}] / \lambda^2 \end{aligned} \quad (4.33a)$$

$$\begin{aligned} U_{Ns} &= i[\beta(n_x \nu_z + n_z \nu_x) - \alpha(n_y \nu_z + n_z \nu_y)] / \lambda^2 \\ T_{Ns} &= [(n_x \nu_y + n_y \nu_x) (\beta^2 - \alpha^2) + 2(n_x \nu_x - n_y \nu_y) \alpha \beta] c_{66} / \lambda^2 \end{aligned} \quad (4.33b)$$

where $(n_j \nu_i)$ represents the dislocation source pairs.

Special case: In 2D (x, z) -plane, we have only 1D-type Fourier transform in the Cartesian system of vector functions. In order to reduce the source functions to 2D plane-strain (anti-plane) deformation, we only need to replace 2π by $\sqrt{2\pi}$ and β by 0 (thus, $\lambda = |\alpha|$) in the expression of the 3D source functions (Pan 1989b).

For a point dislocation at $z = z_s$, the source functions in terms of the cylindrical system of vector functions (omitting factor $\Delta u d A / \sqrt{(2\pi)}$) are

$$\begin{aligned} U_{Ls} &= (n_x \nu_x + n_y \nu_y) c_{13} / c_{33} + n_z \nu_z & (m = 0) \\ U_{Ms} &= [\pm(n_x \nu_z + n_z \nu_x) - i(n_y \nu_z + n_z \nu_y)] / (2\lambda) & (m = \pm 1) \\ T_{Ms} &= [(c_{11} + c_{12}) / 2 - c_{13}^2 / c_{33}] (n_x \nu_x + n_y \nu_y) & (m = 0) \\ &= [(n_y \nu_y - n_x \nu_x) \pm i(n_x \nu_y + n_y \nu_x)] c_{66} / 2 & (m = \pm 2). \end{aligned} \quad (4.34a)$$

$$\begin{aligned} U_{Ns} &= [-i(n_x \nu_z + n_z \nu_x) \mp (n_y \nu_z + n_z \nu_y)] / (2\lambda) & (m = \pm 1) \\ T_{Ns} &= [(n_x \nu_y + n_y \nu_x) \pm (n_x \nu_x - n_y \nu_y)] c_{66} / 2 & (m = \pm 2). \end{aligned} \quad (4.34b)$$

Special case: For an axisymmetric dislocation source, we have only the terms related to $m = 0$. This dislocation source

is physically an expansion source where we have only the opening displacement discontinuity along the normal direction of the dislocation plane. The reduced source functions are

$$\begin{aligned} U_{Ls} &= (n_x \nu_x + n_y \nu_y) c_{13} / c_{33} + n_z \nu_z & (m = 0) \\ T_{Ms} &= [(c_{11} + c_{12}) / 2 - c_{13}^2 / c_{33}] (n_x \nu_x + n_y \nu_y) & (m = 0). \end{aligned} \quad (4.35)$$

Remark 4.2. For general material anisotropy, the source functions can be expanded and solved in terms of 2D Fourier transforms, as presented below for the time-harmonic deformation. Actually, under the assumption of elastostatic deformation, the dislocation-induced fields in general anisotropic and layered solids were also investigated by researchers from solid mechanics of point of view (Ghoniem and Han 2005, Gao and Larson 2015, Vattré and Pan 2019, Yuan *et al* 2019). These works, particularly the most recent ones (Vattré and Pan 2019, Yuan *et al* 2019), could be utilized for direct geophysics applications.

Remark 4.3. Besides the concentrated forces and dislocations, source functions of other concentrated sources, such as the moments and force couples, can also be derived and analyzed (Takeuchi and Saito 1972, Kennett 1983).

Remark 4.4. It should be further noted that if the normal direction of dislocation element is along the depth direction, one does not need to find the equivalent body-force; the discontinuity of the displacements on the given z -level can be directly applied to derive the solutions (see, e.g. Chu *et al* (2013) and Zhao *et al* (2013, 2014)). This further indicates that for this special orientation of the dislocation plane, the source functions related to the traction vectors are zero!

Remark 4.5. For the viscoelastic deformation, the expansion coefficients are in the Laplace domain s . Thus in the source function expressions, the elastic coefficients c_{ij} become the functions of the Laplace variable s . Furthermore, depending on whether the force/dislocation source is impulsive (proportional to the delta function $\delta(t)$) or constant after $t > 0$ (proportional to the Heaviside function $H(t)$), the source functions may need to be modified slightly by a factor.

Remark 4.6. For the time-harmonic case, the source functions for concentrated force and dislocation are the same as those provided above, except that these source functions are now proportional to the time-harmonic factor $e^{-i\omega t}$. Notice that for this case, the general solutions in the given layer and the propagating relations among different layers are different since the eigenvalues and eigenvectors are also functions of the given frequency. This is discussed in the next subsection.

4.4. Time-harmonic GFs in anisotropic and layered elastic half-spaces

Wave propagation in horizontally layered half-spaces or layered plates (elastic without gravity) has been studied extensively in different engineering and science fields.

So many papers and books have been published, and as such, a detailed review would be difficult if not impossible. Nevertheless, some beneficial review papers and books are listed here for possible future reference (e.g. review or thesis by Ursin (1983), Braga (1990), Chimenti (1997), Cormier (2007), books by Ewing *et al* (1957), Brekhovskikh (1980), Kennett (1983), van der Hijden (1987), Chew (1990), Nayfeh (1995), Liu and Xi (2001), Chapman (2004) and Jensen *et al* (2011)). Notice further that although some were on horizontally layered structures, the approaches used could be useful to study wave propagation in the corresponding layered sphere to be discussed in the next section.

As previously stated, if the problem is axisymmetric (associated with isotropic or TI materials), the Hankel transform or cylindrical system of vector functions is commonly used to analyze the time-harmonic deformation in a horizontally layered half-space; otherwise, the Fourier transform or Cartesian system of vector functions needs to be applied. To connect the transformed coefficients from one layer to the other, the Thomson–Haskell propagator matrix method (Thomson 1950, Haskell 1953) can be applied (Zhu and Rivera 2002). Theoretical and numerical seismogram syntheses in elastic and layered half-spaces were investigated by many (Dunkin 1965, Harkrider 1970, Bouchon 1993, 2003, Chen 1993, 1999, Chen *et al* 1996, Chen and Zhang 2001, Chen and Chen 2002, Wu and Chen 2016, Fryer and Frazer 1984, 1987, Chapman 1978, 2003). A numerically stable algorithm for any frequency was proposed by O’Toole and Woodhouse (2011) where a brief review on various algorithms in handling both lower and higher frequencies was given. O’Toole and Woodhouse (2011)’s approach was based on the minor matrix method by Gilbert and Backus (1966). Notice again that many approaches developed for the horizontally layered system can be equally applied to the corresponding layered spherical system.

Besides the works by geophysicists, time-harmonic GFs in layered half-spaces have been also derived by engineers. These include time-harmonic point-force GFs (Kausel and Peek 1982, Apsel and Luco 1983, Luco and Apsel 1983, Guzina and Pak 2001, Pak and Guzina 2002, Khojasteh *et al* 2011), solutions to the periodic surface loading on layered composites (Mal 1988), and time-harmonic point-dislocation GFs (Kundu and Mal 1985).

Below we briefly present the time-harmonic solutions due to a given concentrated source within a generally anisotropic and layered elastic half-space. The solutions are based on the mathematically elegant and computationally powerful Stroh formalism (Ting 1996) along with the stable DVP method. We define the following 2D Fourier transform pairs, corresponding to the horizontal space variables x_α , as (which is already in the frequency domain)

$$\tilde{f}(z, k_\alpha) = \int_{-\infty}^{\infty} \int_{-\infty}^{\infty} f(z, x_\alpha) e^{-ik_\alpha x_\alpha} dx_1 dx_2 \quad (4.36a)$$

$$f(z, x_\alpha) = \frac{1}{(2\pi)^2} \int_{-\infty}^{\infty} \int_{-\infty}^{\infty} \tilde{f}(z, k_\alpha) e^{ik_\alpha x_\alpha} dk_1 dk_2 \quad (4.36b)$$

where the repeated Greek index α takes the summation from 1 to 2.

Applying the Fourier transform (4.36a) to (2.6), we have, in the transformed domain (k_α , also in the frequency ω -domain)

$$-k^2 Q_{jl} \tilde{u}_l + ik(R_{jl}^t + R_{jl}) \tilde{u}_{l,3} + T_{jl} \tilde{u}_{l,33} + \tilde{f}_j + \rho\omega^2 \tilde{u}_j = 0 \quad (4.37)$$

where the superscript t denotes transpose of a vector or matrix, and the matrices $[Q]$, $[R]$, and $[T]$ are defined as

$$Q_{ik} = c_{jiks} m_j m_s, R_{ik} = c_{jiks} m_j n_s, T_{ik} = c_{jiks} n_j n_s \quad (4.38)$$

with

$$\begin{bmatrix} k_1 \\ k_2 \\ 0 \end{bmatrix} = k\mathbf{m} \equiv \sqrt{k_1^2 + k_2^2} \mathbf{m};$$

$$\mathbf{m} = \begin{bmatrix} m_1 \\ m_2 \\ 0 \end{bmatrix} = \begin{bmatrix} \cos \theta \\ \sin \theta \\ 0 \end{bmatrix} \equiv \begin{bmatrix} k_1/k \\ k_2/k \\ 0 \end{bmatrix}; \quad \mathbf{n} = \begin{bmatrix} 0 \\ 0 \\ 1 \end{bmatrix}. \quad (4.39)$$

We also define the traction vector \mathbf{t} (with components t_j) with unit normal n_i ($=0, 0, 1$) for the horizontally layered case), which has nothing to do with the unit vector \mathbf{n} defined in equation (4.39), and the in-plane stress vector \mathbf{s} as

$$\begin{aligned} t_j &= \sigma_{ij} n_i = \sigma_{3j} = c_{3jml} u_{m,l} \\ \mathbf{s} &\equiv (\sigma_{xx}, \sigma_{xy}, \sigma_{yy})^t \\ &= (c_{11ml} u_{m,l}, c_{12ml} u_{m,l}, c_{22ml} u_{m,l})^t \end{aligned} \quad (4.40)$$

In the 2D Fourier-transformed domain, we have the traction and in-plane stresses expressed in terms of the transformed elastic displacements as

$$\begin{aligned} \tilde{\mathbf{t}} &= (c_{31ml} \tilde{u}_{m,l}, c_{32ml} \tilde{u}_{m,l}, c_{33ml} \tilde{u}_{m,l})^t \\ \tilde{\mathbf{s}} &\equiv (\tilde{\sigma}_{xx}, \tilde{\sigma}_{xy}, \tilde{\sigma}_{yy})^t \\ &= (c_{11ml} \tilde{u}_{m,l}, c_{12ml} \tilde{u}_{m,l}, c_{22ml} \tilde{u}_{m,l})^t. \end{aligned} \quad (4.41)$$

We therefore have, in vector/matrix form (with $\tilde{\mathbf{u}} = [\tilde{u}_1 \ \tilde{u}_2 \ \tilde{u}_3]^t$)

$$\begin{aligned} \tilde{\mathbf{t}} &= ik[\mathbf{R}]^t \tilde{\mathbf{u}} + [\mathbf{T}] \tilde{\mathbf{u}}_{,3} \\ \tilde{\mathbf{s}} &= ik[\mathbf{M}_{dc}] \tilde{\mathbf{u}} + [\mathbf{M}_{rc}] \tilde{\mathbf{u}}_{,3} \end{aligned} \quad (4.42)$$

where

$$[\mathbf{M}_{dc}] = \begin{bmatrix} c_{11}m_1 + c_{16}m_2 & c_{16}m_1 + c_{12}m_2 & c_{15}m_1 + c_{14}m_2 \\ c_{61}m_1 + c_{66}m_2 & c_{66}m_1 + c_{62}m_2 & c_{65}m_1 + c_{64}m_2 \\ c_{21}m_1 + c_{26}m_2 & c_{26}m_1 + c_{22}m_2 & c_{25}m_1 + c_{24}m_2 \end{bmatrix} \quad (4.43a)$$

$$[\mathbf{M}_{rc}] = \begin{bmatrix} c_{15} & c_{14} & c_{13} \\ c_{65} & c_{64} & c_{63} \\ c_{25} & c_{24} & c_{23} \end{bmatrix}. \quad (4.43b)$$

Combining equation (4.40) with (4.37), we finally arrive at the following set of first-order ordinary differential equations

$$\frac{d}{dz} \begin{bmatrix} \tilde{\mathbf{u}} \\ \tilde{\mathbf{t}} \end{bmatrix} = \begin{bmatrix} -ik\mathbf{T}^{-1}\mathbf{R}^t & \mathbf{T}^{-1} \\ \mathbf{Q}k^2 - \rho\omega^2\mathbf{I} - k^2\mathbf{R}\mathbf{T}^{-1}\mathbf{R}^t & -ik\mathbf{R}\mathbf{T}^{-1} \end{bmatrix} \begin{bmatrix} \tilde{\mathbf{u}} \\ \tilde{\mathbf{t}} \end{bmatrix} + \begin{bmatrix} \mathbf{0} \\ -\tilde{\mathbf{f}} \end{bmatrix}. \quad (4.44)$$

In any homogeneous and anisotropic elastic layer free of the source, we assume that the solution of the homogeneous equation (4.44) as

$$\tilde{\mathbf{u}} = \mathbf{a}e^{ikpz}, \tilde{\mathbf{t}} = ik\mathbf{b}e^{ikpz} \quad (4.45)$$

where the eigenvalue p and eigenvectors \mathbf{a} and \mathbf{b} are the eigen-solutions of the following eigensystem of equations

$$\begin{bmatrix} -\mathbf{T}^{-1}\mathbf{R}^t & \mathbf{T}^{-1} \\ \mathbf{R}\mathbf{T}^{-1}\mathbf{R}^t - \mathbf{Q} + (\rho\omega^2/k^2)\mathbf{I} & -\mathbf{R}\mathbf{T}^{-1} \end{bmatrix} \begin{bmatrix} \mathbf{a} \\ \mathbf{b} \end{bmatrix} = p \begin{bmatrix} \mathbf{a} \\ \mathbf{b} \end{bmatrix}. \quad (4.46)$$

There are six eigenvalues and their corresponding eigenvectors from equation (4.46), and therefore, we can express the general solution as, in layer j bounded by z_j and z_{j-1} ($z_{j-1} \leq z \leq z_j$, with thickness $h_j = z_j - z_{j-1}$) ($z \equiv x_3$)

$$\begin{bmatrix} ik\tilde{\mathbf{u}} \\ \tilde{\mathbf{t}} \end{bmatrix} = \begin{bmatrix} \mathbf{A}_1 & \mathbf{A}_2 \\ \mathbf{B}_1 & \mathbf{B}_2 \end{bmatrix} \begin{bmatrix} \langle e^{ikp_1(z-z_j)} \rangle & \mathbf{0} \\ \mathbf{0} & \langle e^{ikp_2(z-z_{j-1})} \rangle \end{bmatrix} \begin{bmatrix} \mathbf{c}_1 \\ \mathbf{c}_2 \end{bmatrix} \quad (4.47)$$

where $[\mathbf{c}_1, \mathbf{c}_2]^t$ are coefficient vectors to be determined, and

$$\begin{aligned} \mathbf{A}_1 &= [\mathbf{a}_1, \mathbf{a}_2, \mathbf{a}_3], \quad \mathbf{A}_2 = [\mathbf{a}_4, \mathbf{a}_5, \mathbf{a}_6] \\ \mathbf{B}_1 &= [\mathbf{b}_1, \mathbf{b}_2, \mathbf{b}_3], \quad \mathbf{B}_2 = [\mathbf{b}_4, \mathbf{b}_5, \mathbf{b}_6] \\ \langle e^{ikp_1 z} \rangle &= \text{diag}[e^{ikp_1 z}, e^{ikp_2 z}, e^{ikp_3 z}] \\ \langle e^{ikp_2 z} \rangle &= \text{diag}[e^{ikp_4 z}, e^{ikp_5 z}, e^{ikp_6 z}] \end{aligned} \quad (4.48)$$

with \mathbf{a}_i and \mathbf{b}_i being the eigenvectors corresponding to the eigenvalue p_i . Notice that the eigenvalues are ordered as such that $\text{Im}(p_1) \leq \text{Im}(p_2) \leq \dots \leq \text{Im}(p_5) \leq \text{Im}(p_6)$. Actually, the first three have a negative imaginary part and the last three have a positive imaginary part.

Similar to the static case discussed above, based on the general solution in each layer, we can derive the layer matrix and then the recursive relation between the adjacent layers. If there is a concentrated time-harmonic source (force or dislocation type) within a given layer, we then need to subdivide it into two sublayers and propagate the solutions by making use of the jump conditions (or the source functions) at the source level. These source functions can be easily derived as below.

We first define, similar to equation (4.24), the following source functions for the time-harmonic wave problem as

$$\begin{aligned} ik\tilde{\mathbf{u}}_s &= ik\tilde{\mathbf{u}}(z_s + 0) - ik\tilde{\mathbf{u}}(z_s - 0) \\ \tilde{\mathbf{t}}_s &= \tilde{\mathbf{t}}(z_s + 0) - \tilde{\mathbf{t}}(z_s - 0). \end{aligned} \quad (4.49)$$

We assume that the general time-harmonic concentrated force as (proportional to $e^{-i\omega t}$)

$$f_j(z, x_\alpha) = \delta(x_1)\delta(x_2)\delta(z - z_s)f_j(\omega) \equiv \delta(x)\delta(y)\delta(z - z_s)f_j(\omega). \quad (4.50)$$

After applying the 2D space Fourier transforms, we have

$$\tilde{f}_j(z, k_\alpha) = \delta(z - z_s)f_j(\omega). \quad (4.51)$$

The source functions at $z = z_s$ corresponding to the concentrated time-harmonic force are therefore

$$\begin{aligned} ik\tilde{\mathbf{u}}_s &= \mathbf{0} \\ \tilde{\mathbf{t}}_s &= \mathbf{f}(\omega). \end{aligned} \quad (4.52)$$

For a concentrated dislocation source, its equivalent body force in time-harmonic deformation can be expressed as

$$\begin{aligned} f_l(z, x_\alpha; \omega) &= -\Delta u(\omega) dAc_{ijlp} n_j \nu_i \frac{\partial}{\partial x_p} [\delta(x)\delta(y)\delta(z - z_s)] \\ &= -\Delta u(\omega) dAc_{ijl1} n_j \nu_i \frac{d}{dx} [\delta(x)] \delta(y) \delta(z - z_s) \\ &\quad - \Delta u(\omega) dAc_{ijl2} n_j \nu_i \frac{d}{dy} [\delta(y)] \delta(x) \delta(z - z_s) \\ &\quad - \Delta u(\omega) dAc_{ijl3} n_j \nu_i \delta(x) \delta(y) \frac{d}{dz} [\delta(z - z_s)]. \end{aligned} \quad (4.53)$$

Applying the 2D Fourier transforms over x_α , we have

$$\begin{aligned} -\tilde{f}_l(z, k_\alpha; \omega) &= \Delta u(\omega) dAc_{mj\alpha} ik_\alpha n_j \nu_m \delta(z - z_s) \\ &\quad + \Delta u(\omega) dAc_{mj\beta} n_j \nu_m \frac{d}{dz} [\delta(z - z_s)]. \end{aligned} \quad (4.54)$$

Substituting the inhomogeneous term (4.54) to the first-order differential equation system (4.44), the corresponding discontinuities can be found (i.e. Kennett (1983)). The total discontinuity can be expressed as

$$\begin{bmatrix} \tilde{\mathbf{u}} \\ \tilde{\mathbf{t}} \end{bmatrix}_{z_s+} - \begin{bmatrix} \tilde{\mathbf{u}} \\ \tilde{\mathbf{t}} \end{bmatrix}_{z_s-} = \begin{bmatrix} \mathbf{0} \\ \mathbf{f}^\delta \end{bmatrix} + \begin{bmatrix} \mathbf{T}^{-1} \mathbf{f}^d \\ -i\mathbf{k}\mathbf{R}\mathbf{T}^{-1} \mathbf{f}^d \end{bmatrix} \quad (4.55)$$

where

$$\begin{aligned} \mathbf{f}^\delta &\equiv [f_l^\delta] \equiv \Delta u(\omega) dAc_{mj\alpha} ik_\alpha n_j \nu_m \\ \mathbf{f}^d &\equiv [f_l^d] \equiv \Delta u(\omega) dAc_{mj\beta} n_j \nu_m. \end{aligned} \quad (4.56)$$

Therefore, the source functions of the time-harmonic dislocation applied at $(0, 0, z_s)$ are

$$\begin{aligned} ik\tilde{\mathbf{u}}_s &= ik\mathbf{T}^{-1} \mathbf{f}^d \\ \tilde{\mathbf{t}}_s &= \mathbf{f}^\delta - i\mathbf{k}\mathbf{R}\mathbf{T}^{-1} \mathbf{f}^d. \end{aligned} \quad (4.57)$$

Similar to the static case, we can propagate the solution coefficients from the top surface to the upper level of the source and then from the lower level of the source to the last interface in the bottom. Making use of the given boundary conditions, source functions and the conditions on the last layer interface, the involved unknowns can be solved for the source-induced wave deformation. Should the top and bottom boundaries are traction-free and further without any source, we then arrive at the important dispersion equation, which can be solved numerically by a very efficient and accurate method (Zhu *et al* 2018).

Remark 4.7. If $\omega = 0$, we then reduce the time-harmonic wave problem to the static deformation in a general anisotropic and elastic layered half-space. This reduced problem was also solved for the general magnetoelastic layered structure by Li and Pan (2016) with the purely elastic case as one of the special cases.

4.5. Poroelastic and electromagnetic (EM) coupling

Besides gravity, poroelastic coupling would also influence the post-seismic deformation and stress fields (Booker 1974, Jonsson *et al* 2003, Segall 2010) and even induce aftershock (Nur and Booker 1972, Miller *et al* 2004). In general, underground or the near-surface layer is not dry (or purely elastic), but filled with water. It was Biot (1956) who developed the poroelastic coupling theory so that the coupling between the

solid skeleton and the pore pressure could be properly analyzed. The Biot's poroelasticity theory has many applications, as reviewed by Rice and Cleary (1976) for the general elastic porous media with dislocations, by Detournay and Cheng (1993) in rock mechanics, and by Rudnicki (2001) for both faulting and failure of geomaterials. Notable monographies are those by Wang (2000), Selvadurai (2007), Selvadurai and Suvorov (2016) and Cheng (2016).

In analyzing earthquake activity, it was noticed that the aftershock frequency decays like a diffusive process. Pore fluid diffusion was first proposed by Nur and Booker (1972) as the time-dependent process responsible for aftershocks. Booker (1974) showed that in the case of a simple edge dislocation, shear stresses along a fault may be strongly coupled to pore pressure and could change appreciably over time due to fluid diffusion. When analyzing data of the Landers 1992 earthquake, Peltzer *et al* (1998) argued that poroelastic rebound caused by pore fluid flow may also occur over greater distance from the fault, compensating the vertical ground shift produced by fault afterslip. Bosl and Nur (2002) tested the importance of pore fluid flow in producing aftershocks, and noticed that rising fluid pressure due to pore fluid flow and the resulting Coulomb stress change were strongly correlated with the time and location of aftershock events. InSAR data spanning a period of seven years between Lander and Hector Mine earthquakes also revealed the poroelastic deformation due to fluid-filled upper crust (Fialko 2004). Analysis of afterslip distribution following the 2007 September 12 southern Sumatra earthquake also indicated the significant correlation to the poroelastic deformation (Lubis *et al* 2013). The short-time post-seismic deformation of the 2001 Kunlun earthquake was found to be correlated to the poroelastic rebound (Shao *et al* 2010). The 2011 Tohoku earthquake further induced the groundwater level change (Yan *et al* 2014) and poroelastic rebound (Hu *et al* 2014).

In analyzing earthquake-induced deformation and aftershock, the fault plane permeability needs to be carefully examined. Rudnicki (1987) considered the shear dislocation on an impermeable plane in which the fluid mass flux vanishes. A shear propagating crack in a poroelastic solid was analyzed by Rice and Simons (1976) and Simons (1977) for the permeable plane and by Rudnicki and Koutsibelas (1991) for the impermeable plane. However, in practice, the glide plane is likely to be neither completely permeable nor impermeable, as considered by Song and Rudnicki (2017) in the case of a suddenly introduced shear dislocations on a leaky plane.

The interaction between the pore pressure and solid skeleton needs to be studied using the fully coupled poroelastic model with further consideration of layering in the earth medium. Wang and Kumpel (2003) derived the formulation and designed the corresponding code based on the propagator matrix method whilst Barbot and Fialko (2010b) developed a semi-analytical method based on the Fourier transformation method. The reciprocity relation in poroelasticity was presented by Pan (1991) for the transient case, and by Wang *et al* (2015) for the time-harmonic case. Concentrated dislocations in poroelastic media were also considered by Cheng and Detournay (1998) and Wang and Hu (2016). The fully coupled model with the source functions (including the fluid dilation contribution) was presented in

Pan (1999) for the layered poroelastic half-space. An interesting and related extension is the work by Song *et al* (2016) on the Eshelby inclusion in fluid-filled porous media. It is further noticed that dislocation in poroelastic media is analogue to that in diffusive materials, which has been an active research topic in recent years (i.e. Song *et al* (2019)).

In a fluid-saturated porous elastic medium, besides the coupling between the fluid and solid phases, EM fields could be further coupled due to the well-known electrokinetic effect, which arises from the existence of the electric double layer formed at the boundary of the solid and fluid phases (Pride 1994, Revil *et al* 1999a, 1999b). This multi-coupling among solid, fluid and EM fields substantially complicates the problem. It was Pride (1994) who first derived the complete boundary-value formulation, which can be reduced to the Biot's poroelastic system and the Maxwell system under the decoupled conditions. Gao and Hu (2010) derived the full-space analytic solution of the EM field generated by a moment tensor source. The electrokinetic coupled system has been analyzed by many for the purpose of (1) detecting and characterizing the underground materials by using the coupled seismoelectric or electroseismic signals and (2) interpreting the earthquake-associated EM phenomena (i.e. Gao *et al* (2013a, 2013b)). Haartsen and Pride (1997) applied the combined Fourier–Hankel transforms and solved the electroseismic waves induced by point sources in layered media, using the global matrix method. The generalized reflection and transmission method in purely elastic media was extended to the porous, EM and layered system with point sources (Garambois and Dietrich 2002, Ren *et al* 2010) and with finite faults (Hu and Gao 2011, Ren *et al* 2012). More recent progress can be found in Ren *et al* (2016a, 2016b) and Gao *et al* (2017), and in the review by Jounianux and Zyerman (2016).

4.6. Summary of section 4

Due to the inhomogeneity in the layering direction, static deformation and wave propagation in layered half-spaces (including layered half-planes, and layered plates) are best analyzed via integral transforms, such as the Fourier and Hankel transforms. While Fourier transform can be applied to general material anisotropy, Hankel transform is best for isotropic or TI media. The Cartesian and cylindrical systems of vector functions are easy to be applied and possess certain advantages over the direct scalar transforms. Once the boundary-value problem is converted to the transformed domain, the DVP method can be applied to propagate the solution from one layer to the other, without having any numerical instability issue. We end this section by highlighting the following references with published computer software codes (in FORTRAN or MATLAB).

Okada (1992) solved the response of a rectangular fault in a homogeneous and isotropic elastic half-space. Pan *et al* (2014) extended the solution to a general polygonal fault in a homogeneous and TI elastic half-space. The time-dependent displacement and stress fields due to shear and tensile faults in a TI viscoelastic half-space were solved by Molavi Tabrizi and Pan (2015). Pan *et al* (2015a) derived the displacements and

stresses due to finite faults and opening-mode fractures in a general anisotropic elastic half-space. Wang *et al* (2003b) and Wang *et al* (2006b) obtained the fault-induced deformation in isotropic elastic and layered half-spaces and in the corresponding elastic half-space with gravity and viscoelasticity. Kausel and Peek (1982) studied the dynamic loading in the interior of an isotropic elastic and layered half-space using the thin-layer method. This GF part of the program was used as kernel functions in civil engineering, related to the dynamic response of soil-structure interaction in the computer program named SASSI developed at Berkeley (i.e. Celebi and Schmid (2005)). A PC program on SAW (surface acoustic wave) propagation in anisotropic multilayers was written by Adler *et al* (1990). The DISPERSE software for waves in layered plates and cylinders was published by Lowe and colleagues (Lowe 1992, Lowe and Pavlakovic 2013). Some programs for calculating synthetic seismograms in horizontally layered media were discussed in Cormier (2007). Under static deformation, a BEM program, called Poly3D, was derived by Maerten *et al* (2005) where the analytical dislocation solution is used as the Green's kernel function.

5. GFs in the layered spherical earth

In this section, we review and present various GF solutions in a layered sphere. Besides their obvious applications to Earth science, these solutions can be also applied to problems in other layered planetary bodies (i.e. Zhang (1992), Dehant *et al* (2000) and Batov *et al* (2016)). Both elastostatic deformation and time-harmonic vibration are considered. As for the elastic and self-gravitational layered earth, the following two types of solutions will be reviewed in more details: (1) the solutions under concentrated surface loading, which are related to the famous elastic load Love number and the corresponding load GFs, and (2) the solutions to the concentrated internal dislocation, which related to the dislocation Love number and the corresponding dislocation GFs. The corresponding viscoelastic and time-harmonic solutions will be also discussed. In most cases, the given problem will be solved in each layer (as for the horizontally layered case) in terms of the spherical system of vector functions. The constitutive relation will be assumed to be isotropic or at most TI (or spherical isotropy), except for otherwise indicated. The solutions for the corresponding layered system will be solved via the propagating matrix method, preferably the one we introduced in section 4, i.e. the DVP method. This section is similar to section 4: however, instead of applying the integral transform in terms of either Cartesian or cylindrical system of vector functions there, here we express the solutions in terms of the spherical system of vector functions, which require series summation, instead of integration. A good reference on the systems of vector functions with particular applications in layered spherical Earth is the classic book by Ben-Menahem and Singh (1981). A comprehensive and advanced treatment on global seismology can

be found in (Dahlen and Tromp 1998). A brief review on the basic relations in different coordinate systems and the corresponding systems of vector functions are presented in appendix for easy reference.

5.1. Basic equations and general solutions with gravity

The linearized governing equation for the elastic and self-gravitational spherical Earth is similar to equation (4.1), but with gravity in r -direction. Namely, we have

$$\sigma_{ji,j} - (\rho g u_r)_{,i} - \rho \psi_{,i} + g(\rho u_j)_{,j} \delta_{ir} + f_i + c_{\text{iner}} u_i = 0 \quad (5.1a)$$

$$\psi_{,jj} + 4\pi G(\rho u_j)_{,j} = 0. \quad (5.1b)$$

In equation (5.1), repeated indices take the summation over the spherical coordinates (r, θ, φ) (appendix) and an index following the subscript comma indicates the derivative in the coordinate direction, G is the universal gravitational constant, δ_{ir} the Kronecker delta, σ_{ji} the stresses, ρ and g are the density and gravity, f_i the body forces (per unit volume), u_i the displacements, and ψ is the perturbed gravitational potential (which may include the tidal body-force, surface load, and deformation potentials) with its negative gradient being the perturbed gravity. This sign convention is the same as in Farrell (1972) and Wu and Peltier (1982), but opposite to that in Takeuchi and Saito (1972) and Sun (1992a, 1992b).

In terms of the spherical coordinates, the strain (tensor ε_{ij}) and displacement relations, as well as the 'flux' in r -direction, q_r , can be written as

$$\begin{aligned} \varepsilon_{rr} &= u_{r,r}; \varepsilon_{\theta\theta} = \frac{u_{\theta,\theta} + u_r}{r}; \varepsilon_{\varphi\varphi} = \frac{u_{\varphi,\varphi}}{r \sin \theta} + \frac{u_{\theta} \cot \theta + u_r}{r} \\ 2\varepsilon_{r\theta} &= u_{\theta,r} + \frac{u_{r,\theta} - u_{\theta}}{r}; 2\varepsilon_{r\varphi} = u_{\varphi,r} + \frac{u_{r,\varphi}}{r \sin \theta} - \frac{u_{\varphi}}{r} \\ 2\varepsilon_{\theta\varphi} &= \frac{u_{\varphi,\theta} - u_{\varphi} \cot \theta}{r} + \frac{u_{\theta,\varphi}}{r \sin \theta} \end{aligned} \quad (5.2a)$$

$$q_r = \psi_{,r} + 4\pi G \rho u_r + \frac{n+1}{r} \psi \quad (5.2b)$$

where n is the degree in the spherical system of vector functions as defined in appendix.

The Hooke's law for each of the spherical mantle layer, which is TI with r -direction being its material axis of symmetry, is (Anderson (1961) and Chen *et al* (2015))

$$\begin{aligned} \sigma_{rr} &= c_{33}\varepsilon_{rr} + c_{13}\varepsilon_{\theta\theta} + c_{13}\varepsilon_{\varphi\varphi} \\ \sigma_{\theta\theta} &= c_{13}\varepsilon_{rr} + c_{11}\varepsilon_{\theta\theta} + c_{12}\varepsilon_{\varphi\varphi} \\ \sigma_{\varphi\varphi} &= c_{13}\varepsilon_{rr} + c_{12}\varepsilon_{\theta\theta} + c_{11}\varepsilon_{\varphi\varphi} \\ \sigma_{\theta r} &= 2c_{44}\varepsilon_{\theta r}; \sigma_{\varphi r} = 2c_{44}\varepsilon_{\varphi r}; \sigma_{\theta\varphi} = 2c_{66}\varepsilon_{\theta\varphi} \end{aligned} \quad (5.3a)$$

where $c_{66} = (c_{11} - c_{12})/2$. For the isotropic elastic material, we have (as in equation (2.4))

$$\begin{aligned} c_{11} &= c_{33} = \lambda_e + 2\mu_e \\ c_{12} &= c_{13} = \lambda_e; \quad c_{44} = c_{66} = \mu_e \\ \lambda_v &= \lambda(s); \mu_v = \mu(s) \end{aligned} \quad (5.3b)$$

where λ and μ are the two Lamé elastic constants, and the subscripts e and v are for the elastic and viscoelastic (with

s being the Laplace variable) cases. Notice that TI for the spherical geometry means equally the spherically isotropic material.

We solve the problem in terms of the spherical system of vector functions or the vector spherical harmonics (VSHs), as defined in appendix. In other words, we expand the solutions as

$$\begin{aligned} \mathbf{u}(r, \theta, \varphi) &\equiv u_r \mathbf{e}_r + u_\theta \mathbf{e}_\theta + u_\varphi \mathbf{e}_\varphi \\ &= \sum_{n=0}^{\infty} \sum_{m=-n}^n [U_L(r) \mathbf{L}(\theta, \varphi) + U_M(r) \mathbf{M}(\theta, \varphi) + U_N(r) \mathbf{N}(\theta, \varphi)] \\ \mathbf{t}(r, \theta, \varphi) &\equiv \sigma_{rr} \mathbf{e}_r + \sigma_{r\theta} \mathbf{e}_\theta + \sigma_{r\varphi} \mathbf{e}_\varphi \\ &= \sum_{n=0}^{\infty} \sum_{m=-n}^n [T_L(r) \mathbf{L}(\theta, \varphi) + T_M(r) \mathbf{M}(\theta, \varphi) + T_N(r) \mathbf{N}(\theta, \varphi)] \end{aligned} \quad (5.4a)$$

and

$$\begin{aligned} \phi(r, \theta, \varphi) &= \sum_{n=0}^{\infty} \sum_{m=-n}^n \Phi(r) S(\theta, \varphi; n, m) \\ q_r(r, \theta, \varphi) &= \sum_{n=0}^{\infty} \sum_{m=-n}^n Q(r) S(\theta, \varphi; n, m). \end{aligned} \quad (5.4b)$$

The body force is also expanded as

$$\mathbf{f}(r, \theta, \varphi) = \sum_{n=0}^{\infty} \sum_{m=-n}^n [F_L(r) \mathbf{L}(\theta, \varphi) + F_M(r) \mathbf{M}(\theta, \varphi) + F_N(r) \mathbf{N}(\theta, \varphi)]. \quad (5.4c)$$

Notice that for $n = 0$, the problem is reduced to a spherically symmetric case where the solution depends only on r and that there is no N -type solution.

It can be shown that the N -type solution is purely elastic, independent of the gravity effect. This deformation is toroidal and it is governed by the following equation

$$\frac{d}{dr} \begin{bmatrix} U_N(r) \\ T_N(r) \end{bmatrix} = [\mathbf{A}_N(r)] \begin{bmatrix} U_N(r) \\ T_N(r) \end{bmatrix} - \begin{bmatrix} 0 \\ F_N(r) \end{bmatrix} \quad (5.5)$$

where

$$[\mathbf{A}_N(r)] = \begin{bmatrix} 1/r & 1/c_{44} \\ (N-2)c_{66}/r^2 - c_{\text{iner}} & -3/r \end{bmatrix} \quad (5.6)$$

and $N = n(n+1)$. Under elastostatic (or viscoelastic) deformation and if the material properties are independent of the radial variable r , this equation can be solved by introducing a variable transformation (Pan *et al* 2015b), similar to the LM -type deformation discussed below.

For the LM -type deformation, we introduce

$$\mathbf{U} = [U_L \quad U_M \quad \Phi]^t; \quad \mathbf{T} = [T_L \quad T_M \quad Q]^t; \quad \mathbf{F} = [F_L \quad F_M \quad 0]^t. \quad (5.7)$$

Then, the governing equation can be converted into the following first-order differential equations with r -dependent coefficients as

$$\frac{d}{dr} \begin{bmatrix} \mathbf{U}(r) \\ \mathbf{T}(r) \end{bmatrix} = [\mathbf{A}(r)] \begin{bmatrix} \mathbf{U}(r) \\ \mathbf{T}(r) \end{bmatrix} - \begin{bmatrix} \mathbf{0} \\ \mathbf{F}(r) \end{bmatrix} \quad (5.8)$$

where the coefficient matrix $[\mathbf{A}(r)]$ is defined as

$$[\mathbf{A}(r)] = \begin{bmatrix} -2c_{13}/(c_{33}r) & Nc_{13}/(c_{33}r) & 0 & 1/c_{33} & 0 & 0 \\ -1/r & 1/r & 0 & 0 & 1/c_{44} & 0 \\ -4\pi G\rho & 0 & -(n+1)/r & 0 & 0 & 1 \\ -\frac{4\rho g}{r} + \frac{2[c_{33}(c_{11}+c_{12})-2c_{13}^2]}{c_{33}r^2} - c_{\text{iner}} & \frac{N\rho g}{r} + \frac{[2c_{13}^2 - c_{33}(c_{11}+c_{12})]N}{c_{33}r^2} & -\frac{(n+1)\rho}{r} & \frac{2(c_{13}/c_{33}-1)}{r} & \frac{N}{r} & \rho \\ \frac{\rho g}{r} + \frac{[2c_{13}^2 - c_{33}(c_{11}+c_{12})]}{c_{33}r^2} & -\frac{(c_{11}-c_{12})}{r^2} + N\frac{c_{11}c_{33}-c_{13}^2}{c_{33}r^2} - c_{\text{iner}} & \frac{\rho}{r} & -\frac{c_{13}}{c_{33}r} & -\frac{3}{r} & 0 \\ -4\pi G\rho(n+1)/r & 4\pi G\rho N/r & 0 & 0 & 0 & (n-1)/r \end{bmatrix}. \quad (5.9)$$

For the isotropic case, making use of equation (5.3b), equations (5.6) and (5.9) become

$$[\mathbf{A}_N(r)] = \begin{bmatrix} 1/r & 1/\mu_e \\ (N-2)\mu_e/r^2 - c_{\text{iner}} & -3/r \end{bmatrix} \quad (5.10)$$

$$[\mathbf{A}(r)] = \begin{bmatrix} -2\lambda_e/[(\lambda_e+2\mu_e)r] & N\lambda_e/[(\lambda_e+2\mu_e)r] & 0 & 1/(\lambda_e+2\mu_e) & 0 & 0 \\ -1/r & 1/r & 0 & 0 & 1/\mu_e & 0 \\ -4\pi G\rho & 0 & -(n+1)/r & 0 & 0 & 1 \\ -\frac{4\rho g}{r} + \frac{4\mu_e(3\lambda_e+2\mu_e)}{(\lambda_e+2\mu_e)r^2} - c_{\text{iner}} & \frac{N\rho g}{r} - \frac{2\mu_e(3\lambda_e+2\mu_e)N\mu_e}{(\lambda_e+2\mu_e)r^2} & -\frac{(n+1)\rho}{r} & -\frac{4\mu_e}{(\lambda_e+2\mu_e)r} & \frac{N}{r} & \rho \\ \frac{\rho g}{r} - \frac{2\mu_e(3\lambda_e+2\mu_e)}{(\lambda_e+2\mu_e)r^2} & \frac{2\mu_e[2N(\lambda_e+\mu_e)-(\lambda_e+2\mu_e)]}{(\lambda_e+2\mu_e)r^2} - c_{\text{iner}} & \frac{\rho}{r} & -\frac{\lambda_e}{(\lambda_e+2\mu_e)r} & -\frac{3}{r} & 0 \\ -4\pi G\rho(n+1)/r & 4\pi G\rho N/r & 0 & 0 & 0 & (n-1)/r \end{bmatrix}. \quad (5.11)$$

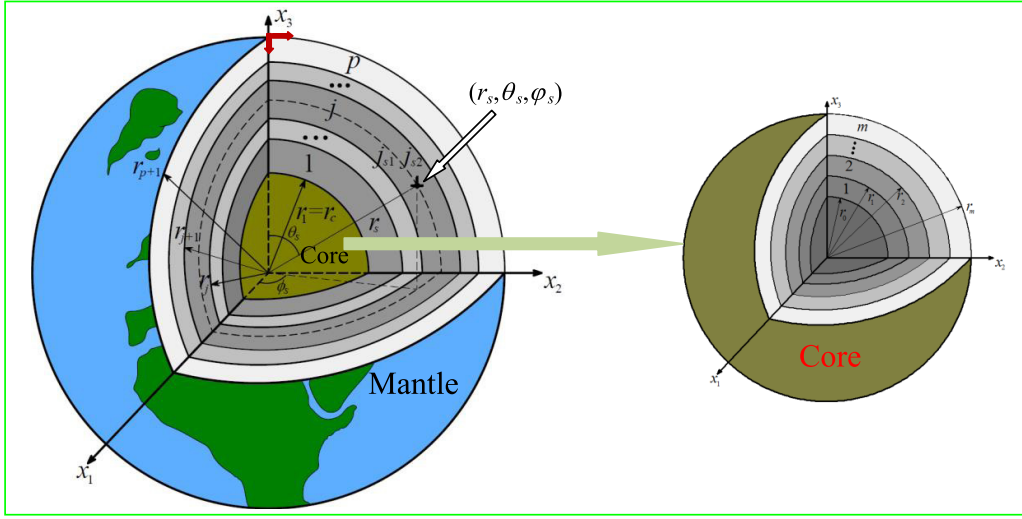


Figure 5. A layered spherical Earth made of p layers in its mantle with a (layered) inner liquid core of radius $r_1 = r_c$ (from the mantle side). The outer surface of the Earth is located at $r_{p+1} = a$. A general concentrated force is applied on the surface and a concentrated dislocation is located at $(r_s, \theta_s, \varphi_s)$ within the mantle layer j . The Earth core is made of m layers over a homogeneous inner core of radius $r = r_0$, which can be solid or liquid. The outer surface of the core is the core-mantle boundary at $r_m = r_c$ (from the core side).

Since the density, gravity, and elastic properties are functions of radius r , equations (5.5) and (5.8) can only be solved numerically. It is usually done using the Runge–Kutta numerical integration (i.e. Longman (1963) and Farrell (1972) for the elastostatic deformation with gravity).

However, if we assume that the Earth is made of multilayers (p layers in its mantle and m layers in its core, as shown in figure 5), then one can solve the elastostatic and viscoelastic deformations of the earth analytically. By looking closely at the data and curves in the preliminary reference Earth model (PREM) (Dziewonski and Anderson 1981), and considering further the possibility of an analytical solution, Pan *et al* (2015b) came up perhaps with the best and yet more realistic Earth model which can be solved analytically. In this spherical and radially heterogeneous Earth model made of multiple layers, the density is constant and gravity varies linearly with radius in each core layer, whilst the density variation is inversely linear with the radius and gravity is constant in each mantle layer. With only 56 mantle layers and 26 core layers, the material properties in the entire radial direction of Earth (in both core and mantle) overlap with the original PREM model (Dziewonski and Anderson 1981). Thus, by dividing the mantle into certain thin layers and assuming that in each

layer its density varies as $\rho(r) = \rho_e/r$, whilst its gravity and (visco)elastic coefficients are uniform, a general analytical solution in each mantle layer can be derived. This is achieved by further introducing, for a given layer j with interfaces at $r = r_{j-1}$ and r_j ($> r_{j-1}$), the following variable transformation as in Pan *et al* (2015b)

$$r = r_{j-1}e^\xi$$

$$0 \leq \xi \leq \xi_j; \quad \xi_j = \ln(r_j/r_{j-1}). \quad (5.12)$$

Under this transformation, equations (5.5) and (5.8) are converted to the following sets with constant coefficients (except for the inertia term)

$$\frac{d}{d\xi} \begin{bmatrix} U_N(\xi) \\ rT_N(\xi) \end{bmatrix} = [C_N] \begin{bmatrix} U_N(\xi) \\ rT_N(\xi) \end{bmatrix} - \begin{bmatrix} \mathbf{0} \\ r^2F_N(r) \end{bmatrix} \quad (5.13a)$$

$$\frac{d}{d\xi} \begin{bmatrix} U(\xi) \\ rT(\xi) \end{bmatrix} = [C] \begin{bmatrix} U(\xi) \\ rT(\xi) \end{bmatrix} - \begin{bmatrix} \mathbf{0} \\ r^2F(r) \end{bmatrix} \quad (5.13b)$$

where the involved coefficient matrices are

$$[C_N] = \begin{bmatrix} 1 & 1/c_{44} \\ (N-2)c_{66} - r^2c_{iner} & -2 \end{bmatrix} \quad (5.14a)$$

$$[C] = \begin{bmatrix} -2c_{13}/c_{33} & Nc_{13}/c_{33} & 0 & 1/c_{33} & 0 & 0 \\ -1 & 1 & 0 & 0 & 1/c_{44} & 0 \\ -4\pi G\rho_e & 0 & -(n+1) & 0 & 0 & 1 \\ -4\rho_e g + \frac{2[c_{33}(c_{11}+c_{12})-2c_{13}^2]}{c_{33}} - r^2c_{iner} & N\rho_e g + \frac{[2c_{13}^2-c_{33}(c_{11}+c_{12})]N}{c_{33}} & -(n+1)\rho_e & 2c_{13}/c_{33} - 1 & N & \rho_e \\ \rho_e g + \frac{[2c_{13}^2-c_{33}(c_{11}+c_{12})]}{c_{33}} & -(c_{11} - c_{12}) + N\frac{c_{11}c_{33}-c_{13}^2}{c_{33}} - r^2c_{iner} & \rho_e & -\frac{c_{13}}{c_{33}} & -2 & 0 \\ -4\pi G\rho_e(n+1) & 4\pi G\rho_e N & 0 & 0 & 0 & n \end{bmatrix}. \quad (5.14b)$$

Similar procedure can be applied to find the analytical solution in the core. Namely, one can divide the core into certain thin layers and assume that in each core layer, the density is constant but gravity is a linear function of r (Pan *et al* 2015b).

Therefore, under the elastostatic (or viscoelastic) deformation without the inertia term (i.e. $c_{\text{iner}} = 0$), we can derive analytically the general solutions of equation (5.13) (without body force), and thus the recursive relations between the layers based on the DVP method, similar to those in section 4. Making use of the recursive relation repeatedly from the core-mantle boundary $r = r_c$ (r_1) to the surface of the Earth at $r = a$ ($r = r_{p+1}$), we finally obtain the following two sets of relations (i.e. for both **LM**- and **N**-types)

$$\begin{bmatrix} \mathbf{U}(r_c) \\ a\mathbf{T}(a) \end{bmatrix} = \begin{bmatrix} \mathbf{S}_{11}^{1:p} & \mathbf{S}_{12}^{1:p} \\ \mathbf{S}_{21}^{1:p} & \mathbf{S}_{22}^{1:p} \end{bmatrix} \begin{bmatrix} \mathbf{U}(a) \\ r_c\mathbf{T}(r_c) \end{bmatrix} \quad (5.15a)$$

$$\begin{bmatrix} U_N(r_c) \\ aT_N(a) \end{bmatrix} = \begin{bmatrix} N_{11}^{1:p} & N_{12}^{1:p} \\ N_{21}^{1:p} & N_{22}^{1:p} \end{bmatrix} \begin{bmatrix} U_N(a) \\ r_c T_N(r_c) \end{bmatrix} \quad (5.15b)$$

where the superscripts ‘1:p’ indicate the combined recursive relations between the core-mantle boundary (the lower interface of the first mantle layer, i.e. the mantle side of the core-mantle boundary) and the surface (the upper interface of the last or top-mantle layer p), and the subscripts ‘ ij ’ ($i, j = 1, 2$) are the indices of the submatrix or elements of the matrix.

Equations (5.15a) and (5.15b) need to be solved using the core-mantle boundary conditions. First, for the **N**-type, since the outer core is liquid, we have $T_N(r_c) = 0$ so that equation (5.15b) can be solved for the given boundary conditions on the surface of the Earth at $r = a$. As for the **LM**-type deformation, for the given layered (or homogeneous) core model, we can propagate from the most inner homogeneous core to the core-mantle boundary to obtain the relation between the expansion coefficients on the core-mantle boundary (on the core side) and the three coefficients (c_i below) in the most inner homogeneous (solid or liquid) core as

$$\begin{bmatrix} \mathbf{U}(r_c) \\ r_c\mathbf{T}(r_c) \end{bmatrix} = [\mathbf{B}_{cm}] \begin{bmatrix} c_1 \\ c_2 \\ c_3 \end{bmatrix} \equiv [\mathbf{B}_{cm}] [\mathbf{c}] \quad (5.16)$$

where $[\mathbf{B}_{cm}]$ is the known core-mantle boundary matrix (with subscripts ‘ cm ’ for core-mantle) for the given core model (Pan *et al* 2015b). Combining equations (5.16) and (5.15a), we can then solve the involved unknown coefficients for the given boundary condition on the surface of the Earth $r = a$. This solves the surface loading deformation and thus the corresponding loading Love numbers and GFs.

It is noted that the core models and core-mantle boundary used here are similar to those in Saito (1974) and Wu and Peltier (1982). Some detailed discussions on this topic can be found in Chinnery (1975) and Crossley and Gubbins (1975).

If there is a given concentrated source, force or dislocation, located at r_s in the mantle layer j (figure 5), then we just need to subdivide this layer into two sublayers j_1 (j_{s1}) and j_2 (j_{s2}). In terms of the expansion coefficients in the spherical system of vector functions, the source functions $\mathbf{U}_s, \mathbf{T}_s, U_{Ns}$,

and T_{Ns} are defined in terms of the following discontinuities at the source level $r = r_s$ as (with $r_{j_2} = r_s + 0$, and $r_{j_1} = r_s - 0$) (again, there is no discontinuity or jump for the gravity related coefficients Φ and Q)

$$\begin{aligned} \mathbf{U}_s &= \mathbf{U}(r_{j_2}) - \mathbf{U}(r_{j_1}) \equiv \mathbf{U}(r_s + 0) - \mathbf{U}(r_s - 0) \\ \mathbf{T}_s &= \mathbf{T}(r_{j_2}) - \mathbf{T}(r_{j_1}) \equiv \mathbf{T}(r_s + 0) - \mathbf{T}(r_s - 0) \\ U_{Ns} &= U_N(r_{j_2}) - U_N(r_{j_1}) \equiv U_N(r_s + 0) - U_N(r_s - 0) \\ T_{Ns} &= T_N(r_{j_2}) - T_N(r_{j_1}) \equiv T_N(r_s + 0) - T_N(r_s - 0). \end{aligned} \quad (5.17)$$

Now in the mantle, we propagate the recursive relation from the surface to the upper side of the source and then from the lower side of the source to the core-mantle boundary to arrive at the following two sets of equations as

$$\begin{bmatrix} \mathbf{U}(r_{j_2}) \\ a\mathbf{T}(a) \end{bmatrix} = \begin{bmatrix} \mathbf{S}_{11}^{j_2:p} & \mathbf{S}_{12}^{j_2:p} \\ \mathbf{S}_{21}^{j_2:p} & \mathbf{S}_{22}^{j_2:p} \end{bmatrix} \begin{bmatrix} \mathbf{U}(a) \\ r_{j_2}\mathbf{T}(r_{j_2}) \end{bmatrix} \quad (5.18a)$$

$$\begin{bmatrix} U_N(r_{j_2}) \\ aT_N(a) \end{bmatrix} = \begin{bmatrix} N_{11}^{j_2:p} & N_{12}^{j_2:p} \\ N_{21}^{j_2:p} & N_{22}^{j_2:p} \end{bmatrix} \begin{bmatrix} U_N(a) \\ r_{j_2}T_N(r_{j_2}) \end{bmatrix} \quad (5.18b)$$

and

$$\begin{bmatrix} \mathbf{U}(r_c) \\ r_{j_1}\mathbf{T}(r_{j_1}) \end{bmatrix} = \begin{bmatrix} \mathbf{S}_{11}^{1:j_1} & \mathbf{S}_{12}^{1:j_1} \\ \mathbf{S}_{21}^{1:j_1} & \mathbf{S}_{22}^{1:j_1} \end{bmatrix} \begin{bmatrix} \mathbf{U}(r_{j_1}) \\ r_c\mathbf{T}(r_c) \end{bmatrix} \quad (5.18c)$$

$$\begin{bmatrix} U_N(r_c) \\ r_{j_1}T_N(r_{j_1}) \end{bmatrix} = \begin{bmatrix} N_{11}^{1:j_1} & N_{12}^{1:j_1} \\ N_{21}^{1:j_1} & N_{22}^{1:j_1} \end{bmatrix} \begin{bmatrix} U_N(r_{j_1}) \\ r_c T_N(r_c) \end{bmatrix}. \quad (5.18d)$$

Similarly, combining equations (5.16)–(5.18), the involved unknowns can be solved.

In summary, for the surface loading case, one solves the involved unknowns from equations (5.15) and (5.16), and the solved expansion coefficients $\mathbf{U}(a)$ and $U_N(a)$ will give us the elastic loading Love numbers (ELLNs). For the given internal dislocation case, one can solve the involved knowns from equations (5.16) to (5.18), and the solved expansion coefficients $\mathbf{U}(a)$ and $U_N(a)$ will give us the dislocation Love numbers (DLNs).

Remark 5.1. Another type of important analytical solution was provided by Gilbert and Backus (1968). They derived the analytical solutions for time-harmonic vibration of (isotropic) elastic-gravitational and layered sphere in terms of spherical Bessel functions. They assumed that all the material properties as well as the density were uniform in each layer whilst the gravity in each layer varied as $g(r) = kr$, a linear function of radius r . This solution contains many special cases including the corresponding elastostatic deformation and the elastic waves in layered sphere (without gravity) as special solutions.

5.2. Source functions of concentrated forces and dislocations

Without loss of generality, we assume that there is a point force or point dislocation of unit magnitude applied at $(r, \theta, \varphi) = (r_s, 0, 0)$ in layer j of the layered Earth (in a mantle layer). Thus, in terms of the expansion coefficients in the

spherical system of vector functions, the source functions U_s , T_s , U_{Ns} , and T_{Ns} defined in equation (5.17) can be derived and they are listed below.

For a concentrated force at $(r, \theta, \varphi) = (r_s, 0, 0)$, we have

$$f_j(r, \theta, \varphi) = \frac{\delta(r - r_s)\delta(\theta)\delta(\varphi)}{r^2 \sin \theta} n_j. \quad (5.19)$$

Then the expansion coefficients of the concentrated force is

$$\begin{aligned} F_L &= \frac{1}{r_s^2} \sqrt{\frac{(2n+1)}{4\pi}} n_z \delta(r - r_s); \quad m = 0 \\ F_M &= -\frac{1}{2r_s^2} \sqrt{\frac{(2n+1)}{4\pi n(n+1)}} (\mp n_x + i n_y) \delta(r - r_s); \quad m = \pm 1 \\ F_N &= -\frac{1}{2r_s^2} \sqrt{\frac{(2n+1)}{4\pi n(n+1)}} (i n_x \pm n_y) \delta(r - r_s); \quad m = \pm 1. \end{aligned} \quad (5.20)$$

Therefore the source functions of the concentrated force are (only the nonzero components)

$$\begin{aligned} T_{Ls} &= -\frac{1}{r_s^2} \sqrt{\frac{(2n+1)}{4\pi}} n_z; \quad m = 0 \\ T_{Ms} &= \frac{1}{2r_s^2} \sqrt{\frac{(2n+1)}{4\pi n(n+1)}} (\mp n_x + i n_y); \quad m = \pm 1 \\ T_{Ns} &= \frac{1}{2r_s^2} \sqrt{\frac{(2n+1)}{4\pi n(n+1)}} (i n_x \pm n_y); \quad m = \pm 1. \end{aligned} \quad (5.21)$$

Once we have the GF solution due to a concentrated force, the Betti's reciprocity in section 2 can be applied to find the GF solution due to a concentrated dislocation. On the other hand, the source functions for a point dislocation in a TI medium can be also derived directly as commonly applied in geophysics. We first express the dislocation as an equivalent body-force, and then expand the latter in terms of the spherical system of vector functions. In other words, to find the source functions of the point dislocation, we rely on the equivalent body-force expression of a general dislocation over the internal area A with normal n_i (equation (2.31) and also Aki and Richards (1980)) as

$$f_p(\mathbf{r}) = -\int_A c_{ijpq} b_j(\mathbf{r}_s) n_i(\mathbf{r}_s) \frac{\partial}{\partial r_q} \delta(\mathbf{r} - \mathbf{r}_s) dA(\mathbf{r}_s) \quad (5.22)$$

where ∂r_q ($q = 1, 2, 3$) stands for $(\partial r, r\partial\theta, r\sin\theta\partial\varphi)$. For a concentrated dislocation source, we have $b_j = \Delta u_j$ (where ν_j is the unit vector of the dislocation, or the Burgers vector). By also assuming that the source is fixed at $\mathbf{r}_s = (r_s, 0, 0)$, we have

$$f_p(r, \theta, \varphi) = -\Delta u d A n_i \nu_j c_{ijpq} \frac{\partial}{\partial r_q} \left[\frac{\delta(r - r_s)}{r^2} \frac{\delta(\theta)}{\sin \theta} \delta(\varphi) \right]. \quad (5.23)$$

Then, expanding the equivalent force (5.23) in terms of the spherical system of vector functions, it can be shown that the expansion coefficients can be separated into two parts as (similar to those in section 4)

$$\begin{bmatrix} F_L(r) \\ F_M(r) \\ F_N(r) \end{bmatrix} = \begin{bmatrix} F_L^\delta \\ F_M^\delta \\ F_N^\delta \end{bmatrix} \frac{\delta(r - r_s)}{r_s^3} + \begin{bmatrix} F_L^d \\ F_M^d \\ F_N^d \end{bmatrix} \frac{\delta'(r - r_s)}{r_s^2}. \quad (5.24)$$

While the first term on the right-hand side induces the discontinuity of the traction expansion coefficients, the second term causes discontinuities in both the displacement and traction expansion coefficients. Making use of the coefficient matrix and jump conditions related to the derivative of the delta function (Kennett 1983), the following results (omitting

the common factor of the dislocation $\Delta u d A$) can be found (Takeuchi and Saito 1972, Kennett 1983)

$$\begin{aligned} U_{Ns} &= \frac{1}{2r_s^2} \sqrt{\frac{(2n+1)}{4\pi n(n+1)}} [\mp (n_y \nu_z + n_z \nu_y) - i(n_z \nu_x + n_x \nu_z)]; \quad m = \pm 1 \\ r_s T_{Ns} &= \frac{c_{66}}{2r_s^2} \sqrt{\frac{(2n+1)(n+2)(n-1)}{4\pi n(n+1)}} [(n_x \nu_y + n_y \nu_x) \pm i(n_x \nu_x - n_y \nu_y)]; \quad m = \pm 2 \end{aligned} \quad (5.25)$$

$$\begin{aligned} U_{Ls} &= \frac{1}{r_s^2} \sqrt{\frac{(2n+1)}{4\pi}} [n_z \nu_z + (n_x \nu_x + n_y \nu_y) c_{13}/c_{33}]; \quad m = 0 \\ r_s T_{Ls} &= \frac{1}{r_s^2} \sqrt{\frac{(2n+1)}{\pi}} [2(c_{13}^2/c_{33} - c_{11} + c_{66})(n_x \nu_x + n_y \nu_y)]; \quad m = 0 \\ U_{Ms} &= \frac{1}{2r_s^2} \sqrt{\frac{(2n+1)}{4\pi n(n+1)}} [\pm (n_z \nu_x + n_x \nu_z) - i(n_y \nu_z + n_z \nu_y)]; \quad m = \pm 1 \\ r_s T_{Ms} &= \frac{1}{r_s^2} \sqrt{\frac{(2n+1)}{4\pi}} (c_{11} - c_{66} - c_{13}^2/c_{33})(n_x \nu_x + n_y \nu_y); \quad m = 0 \\ &= \frac{c_{66}}{2r_s^2} \sqrt{\frac{(2n+1)(n+2)(n-1)}{4\pi n(n+1)}} [(-n_x \nu_x + n_y \nu_y) \pm i(n_x \nu_y + n_y \nu_x)]; \quad m = \pm 2. \end{aligned} \quad (5.26)$$

We point out that there are slight differences on the factors related to n between equation (5.26) and those in Takeuchi and Saito (1972). This is due to the different definitions of the spherical functions. Also, there is a typo in sign for the source function expression of the N -type in Takeuchi and Saito (1972), which has been corrected here. Source functions of other types (i.e. single couple, double couple, etc) can be found in Takeuchi and Saito (1972) and Kagan (1987a, 1987b).

5.3. Solutions in purely elastic and layered spheres

5.3.1. Elastostatic homogeneous or layered spheres. Static deformation of an isotropic or TI sphere can be analytically solved by neglecting the density- (thus the gravity) and c_{iner} -related terms in equations (5.13) and (5.14). For deformation in spherical domains, a good reference from the mathematical point of view is the book by Lure (1964) where the spherical system of vector functions were used and some general solutions were presented. We discuss the surface and internal loading cases below.

Case 1. Under surface loading. For a uniform isotropic sphere under non-symmetric loading, the general solutions in terms of the spherical system of vector functions were derived by McClung (1989). Caputo (1961, 1962) derived the analytical solution and presented numerical examples for a layered isotropic elastic sphere under an axially symmetric surface mass distribution. Based on the state-space method and variables separation techniques, Chen and Ding (2001b) and Chen *et al* (2001) investigated, respectively, the static deformation of multilayered elastic and piezoelectric spheres. Heyliger and Wu (1999) derived an analytical solution for the radial deformation of a layered piezoelectric sphere, and most recently by Chen *et al* (2015) for the static deformation of layered magnetoelastoelectric spheres. We mention that most analytical solutions are for the spherically isotropic or TI materials. However, since the method in Heyliger and Wu (1999) is based on the discrete-layer method, their approach can be applied to the general anisotropic material, including the TI elastic and also the isotropic elastic as special cases. Notice that besides its important application in geophysics, the surface GFs in an elastic

sphere can be applied to the important contact problem in mechanics (Titovich and Norris 2012).

Case 2. Under internal loading. More specifically under internal dislocations, the deformation of the elastic (layered) sphere was also investigated. This includes the dislocation loop and screw dislocation in an elastic sphere (Willis *et al* 1983, Polonsky *et al* 1991) and circular dislocation loop in an elastic sphere and a spherical shell (Bondarenko and Litoshenko 1997, Kolesnikova and Romanov 2010, Kolesnikova *et al* 2013). For a static dislocation in a homogeneous and isotropic spherical earth, Ben-Menahem *et al* (1969, 1970) derived the analytical solution for both concentrated and finite dislocations. The latter paper by Ben-Menahem *et al* (1970) is particularly important since it solved and presented numerical results within a homogeneous and purely elastic isotropic sphere by finite strike-slip fault and dip-slip fault. This analytical solution is analogous to Okada (1992) for a homogeneous half-space with finite fault, and as such, it is extremely important. Unfortunately, there is no computer code available for such an important contribution. For the corresponding isotropic and layered earth, Singh (1972) derived the analytical static deformation caused by a concentrated internal dislocation and Pollitz (1996) superposed the point-dislocation GFs to find the finite-fault induced co-seismic deformation. Pollitz (1992) also analyzed the post-seismic relaxation in layered earth with a linear Maxwell rheology by finite fault based on the NME method (Schapery 1962), and studied the gravity anomaly from faulting in a layered spherical earth using the decoupled model between elastic and gravitational deformations (Pollitz 1997a). A FORTRAN code, named STATIC1D, was also developed by Pollitz.

Based on the analytical solution of the static deformation in a homogeneous and isotropic spherical Earth, Tang and Sun (2018a) recently derived the closed-form expressions of the viscoelastic dislocation Love number and the corresponding GFs due to concentrated dislocations within a homogeneous Maxwell Earth model. While the solution neglects the coupling between the elastic and gravitational fields, it serves as important benchmark for analyzing viscoelastic deformation in the real Earth. Based on the derived formulation, the surface loading Love number and the corresponding GFs can be also derived.

5.3.2. Time-harmonic deformation and waves in homogeneous or layered elastic sphere. Two good references on waves and vibrations in a homogeneous sphere are the books by Lure (1964) and Eringen and Suhubi (1974) where the solutions were expressed in terms of the spherical system of vector functions with the coefficients being spherical Bessel functions of the first and second kind, or a linear combination of them.

While free vibration of a given finite body (and further the corresponding dispersion curve) is not a GF problem, it is important and very fundamental from the following point of view: (1) it helps to invert the material property of the body,

as in the classical work by Lamb (1882) for the elastic sphere, and many works followed on various basic issues of vibration of an elastic sphere, i.e. the series work by Sato and colleagues (Sato and Usami 1962a, 1962b, Sato *et al* 1962, 1963); (2) the eigenvalues (i.e. the eigen-frequency or natural frequency) and eigen-modes of the free vibration can be superposed to solve the corresponding forced (time-harmonic) vibration or deformation, i.e. the GFs induced by the concentrated unit time-harmonic source. In physics and material engineering, the vibration features of a given finite body (spherical or rectangular shapes) derived and observed can be correlated to determine the effective properties of the medium, particularly the anisotropic elasticity coefficients of the body (Ohno 1976, Ohno *et al* 1986, Visscher *et al* 1991). This further has particular applications to the nanoscale objects, like nanoparticles (Saviot *et al* 2004, Saviot and Murray 2005, 2009).

In geophysics, Bhattacharya (1976, 2005) studies the waves and calculated the synthetic seismograms induced by general discontinuities in layered spheres by assuming that in each layer the density as well as the compressional and shear wave velocities were certain functions of the radial coordinate r . Bhattacharya (1978) also solved the Rayleigh waves from a point source in the layered sphere using the analytical solution in each layer in terms of the spherical Bessel functions, i.e. the one similar to Gilbert and Backus (1968) and McClung (1991). Complete synthetic seismograms for a TI earth were also numerically computed by Friederich and Dalkolmo (1995) with the corresponding program code called GEMINI.

In mechanics community, McClung (1991) derive the solution for the general (or asymmetric) vibration of a homogeneous and isotropic elastic sphere. Chen and colleagues (Chen 2000, 2001, Chen and Ding 2001a, Chen *et al* 2002) proposed the state-space method and the Taylor's expansion theorem for the free vibration of multi-layered TI hollow piezoelectric spheres, which contain the purely elastic solutions as special cases. Radial vibration of piezoelectric and magnetic hollow spheres was also solved by Wang and Ding (2007). Norris and Shuvalov (2012) studied the time-harmonic vibration in radially inhomogeneous TI sphere using the Stroh formalism. Qiao *et al* (2016a, 2016b) analytically derived the solutions for the coated elastic spherical shell or the functionally graded spherical shell. It is noted that the analytical approach applies only to the TI material. For the general material anisotropy, other semi-analytical methods need to be applied, such as the discrete-layer model developed by Heyliger *et al* (1994), which has been applied to layered, functionally graded and piezoelectric spheres by Heyliger and Wu (1999) and Wu and Heyliger (2001) and to the magneto-electroelastic layered spheres by Heyliger and Pan (2016). This discrete-layer model requires discretization in r -direction only, whilst in the other two directions, known shape functions are used so that it is more accurate and efficient than the direct FEM.

5.4. Surface loading Love numbers and GFs in elastostatic and viscoelastic self-gravitational and layered Earth

Earth deformation in response to external (surface) mass loading has been an exciting and fundamental research topic

in geophysics since Love (e.g. Love (1911), Farrell (1972), Spada *et al* (2011), Wang *et al* (2012), and references therein). GFs to concentrated surface loading can be applied to broad areas of Earth science, including atmospheric loading (i.e. Merriam (1992), Guo *et al* (2004), Petrov and Boy (2004), Tregoning and van Dam (2005), Gitlein *et al* (2013), Mikolaj *et al* (2016)), tidal ocean loading (i.e. Agnew (1996, 1997), Yuan *et al* (2013) and Martens *et al* (2016)), non-tidal ocean loading (i.e. Williams and Penna (2011)), continental water storage (i.e. Bevis *et al* (2005), Fu *et al* (2012), Wahr *et al* (2013) and Argus *et al* (2014b)) and ice mass loading (i.e. Khan *et al* (2007), Marzeion *et al* (2012) and Pfeffer *et al* (2014)). The 2002 review on the IERS workshop by Plag and van Dam (2002) summarized the status and remaining scientific issues related to surface loading on the Earth where the ELLNs are the key elements. A recent review on the important applications of GFs can be found in the EOS report by Melini *et al* (2015).

Besides the elastic deformation, time-dependent response (viscoelastic deformation) of the Earth is also important for us to understand the history of the Earth. For instance, the glacial isostatic adjustment (GIA) information could be applied to different fields related to Earth: oceanography as related to relative sea level change, space gravity as mass redistribution and balance, and geodynamics as related to Earth rheology. We review the elastostatic and viscoelastic surface loading Love numbers and GFs below separately.

5.4.1. Elastostatic loading Love numbers and GFs. Since Love (1911), other earlier contributions on surface loading on the Earth were by Stoneley (1926), Takeuchi (1950) and Slichter and Caputo (1960). For the elastic earth with gravity under surface load, Love (1911) induced the dimensionless quantities (or numbers) h and k to describe the earth tide, and Shida (1912) added the number l . Together, they are sometimes called Love and Shida numbers (Krásná *et al* 2013), or most commonly just called Love numbers. One needs to keep in mind that besides the surface loading Love numbers, there are also the tidal Love numbers which relate to the deformation of the sphere by luni-solar tidal force (Wahr 1981) and the DLNs to be discussed below. Besides the existing relations between the tidal and surface-loading Love numbers (Molodensky 1977, Pan and Ding 1986), the tidal Love number is further physically significant in astronomical systems (Yip and Leung 2017), particularly the I-Love-Q relation (Yagi and Yunes 2013, 2014, 2017) which can be applied to astrophysics, fundamental physics, and gravitational waves (Abbott *et al* 2016). The relation between the surface loading Love number and the dislocation Love number has been also useful as to be discussed later.

For elastic, self-gravitational and layered Earth, Longman (1962, 1963) derived the GFs for the first time where the radius-dependent coefficients in the first-order differential equation system (i.e. the matrix $[A(r)]$ in equation (5.11)) were solved numerically. Farrell (1972) provided a well-written review where the singularity issue at the source point and thus the convergence issue with large degree n were also

discussed. Two important approaches were suggested to calculate the ELLNs and to speed up the convergence of the series summation in the GF expression: The disc factor instead of the concentrated delta function loading and the Euler's transformation on the summation of an alternating series. Furthermore, Farrell (1972) derived the analytical expressions for the ELLNs at infinity and proposed the Kummer's transformation for the series summation. In terms of this transformation, each term of the series is subtracted by the ELLNs at infinity and then added back. For instance, the series terms containing h_n will be replaced by two series with $(h_n - h_\infty)$ and h_∞ , where the first series related to $(h_n - h_\infty)$ behaves well and the second one related to h_∞ has exact closed-form expression. Published in the same year as Farrell's review paper, the paper by Takeuchi and Saito (1972) is an equally important reference where, while it concentrated on seismic waves, solutions in both layered half-space and layered sphere were presented including further various source functions.

So far the surface loading problem in a layered elastic (or viscoelastic) and self-gravitating Earth has been solved analytically only for the case of an incompressible Earth, while the compressible case is usually solved numerically (e.g. Farrell (1972), Guo *et al* (2004)), except for the work by Gilbert and Backus (1968) where the gravity in each layer of the Earth was characterized as a linear function of the radial coordinate r . While the analytical solutions based on the Gilbert–Backus formulation can be extended to the layered spherical Earth, such an approximation would be unsatisfactory at low harmonic degrees and if the contribution of the internal buoyancy modes could not be neglected (Cambiotti *et al* 2009).

Pan *et al* (2015b) proposed an analytical approach for solving the layered earth problem with gravity and under concentrated surface loading. In their paper, a simple and reasonable assumption was made on the density and gravity in the layer which guarantees an analytical solution. Furthermore, the effect of material anisotropy was first analyzed in that paper. In a more recent paper, based on the analytical solution of Pan *et al* (2015b), Chen *et al* (2018b) introduced the stiffness matrix method (SMM), and by doing so, they can basically calculate the ELLNs to any degree one wishes. Thus, with this new analytical solution and the corresponding MATLAB code ELLNs.m, one can calculate all the ELLNs and thus the corresponding GFs under surface loading.

5.4.2. Viscoelastic loading Love numbers and GFs. To understand the history of the Earth, the viscoelastic response of the Earth under time-dependent surface loading is required (i.e. Mitrovica and Peltier (1991), Peltier (2004), Purcell *et al* (2011, 2016), Argus *et al* (2014a and 2014b) and Peltier *et al* (2015)). It was discussed in section 2 that the viscoelastic response can be solved by applying the correspondence principle if the involved problem is linear. When time is involved, the point force (or mass) on the surface would depend not only on the space location on the surface but also on time. In studying the viscoelastic surface GFs, the time-dependence of the point force can be either impulsive, i.e. proportional to $\delta(t)$ or Heaviside, i.e. proportional to $H(t)$.

Assuming that the earth's time-dependence can be described by a Maxwell body, Peltier (1974) first solved the impulsive response of the layered earth (i.e. the concentrated force on the surface is proportional to $\delta(t)$). The Laplace-domain (i.e. the s -domain) solutions were derived by the correspondence principle and the time-domain solutions were obtained using the simple NME method as proposed by Schapery (1962). This NME method was refined later by Wu and Peltier (1982), Sabadini *et al* (1982), and Peltier (1985). Besides the Maxwell model, other linear viscoelastic models of the Earth were also studied, i.e. Han and Wahr (1997) for anisotropic viscosity and Spada (2008) for many other linear rheological laws. Spada (2008) has also developed a FORTRAN program, called ALMA, for these different rheological models.

While the NME method is analytical and provides an analytical solution directly in terms of time t , its application to multilayered and/or compressible earth is not feasible as investigated in details, say by Tanaka *et al* (2006) and Spada and Boschi (2006). To overcome the numerical difficulties, Tanaka *et al* (2006) proposed to evaluate the inverse Laplace integration numerically by changing the integration path in the complex plane so that it includes all the poles. Spada and Boschi (2006), on the other hand, proposed the Post–Widder–Gaver (PWG) approach.

Just like any integral transform, a better method needs to be explored for carrying out the inverse Laplace transform. As is well known, besides the NME method of Schapery (1962), several numerical algorithms have been already proposed to carry out the inverse Laplace transform (Weeks 1966, Dubner and Abate 1968, Stehfest 1970, Durbin 1974, Talbot 1979, De Hoog *et al* 1982, Honig and Hirdes 1984). Furthermore, comparisons among different algorithms can be found in Bellman *et al* (1966), Davies and Martin (1979), Duffy (1993), Cohen (2007), and Kuhlman (2013), Naeni *et al* (2015) and Wang and Zhan (2015). It seems that the Fourier series method works for the most common time behaviors and is more robust than others, whilst the involved free parameters can be found optimally as in Honig and Hirdes (1984). Furthermore, Honig and Hirdes (1984) adopted three different algorithms to accelerate the convergence of the Fourier series and published the LAPIN code in FORTRAN. The code was recently converted into MATLAB and applied to post-seismic deformation by a fault (Molavi Tabrizi and Pan 2015). The Fourier series expansion method was made automatic by D'Amore *et al* (1999a, 1999b) and again coded in FORTRAN as INVLTF. This automatic routine code was claimed to be faster than LAPIN by factors of 6 to 7. All these indicate that the Fourier series based method could be adopted and applied to the viscoelastic response of the spherically (and flatly) layered earth under surface loading and by internal dislocation.

5.5. DLNs and GFs in elastostatic and viscoelastic self-gravitational and layered Earth

Besides the surface loading on the Earth surface, another important type of loading is due to the internal earthquake or internal dislocation (fault). Thus, both elastic and viscoelastic

response of the layered Earth to the dislocation has important applications in geophysics.

To solve the internal loading response of the Earth, the following two approaches can be applied: (1) making use of the surface load GFs derived in previous sub-section 5.4 via Betti's reciprocity or (2) directly deriving the new dislocation-induced GFs. For approach one, they can be related by using equation (2.28), which relates the force-induced stress to the dislocation-induced displacement. Equation (2.28) indicates that in order to find the surface displacement induced by an internal dislocation, one needs only to solve the surface force-induced stress at the location where the internal dislocation is located (at $\mathbf{r} = \mathbf{r}_s$). The reciprocity theorem in spherical earths can be also found in Boschi (1973) and Pan and Ding (1986). We point out that it was Okubo (1993) who derived the important relations between point dislocation and the force (tidal and surface loading), which was further investigated by Sun and Dong (2013). More specifically, the spherical coefficients (say for the *LM*-type) \mathbf{U} and \mathbf{T} on the surface $r = a$ due to a point dislocation buried at $\mathbf{r} = \mathbf{r}_s$, can be expressed in terms of the tidal/surface load induced coefficients \mathbf{U} and \mathbf{T} at $\mathbf{r} = \mathbf{r}_s$. This gives the relation between the ELLNs and DLNs via reciprocity. The second approach is to derive directly the dislocation solution induced by the dislocation source function. We review the main contributions in terms of elastostatic and viscoelastic deformation separately below.

5.5.1. Elastostatic DLNs and GFs. While Takeuchi and Saito (1972) presented the general formulation, the detailed derivation and solution for the point-dislocation GFs within an elastic, gravitational and layered spherical earth was first derived by Sun (1992a, 1992b). More specifically, Sun (1992a, 1992b) defined and derived the DLNs and the corresponding GFs in terms of four independent point-dislocation sources in such an earth model. Sun (1992a, 1992b) further proposed a truncation criterion for the infinite DLNs series in order to accurately and efficiently calculate the GFs via superposition. Sun's solution has been analyzed and applied extensively to various problems. First, the point-dislocation GFs was presented by Sun and Okubo (1993, 1994, 1995) for layered spherical earth with isotropic elasticity in each layer. These studies contain two parts: The DLNs and the corresponding GFs where the DLNs are the expansion coefficients and GFs are the point-dislocation-induced elastic displacement, gravity change, etc within the earth (Sun *et al* 1996). These GF solutions were then extended to the finite fault case (by superposition) by Sun and Okubo (1998). Applications can be found for co-seismic deformations and/or gravity changes induced by the earthquakes in Alaska and Hokkaido (Sun and Okubo 2004), the Chi–Chi and Kunlun earthquakes (Fu and Sun, 2004), Sumatra–Andaman earthquake (Fu and Sun 2006), Wenchuan earthquake (Wang *et al* 2010), Tohoku–Oki earthquake (Sun and Zhou 2012, Zhou *et al* 2012, 2014), and L'Aquila earthquake (Cambiotti *et al* 2017). The possibility of determining the DLNs using GRACE satellite mission gravity data was investigated by Yang *et al* (2015). The changes in Earth rotation, Earth volume, and coseismic gravitational potential energy

due to dislocations were studied, respectively, by Xu and Chao (2017), Xu and Sun (2014) and Xu *et al* (2014).

In order to apply the point-dislocation GFs, one needs their accurate analytical expressions. Unfortunately, since these GFs contain infinite series in degree n (of the spherical harmonics), summation to infinity is impossible in general. For the surface loading case, one can derive the exact-closed form ELLNs at infinity (Farrell 1972). For the problem with internal loading, it is different. Starting from Okubo (1988), who first presented six sets of independent asymptotic solutions, various efforts have been made to derive the asymptotic and closed-form GFs (Sun 2003, 2004a, 2004b, Tang and Sun 2017). Takagi and Okubo (2017) proposed further a new method to calculate all the GFs (displacements, strain, etc) in a uniform sphere with better convergence.

The effect of Earth layering, gravity and curvature on the co-seismic (or post-seismic) deformation has been actively studied (Sun and Okubo 2002, Dong *et al* 2014, 2016). Through numerical examples, Dong *et al* (2014) showed that, for a typical earthquake located at a depth less than 100 km, the largest effect on the dislocation-induced deformation is the Earth layering, followed by gravity, with the curvature effect being the least. However the curvature effect can be as large as 30% if the fault source location is deep (i.e. around 400 km), and it is the largest in the far-field deformation (Dong *et al* 2016).

The relative contribution from different coupling terms was first investigated qualitatively by Segall (2010) who normalized the elastic-gravitational governing equation by introducing the so-called ‘big G ’ term (proportional to G and distance squared as Gd^2) and ‘little g ’ (proportional to g and distance as gd). Regarding d as the distance from the source to the observation station, it was found that for most co-seismic applications where the observation is at tens of km to at most a few hundred km from the source, the big G terms can be safely neglected, and even the little g effect is small (Pollitz 1997b, Segall 2010, Gomez *et al* 2017). However, for a very large earthquake, its effect can be thousand km away, and consequently, the little g and even the big G may need to be included (Gomez *et al* 2017).

It should be mentioned that very recently, Zhou *et al* (2019) derived analytical expressions of the DLNs for a layered, spherical, TI and self-gravitating Earth. This solution is based on the spherical system of vector functions (or the VSHs) and the new DVP method presented above, instead of the SMM used in Chen *et al* (2018b). The DLNs can be obtained with high accuracy to an arbitrarily high degree, thereby allowing a wide range of applications based on high resolution Earth models. Compared to the traditional numerical integration approach, the analytical solution by Zhou *et al* (2019) is at least three orders of magnitude faster. An MATLAB code for computing the analytical DLNs is also provided, along with a user manual.

5.5.2. Viscoelastic DLNs and GFs. Pollitz (1997b) derived the dislocation GF solutions and studied the gravitational and viscoelastic post-seismic relation in layered spherical Earth. Since there was only one viscoelastic layer, the time-domain

solution can be expressed in terms of the NME method (Schapery 1962). To overcome the numerical instabilities, the method of second-order minors was used (Gilbert and Backus 1966, Takeuchi and Saito 1972). Once the viscoelastic GFs were derived (due to a concentrated point dislocation), viscoelastic response to a finite fault can be superposed by numerical integration over the fault. A FORTRAN program called VISCO1D-v3 was developed and it can be applied to analyze large earthquake-induced post-seismic deformation of the global Earth (i.e. Pollitz *et al* 2006).

Making use of the reciprocity relation (Okubo 1993, Sun and Dong 2013), Tang and Sun (2018b) derived the asymptotic GF solutions of the co- and post-seismic displacements in a homogeneous Maxwell and gravitational sphere. Since the asymptotic solutions are analytical in terms of source/field positions and time, they are good benchmarks for various numerical methods proposed for Earth deformation modeling (involving series summation truncation and/or numerical inverse Laplace transform).

5.6. Time-harmonic waves and seismograms in elastic, self-gravitational and layered Earth

For this general case, i.e. in equation (5.1), we keep the inertia term (c_{iner}). We mention that Gilbert and Backus (1968), Smylie and Mansinha (1971) and Dahlen (1972) have contributed to the formulation. Furthermore, Gilbert and Backus (1968) derived the analytical solutions under the assumptions of constant density and linear gravity (as $g(r) = g_0 r$) in each isotropic layers (with constant density and elastic moduli). Saito (1967) presented a theory on calculating the amplitudes of the free oscillations caused by a point source in a spherically symmetric earth model, as also the classic paper by Takeuchi and Saito (1972) on seismic surface waves in layered earth.

Qureshi and Bhattacharya (2008) derived the solutions for Rayleigh wave (LM -type) with gravity in a radially heterogeneous isotropic and spherical Earth where the heterogeneity for the density, gravity and two Lamé coefficients were assumed to be special functions of r so that an analytical solution of the time-harmonic wave can be obtained. Al-Attar and Woodhouse (2008) calculated the seismic displacement fields in self-gravitating earth models by applying the minors vectors and symplectic structure method. The solution is stable and it can be applied to the TI PREM earth model (Woodhouse and Deuss 2007). More recently, Wang *et al* (2017) presented the complete formulation and further published the FORTRAN code QSSP for seismic waves in layered and gravitational Earth.

5.7. Future GFs and analytical solutions

This section contains a large and important topic and so many earth scientists have contributed to the development of the GFs and analytical solutions. Yet GFs or analytical solutions in the new horizons are waiting for us to explore, as briefly discussed in the following three key areas.

It is well-known that the upper mantle of the earth is elastically anisotropic (Dziewonski and Anderson 1981, Marone

and Romanowicz 2007, Lebedev and van der Hilst 2008, Kustowski *et al* 2008, Long and Becker 2010). The question is: would the upper mantle be viscously anisotropic? McNamara *et al* (2002) reported the development of anisotropic structures even in the Earth's lower mantle by solid-state convection. Hansen *et al* (2012) measured the viscous anisotropy of upper mantle materials olivine aggregates in their laboratory, which were consistent with previous reports (Durham and Goetze 1977, Durham *et al* 1977, Honda 1986, Christensen 1987, Lev and Hager 2008a). Hansen *et al* (2016a, 2016b) further studied the viscous anisotropy of textured olivine aggregates, both experimentally and analytically. These new anisotropic viscosity models include both normal and shearing viscosities, and it was further reported that the normal viscosity value could be much larger than the shear, 10–15 times large (Hansen *et al* 2012)! Therefore, it would be very appealing to develop a consistent anisotropic viscoelastic model so that it can simulate the correct mantle behavior and thus predict the accurate GIA observed on the surface of the Earth. However, since a consistent anisotropic viscoelastic model has to satisfy certain conditions as discussed by Carcione (1990), so far, there is still no available reliable anisotropic viscoelastic model for the Earth's long-term response, such as the GIA, not to mention the corresponding GFs. Also in Earth's mantle, the deformation mechanism of the olivine-rich rocks there could be further associated with disclinations (Cordier *et al* 2014). This would require us to apply the GFs of the disclinations which relates to the relative rotational displacements, instead of the translational displacements (as in the dislocation case) of the two surfaces of the fault. Fundamental theories and the corresponding solutions in deWit (1973a, 1973b, 1973c) and Romanov and Vladimirov (1992) would be the starting point to explore the possible GFs and analytical solutions.

Closely related to the Earth gravitational elasticity and viscoelasticity is on the gravitational instability. It was Love (1911) who first derived analytically the gravitational instability condition for a homogeneous, hydrostatically pre-stressed and self-gravitating elastic sphere. When analyzing the corresponding viscoelastic spherical Earth, the instability condition is termed as Rayleigh–Taylor stability (Plag and Juttner 1995). Vermeersen and Mitrovica (2000) revisited Love's elasticity instability condition, and extended it to both homogeneous and layered Earth with Maxwell viscoelastic model. For a homogeneous viscoelastic sphere, they concluded that the instability condition is independent of viscosity and only occurs when the corresponding elastic sphere is already unstable (Vermeersen and Mitrovica 2000). In terms of the NME method, Han and Wahr (1995) and Fang and Hager (1995) were able to distinguish two types of important modes: The advection or the viscosity mode due to the viscosity jump between adjacent layers, and the buoyancy mode due to the density jump between adjacent layers. It was shown that due to the existence of infinite (or continuous) modes in layered viscoelastic and gravitational Earth, the NME method would be no longer valid (Fang and Hager 1995, Han and Wahr 1995). By assuming that the Earth is made of a homogeneous and compressible viscoelastic half-space under initial stress (i.e. the gravity), Klemann *et al* (2003) were able to

carry out detailed analyses by distinguishing various different forces associated with different sources (viscous, initial stress, density discontinuity, etc). Based on a Maxwell Earth model and in terms of also the NME method, Cambiotti *et al* (2009) analyzed the relative role and importance of the advection and buoyancy force using both the analytical solution of Gilbert and Backus (1968) and the numerical Runge–Kutta scheme. For the layered Maxwell earth models, Cambiotti and Sabadini (2010) further studied the effect of compressional and compositional stratifications on the viscoelastic relaxation modes and identified a new class, called the compositional C-modes. More recently, Mondal and Korenaga (2018a, 2018b) investigated the Rayleigh–Taylor instability for both a two-layered self-gravitating viscous sphere and the corresponding multi-layered sphere. The growth rate of this instability is important to understand the formation and dynamics of the Earth and other planets. While Earth anisotropic viscosity is important, only Lev and Hager (2008b) considered its effect on stability by building a 2D FEM model. They concluded that, for investigating lithospheric instability and other possible processes in the mantle, the isotropic viscosity model, like the Maxwell model, may not be adequate, and thus an anisotropic viscous model needs to be included (Lev and Hager 2008b). Again, this calls for the GFs in the corresponding anisotropic viscoelastic, self-gravitating, and layered spherical Earth.

The third topic is on GFs and analytical solutions in 3D heterogeneous Earth. It is well known that, besides layering in the radial direction, our Earth is actually in an ellipsoidal shape and it is further laterally inhomogeneous (or laterally heterogeneous) in general. When the scale of heterogeneity is small compared to the Earth's radius (i.e. the difference between the ellipsoidal and spherical Earth is about 1/300), the perturbation method as described well in Dahlen and Tromp (1998) can be applied to derive semi-analytical solutions. Wahr (1981) studied the effect of ellipsoid on the body tide. D'Agostino *et al* (1997) presented the relation between postglacial rebound and lateral viscosity variations. Metivier *et al* (2005, 2006) investigated, respectively, the effect of ellipticity on the surface loading induced field and the atmospheric loading induced field. The effect of large mantle density heterogeneity on body tides was also carried out by Metivier *et al* (2007). Based on the eccentricity nested spherical model, Martinec and Wolf (1999) derived analytically the gravitational viscoelastic relaxation. Based on the first-order perturbation, Fu and Sun (2007) studied the effect of the ellipticity on the earth tide, and Fu and Sun (2008) and Fu *et al* (2010) presented, respectively, the semi-analytical dislocation solution of the coseismic gravity and displacement changes. However, if the heterogeneity scale is relatively large, one has to apply the numerical method to solve the corresponding boundary-value problem of the Earth, by either the FEM as in Cheng *et al* (2019) or the spectral element method as in Langer *et al* (2019).

5.8. Summary of section 5

In this section, we have reviewed all the GF solutions in spherical and layered earth, with and without gravity. Both the static and time-harmonic (vibrational) deformations are

discussed, and so is the viscoelastic GF via the correspondence principle. The concentrated source could be force and dislocation, either as Heaviside or impulsive in time. The solutions are expressed in terms of the spherical system of vector functions, and for layered sphere, in terms of the DVP method. The key application of GFs in layered spherical earth is to investigate the effect of the Earth sphericity and radial structure, which are particularly important on global deformation of the entire earth. For instance, a large earthquake would induce deformation in the far-field which cannot be simulated by the corresponding flat Earth model.

We end this section by listing several codes related to layered and spherical Earth, which have been developed for calculating both elastic and viscoelastic Love numbers and the corresponding GFs. Some of the loading Love numbers were discussed in Spada *et al* (2011), including the TABOO, PMTF, ALMA, FastLove-HiDeg, MHPLove, and VEENT (based on the numerical integration and spherical expansion), along with those using the purely numerical methods (i.e. the FEM). Recently, the analytical code ELLNs in MATLAB was published by Chen *et al* (2018a). It is based on the analytical solution by Pan *et al* (2015b) combined with the SMM (i.e. Wang and Rokhlin (2001) and Rokhlin and Wang (2002)) so that it can be applied to calculate the ELLNs to any high degree n . Pollitz published a FORTRAN code called STATIC1D for the static response induced by an internal fault (Pollitz 1996, 1997a). The corresponding viscoelastic deformation was also coded by him, named VISCO1D-v3, for calculating the post-seismic deformation caused by an internal fault (Pollitz 1997b, Pollitz *et al* 2006) with applications (Pollitz *et al* 2011). Wang *et al* (2017) published the FORTRAN code QSSP for computing the complete synthetic seismograms, with the Earth model being a very general spherically layered one which contains self-gravity with atmosphere, ocean, mantle and core interactions. Some previous existing codes were also briefly discussed in Wang *et al* (2017). Very recently, Zhou *et al* (2019) published the analytical MATLAB code DLN.m for the elastogravitational DLNs in spherically layered Earth, based on the DVP method as discussed above.

6. GF singularity in layered systems

In this section, we discuss the GF singularity and associated infinity issues in layered systems. We concentrate only on the flatly layered half-space and spherically layered earth structures. To study the singularity in GFs in a layered system, we first present the layer matrix methods involved in deriving the GFs and then analyze the associated singularity in the GF expression. Singularity can be either very pleasant or very unfriendly, in geophysics, as well as its allied fields. Therefore, mastering singularity is a must!

6.1. Various propagating matrix methods

Flatly layered half-spaces (or plates) and spherically layered structures (or particles) can be found everywhere, and as such, researchers from different engineering and science fields have

contributed to their modeling and simulation. In general, by applying the proper transformation, namely, the cylindrical system of vector functions in terms of infinite integration for flatly layered structure as in section 4 or the spherical system of vector functions in terms of infinite series summation for spherically layered structure as in section 5, one can reduce the problem to a set of ordinary differential equations for the expansion coefficients. We take the *LM*-type deformation in the elastostatic and flatly layered half-space as an example. From section 4, in each layer, the general solutions for the expansion (or transformed) displacement and traction vectors \mathbf{U} and \mathbf{T} as in equation (4.15a), are listed below for easy discussion

$$\begin{bmatrix} \mathbf{U}(z) \\ \mathbf{T}(z) \end{bmatrix} = \begin{bmatrix} \mathbf{E}_{11} & \mathbf{E}_{12} \\ \mathbf{E}_{21} & \mathbf{E}_{22} \end{bmatrix} \begin{bmatrix} \langle e^{\lambda p_{12}^* (z-z_j)} \rangle & \mathbf{0} \\ \mathbf{0} & \langle e^{\lambda p_{34}^* (z-z_{j-1})} \rangle \end{bmatrix} \begin{bmatrix} \mathbf{c}_+ \\ \mathbf{c}_- \end{bmatrix} \quad (6.1)$$

where z_{j-1} and z_j are the upper and lower interfaces of layer j , λ the transform variable (or the integral variable, which varies from 0 to $+\infty$). p_{ij}^* are the eigenvalues (four of them) and $[\mathbf{E}_{ij}]$ the corresponding eigenvectors. Both the eigenvalues and eigenvectors are functions of the frequency (for time-harmonic deformation) as well as material properties in the layer. Also, \mathbf{c}_+ and \mathbf{c}_- are the two coefficient vectors to be determined. Notice that in the corresponding spherically layered system, the degrees $n(n+1)$ in the spherical functions (in section 5) would correspond to the transform variable λ .

Since within the four eigenvalues, two of them have positive real parts and the other two negative real parts, the general solution (6.1) is well behaved. For a given layered system with a given point dislocation source, we can subdivide the source layer into two sublayers. By applying equation (6.1) to each layer and making use of the conditions at each interface (including those on the surfaces and source level), we can assemble a global system of equations for solving all the coefficients in each layer. The global matrix thus formed is stable since in each layer, there is no growing exponential term in the elements of the matrix.

However, for handling a multilayered system more efficiently and conveniently, the propagator matrix-related methods are preferable. While various methods were proposed, we only briefly review the key ones and their connections, as well as the main features among them, as further illustrated in figure 6.

The traditional propagator matrix method (PMM), which is also called the Thomson–Haskell matrix method, was proposed by Thomson (1950) and Haskell (1953). Directly applying equation (6.1) to the upper (z_{j-1}) and lower (z_j) interfaces of layer j and eliminating the involved coefficients, one obtains the following propagating relation between the two interfaces of the layer with thickness h_j

$$\begin{bmatrix} \mathbf{U}(z_j) \\ \mathbf{T}(z_j) \end{bmatrix} = [\mathbf{P}^j] \begin{bmatrix} \mathbf{U}(z_{j-1}) \\ \mathbf{T}(z_{j-1}) \end{bmatrix} \quad (6.2)$$

where

$$[\mathbf{P}^j] = \begin{bmatrix} \mathbf{E}_{11} & \mathbf{E}_{12} \\ \mathbf{E}_{21} & \mathbf{E}_{22} \end{bmatrix} \begin{bmatrix} \langle e^{\lambda p_{12}^* h_j} \rangle & \mathbf{0} \\ \mathbf{0} & \langle e^{\lambda p_{34}^* h_j} \rangle \end{bmatrix} \begin{bmatrix} \mathbf{E}_{11} & \mathbf{E}_{12} \\ \mathbf{E}_{21} & \mathbf{E}_{22} \end{bmatrix}^{-1}. \quad (6.3)$$

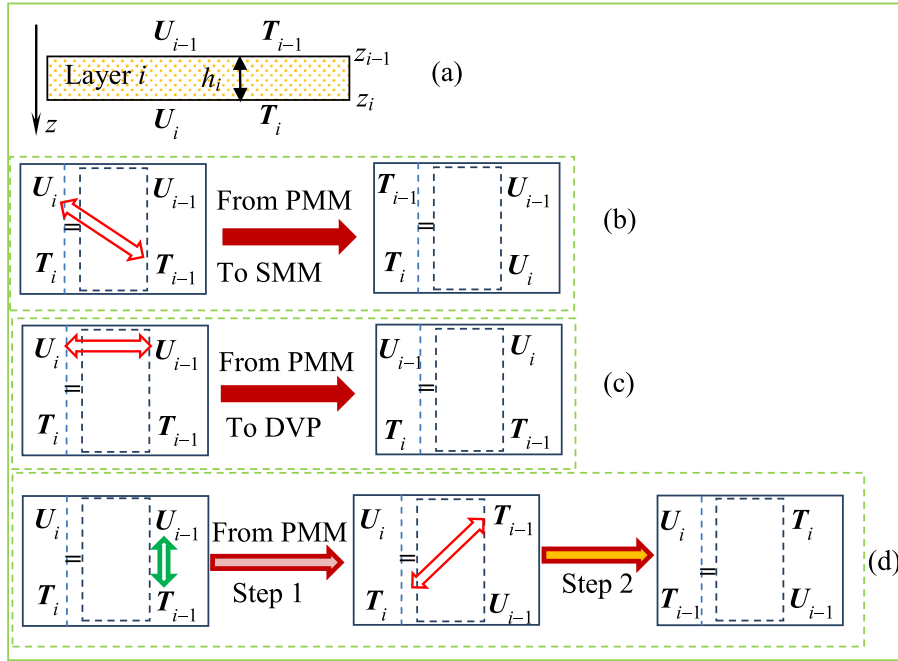


Figure 6. Various layer matrix methods and their relations. The layer geometry with the four coefficient vectors (displacement U and traction T) in (a), relation between PMM and SMM in (b), relation between PMM and DVP in (c), and a new layer matrix (which is similar to DVP in terms of their limiting behaviors) obtained via two steps switches among the four coefficient vectors in (d).

Furthermore, assuming that the interfaces between different layers are continuous (except for the surfaces and those at the source level), we can easily propagate equation (6.3) from one layer to the next to obtain the following propagating relation

$$\begin{bmatrix} U(z_{j+1}) \\ T(z_{j+1}) \end{bmatrix} = [P^{j+1}] [P^j] \begin{bmatrix} U(z_{j-1}) \\ T(z_{j-1}) \end{bmatrix} \equiv [P^{j+1j}] \begin{bmatrix} U(z_{j-1}) \\ T(z_{j-1}) \end{bmatrix}. \quad (6.4)$$

While relation (6.4) is very simple and easy in applying to the multilayered system, there is a very major issue: Noticing that since p_{ij}^* have both positive and negative real parts, this PMM relation (6.2) contains the exponentially growing term. Therefore, an overflow could occur if the integral variable λ is very large, or the layer thickness h_j is very large, or the eigenvalues p_{ij}^* (as functions of the layer material properties and also of the frequency for the time-harmonic deformation) are very large.

To overcome this problem, many methods have been proposed, with perhaps the delta matrix or minor matrix method (Dunkin 1965, Gilbert and Backus 1968) being the earliest one. In geophysics, Spencer (1960) first introduced the generalized reflection and transmission coefficients when analyzing waves in layered half-space. The detailed formulation using the reflection and transmission matrices was developed by Kennett (1974) and Kennett and Kerry (1979) for isotropic and layered media. This can be achieved by eliminating the displacement and traction vectors in the layer and expressing the reflection and transmission coefficients (similar to the coefficients c_+ and c_- in equation (6.1)) on both interfaces in terms of the reflections and transmission matrices. Fryer and Frazer (1984, 1987) extended the formulation to the general anisotropic layered media. Wang (1999) proposed a simple orthonormalization method and Ma *et al* (2012) further

compared this method with the minor matrix method and the reflection-transmission matrix method.

In mechanics, the SMM was developed by Wang and Rokhlin (2001) and Rokhlin and Wang (2002), inspired from the FEM formulation. The precise integration method (PIM) was developed by Zhong *et al* (2004), Gao *et al* (2006) and Ai and Cheng (2014). The method of reverberation-ray matrix (MRRM) was proposed by Pao *et al* (2007), and its detailed theory/formulation was presented by Chen *et al* (2011). Cai and Pan (2018) proposed the dual-boundary strategy for enhancing the solution in any layer matrix method, and compared the three common methods (i.e. PMM, SMM, and PIM). Notice that the reflection-transmission matrix method is more commonly called the generalized reflection-transmission matrix method since other components, such as the conversions of different wave types on the interface, would also contribute to the reflection and transmission coefficients (i.e. Apsel and Luco (1983), Luco and Apsel (1983) and Guzina and Pak (2001)).

Below, we briefly present the SMM and DVP methods as they are unfamiliar to geophysics and yet are very powerful approaches to avoid the exponentially growing terms in the multilayer solutions. Again, the SMM is perhaps inspired by the FEM where the forces at different locations are related to the displacements at these locations by the stiffness matrix. Similar to FEM, based on SMM, the layer matrix is expressed as

$$\begin{bmatrix} T(z_{j-1}) \\ T(z_j) \end{bmatrix} = [K^j] \begin{bmatrix} U(z_{j-1}) \\ U(z_j) \end{bmatrix} \quad (6.5)$$

where the submatrices of $[K^j]$ can be obtained from equation (6.1) by eliminating the coefficients in the layer

$$[\mathbf{K}^j] \equiv \begin{bmatrix} \mathbf{K}_{11}^j & \mathbf{K}_{12}^j \\ \mathbf{K}_{21}^j & \mathbf{K}_{22}^j \end{bmatrix} = \begin{bmatrix} \mathbf{E}_{22} & \mathbf{E}_{21} \langle e^{-\lambda p_{12}^* h_j} \rangle \\ \mathbf{E}_{22} \langle e^{\lambda p_{34}^* h_j} \rangle & \mathbf{E}_{21} \end{bmatrix} \times \begin{bmatrix} \mathbf{E}_{12} & \mathbf{E}_{11} \langle e^{-\lambda p_{12}^* h_j} \rangle \\ \mathbf{E}_{12} \langle e^{\lambda p_{34}^* h_j} \rangle & \mathbf{E}_{11} \end{bmatrix}^{-1}. \quad (6.6)$$

It can be observed that all the submatrices in $[\mathbf{K}^j]$ are regular without exponentially growing terms.

To propagate the coefficients from one layer to the next (i.e. from interface z_{j-1} to interface z_{j+1}), the following recursive relation (instead of the propagating relation (6.4)) can be derived by assuming that on their common interface z_j both displacement and traction vectors are continuous (i.e. Chen *et al* (2018a))

$$\begin{bmatrix} \mathbf{T}(z_{j-1}) \\ \mathbf{T}(z_{j+1}) \end{bmatrix} = [\mathbf{K}^{j:j+1}] \begin{bmatrix} \mathbf{U}(z_{j-1}) \\ \mathbf{U}(z_{j+1}) \end{bmatrix} \quad (6.7)$$

where

$$[\mathbf{K}^{j:j+1}] = \begin{bmatrix} \mathbf{K}_{11}^j + \mathbf{K}_{12}^j (\mathbf{K}_{11}^{j+1} - \mathbf{K}_{22}^j)^{-1} \mathbf{K}_{21}^j & -\mathbf{K}_{12}^j (\mathbf{K}_{11}^{j+1} - \mathbf{K}_{22}^j)^{-1} \mathbf{K}_{12}^{j+1} \\ \mathbf{K}_{21}^{j+1} (\mathbf{K}_{11}^{j+1} - \mathbf{K}_{22}^j)^{-1} \mathbf{K}_{21}^j & \mathbf{K}_{22}^{j+1} - \mathbf{K}_{21}^{j+1} (\mathbf{K}_{11}^{j+1} - \mathbf{K}_{22}^j)^{-1} \mathbf{K}_{12}^{j+1} \end{bmatrix}. \quad (6.8)$$

The DVP method as introduced in this review is inspired by the PIM (Zhong *et al* 2004). The layer matrix and recursive relations have been already derived in section 4.

We point out again that the layer matrix $[\mathbf{P}]$ in PMM, $[\mathbf{K}]$ in SMM, and $[\mathbf{S}]$ in DVP can all be connected with each other (see figure 6 for their relations). Actually, besides the SMM and DVP methods, there are also other methods which can be utilized to avoid the exponentially growing terms in the layer matrix (as illustrated in figure 6). The SMM and other two methods (minor matrices and orthonormalization) can be further connected to the generalized reflection and transmission matrices as shown by Wang and Rokhlin (2001) and Ma *et al* (2012)). The SMM is further unconditionally stable when the exponential factor $\lambda h p^*$ is very large (Wang and Rokhlin 2001). However, the low limit is also important. We discuss both limits below using the SMM and DVP as examples.

From equation (6.6), it can be shown that if the exponential factor $\lambda h p^*$ approaches zero (corresponding to static deformation, lower-frequency response, or very thin layer, etc), the layer matrix of SMM becomes singular whilst that of the DVP approaches an identity matrix (from equations (4.18) and (4.19)). As such, the SMM could be problematic near this limit, whilst the layer matrix in the DVP is perfectly well!

When the exponential factor $\lambda h p^*$ approaches infinity, the limits for both SMM and DVP are

$$\begin{bmatrix} \mathbf{K}_{11}^j & \mathbf{K}_{12}^j \\ \mathbf{K}_{21}^j & \mathbf{K}_{22}^j \end{bmatrix} = \begin{bmatrix} \mathbf{E}_{22} & \mathbf{0} \\ \mathbf{0} & \mathbf{E}_{21} \end{bmatrix} \begin{bmatrix} \mathbf{E}_{12} & \mathbf{0} \\ \mathbf{0} & \mathbf{E}_{11} \end{bmatrix}^{-1} = \begin{bmatrix} \mathbf{E}_{22} \mathbf{E}_{12}^{-1} & \mathbf{0} \\ \mathbf{0} & \mathbf{E}_{21} \mathbf{E}_{11}^{-1} \end{bmatrix} \quad (6.9a)$$

$$\begin{bmatrix} \mathbf{S}_{11}^j & \mathbf{S}_{12}^j \\ \mathbf{S}_{21}^j & \mathbf{S}_{22}^j \end{bmatrix} = \begin{bmatrix} \mathbf{0} & \mathbf{E}_{12} \\ \mathbf{E}_{21} & \mathbf{0} \end{bmatrix} \begin{bmatrix} \mathbf{E}_{11} & \mathbf{0} \\ \mathbf{0} & \mathbf{E}_{22} \end{bmatrix}^{-1} = \begin{bmatrix} \mathbf{0} & \mathbf{E}_{12} \mathbf{E}_{22}^{-1} \\ \mathbf{E}_{21} \mathbf{E}_{11}^{-1} & \mathbf{0} \end{bmatrix}. \quad (6.9b)$$

As such, both SMM and DVP are equally well at this limit (corresponding to a very large λ , very large layer thickness,

very large eigenvalues due to high frequency, or their combination)! Furthermore, the recursive relations based on both SMM and DVP will be also perfectly fine with the resulting matrix structure similar to the layer matrix structure in equation (6.9).

In summary, the DVP method seems to be a very reliable one in handling layered structures; no matter if it is for the static deformation or vibration, for a flatly layered half-space or a spherically layered earth. This DVP method has been further demonstrated recently by applying it to various engineering and earth science problems (Moshtagh *et al* 2017, 2018, Liu and Pan 2018, Liu *et al* 2018, Pan *et al* 2018, Zhang and Pan 2019a, 2019b, Vattre and Pan 2019, Zhou *et al* 2019).

6.2. Singularity of GFs in layered system

Even after taking care of the exponentially growing terms, the integration (for flat layering) or series summation (for spherical layering) involved in the GF solution cannot go all the way to infinity and we have to truncate the integral or summation at a prescribed error criterion. It is obvious that for the same given error criterion, the truncation (the largest integral or summation limit) will depend on the behavior of the integrand or each series term, which in turn depends on the relative position of the source and field points in the GFs. Since the physical-domain GF is singular at the source point (see section 1), numerical difficulty would occur when the field point (or observation point) is near the source point. For the layered system, we face one extra difficulty on calculating the physical-domain GF: This is when the field point is on the same z - (or r -) level (or depth) of the source point.

For layered spherical Earth under surface loading, Farrell (1972) proposed two approaches to accelerate the slowly converging series of the Legendre polynomials in the GF solution: One is the Kummer's transformation already discussed in section 5, and the disc factor (method) instead of the concentrated surface loading. Wang and Wang (2007) proposed the differential transform method which can be applied to both flatly layered and spherically layered structures (associated with infinite integration and summation, respectively). The method proposed by Wang and Wang (2007) is more efficient, except for the extremely near-source region.

It should be pointed out that the singularity in the GF is a local feature. In other words, the singularity in GF is related to the local material property only. For instance, for the half-space (or half-plane) GFs derived in section 2, one can observe that when the field point approaches the internal source point in a half-space (or half-plane), the GF variation or behavior is the same as that in the corresponding full-space (or full-plane). As such, perhaps the best and most efficient method would be to subtract out the singularity under the integration (within the summation) and then add it back after the integration (summation), similar to those in Pan *et al* (2001). Taking the flatly layered case as example, and using the vertical displacement u_z in (4.4) as example. For instance, for the source located at $(0, 0, z_s)$ and the field point (r, θ, z) in the same layer as the source, we have,

$$u_z(r, \theta, z; z_s) = \sum_m \int_0^{+\infty} U_L(z) S(r, \theta; \lambda, m) \lambda d\lambda. \quad (6.10)$$

Making use of the analytical full-space GF solution, equation (6.10) can be modified to

$$u_z(r, \theta, z; z_s) = \sum_m \int_0^{+\infty} [U_L(z) - U_L^\infty(z)] S(r, \theta; \lambda, m) \lambda d\lambda + u_z^\infty(r, \theta, z; z_s) \quad (6.11)$$

where

$$u_z^\infty(r, \theta, z; z_s) = \sum_m \int_0^{+\infty} U_L^\infty(z) S(r, \theta; \lambda, m) \lambda d\lambda \quad (6.12)$$

is the full-space GF displacement component in the physical-domain, which is expressed in terms of its transformed components. This GF (6.12) in both physical and transformed domains is in general available in exact-closed forms (i.e. for the point-force and point dislocation GFs, see Song *et al* (2019)). Since near the source location, the modified integrand within the square bracket [] in equation (6.11) becomes regular, its integration converges fast. A similar approach could be applied to the case where the source is located on the interface or surface. For this case, instead of the analytical GFs in the full-space (or full-plane), one needs to use the corresponding analytical bimaterial or half-space (half-plane) GFs in equation (6.11), which are also mostly available (Pan and Chen 2015). As for the homogeneous sphere case, Ben-Menahem and Singh (1968) derived the GF solutions in the physical domain and also in terms of the spherical system of vector functions. These expressions could be directly applied to take care of the singularity and thus to accelerate the convergence of the series summation. Alternatively, the recent approach by Zhou *et al* (2019) can be directly applied to calculate analytically the limit values of the DLNs (and also the ELLNs) so that combining with the Kummer's transformation, one can take care of the singularity in the GF expression.

6.3. Summary of section 6

Due to the inherent singularity in GF (when field point approaches source point), GF solution in layered systems has been always a challenge. For the flatly layered half-space and spherically layered earth structure, the GF is expressed, respectively, in terms of infinite integral (say via the cylindrical system of vector functions) or infinite series summation (via the spherical system of vector functions). When the field point is close to the source, the integral or series summation needs to be carried out all the way to a very large value. Besides this, both the integrand function and series term are oscillatory and slowly convergent. As such, the first step in dealing with the GF in a layered system is to make sure that the layer matrix and its recursive relation are very stable everywhere, with some of these matrices being discussed in section 6.1. The second step, if possible, is to subtract out the singularity (which is local) so that the involved integrand or series term becomes regular, thus converges fast, as studied in section 6.2.

Statements and Acknowledgements

While the author has tried his best to review the important and key contributions relevant to the topic, there may be articles still missing. For this, the author apologizes and will certainly include the missing one(s) in his future related articles. As such, the author encourages readers to communicate with him by sharing their works. The author's works on GFs have been greatly influenced and advanced by collaborating with many colleagues (including his former students) as cited in this review. Furthermore, in preparing this article, the author has also received tremendous help/support from many colleagues and scientists: X Chen, W A Griffith, H Hu, W Sun, R Wang, J Zhou from geophysics; J J Liao, C D Wang, and Z Q Yue from civil engineering; A Vattre from material science; and W Q Chen from mechanics. This topic review is encouraged and recommended by Editor M Bevis.

Appendix. Basic mathematical operators and systems of vector functions

Two important references on different systems of vector functions are the books by Ben-Menahem and Singh (1968) and Ulitko (1979). Many useful mathematical expressions in different systems of vector functions can be also found in Morse and Feshbach (1953). Here we just list the most important and commonly used relations.

A.1. Three systems of coordinates

The definitions for the Cartesian, cylindrical and spherical coordinate systems are shown, respectively, in figures A1–A3 for easy reference.

A.2. Basic mathematical operators (vector gradient, cross product, Laplace, divergent)

A.2.1. Gradient of a scalar function f in Cartesian, cylindrical, and spherical coordinates

$$\begin{aligned} \nabla f &= \frac{\partial f}{\partial x} \mathbf{e}_x + \frac{\partial f}{\partial y} \mathbf{e}_y + \frac{\partial f}{\partial z} \mathbf{e}_z \\ \nabla f &= \frac{\partial f}{\partial r} \mathbf{e}_r + \frac{\partial f}{r \partial \theta} \mathbf{e}_\theta + \frac{\partial f}{\partial z} \mathbf{e}_z \\ \nabla f &= \frac{\partial f}{\partial r} \mathbf{e}_r + \frac{\partial f}{r \partial \theta} \mathbf{e}_\theta + \frac{\partial f}{r \sin \theta \partial \varphi} \mathbf{e}_\varphi. \end{aligned} \quad (A.1)$$

A.2.2. Divergence of a vector function \mathbf{u} in Cartesian, cylindrical, and spherical coordinates

$$\begin{aligned} \nabla \cdot \mathbf{u} &= \frac{\partial u_x}{\partial x} + \frac{\partial u_y}{\partial y} + \frac{\partial u_z}{\partial z} \\ \nabla \cdot \mathbf{u} &= \frac{\partial(r u_r)}{r \partial r} + \frac{\partial u_\theta}{r \partial \theta} + \frac{\partial u_z}{\partial z} \\ \nabla \cdot \mathbf{u} &= \frac{1}{r^2} \frac{\partial(r^2 u_r)}{\partial r} + \frac{1}{r \sin \theta} \frac{\partial(\sin \theta u_\theta)}{\partial \theta} + \frac{1}{r \sin \theta} \frac{\partial u_\varphi}{\partial \varphi}. \end{aligned} \quad (A.2)$$

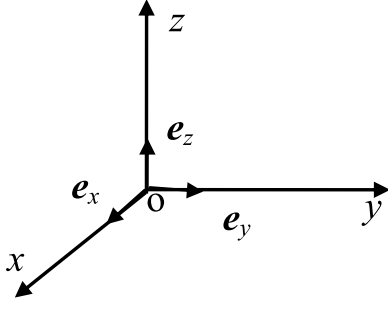


Figure A1. Cartesian coordinates (x, y, z) , with $-\infty < x, y, z < \infty$.

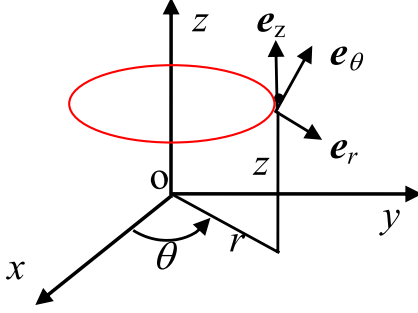


Figure A2. Cylindrical coordinates (r, θ, z) , with $0 \leq r < \infty$, $0 \leq \theta < 2\pi$, $-\infty < z < \infty$.

A.2.3. Cross-product of gradient operator vector and a vector function \mathbf{u} in Cartesian, cylindrical, and spherical coordinates

$$\begin{aligned}\nabla \times \mathbf{u} &= \left[\frac{\partial u_z}{\partial y} - \frac{\partial u_y}{\partial z} \right] \mathbf{e}_x + \left[\frac{\partial u_x}{\partial z} - \frac{\partial u_z}{\partial x} \right] \mathbf{e}_y + \left[\frac{\partial u_y}{\partial x} - \frac{\partial u_x}{\partial y} \right] \mathbf{e}_z \\ \nabla \times \mathbf{u} &= \left[\frac{\partial u_z}{r \partial \theta} - \frac{\partial u_\theta}{\partial z} \right] \mathbf{e}_r + \left[\frac{\partial u_r}{\partial z} - \frac{\partial u_z}{\partial r} \right] \mathbf{e}_\theta + \left[\frac{\partial(r u_\theta)}{r \partial r} - \frac{\partial u_r}{r \partial \theta} \right] \mathbf{e}_z \\ \nabla \times \mathbf{u} &= \frac{1}{r \sin \theta} \left[\frac{\partial(\sin \theta u_\varphi)}{\partial \theta} - \frac{\partial u_\theta}{\partial \varphi} \right] \mathbf{e}_r \\ &+ \left[\frac{1}{r \sin \theta} \frac{\partial u_r}{\partial \varphi} - \frac{1}{r} \frac{\partial(r u_\varphi)}{\partial r} \right] \mathbf{e}_\theta + \left[\frac{\partial(r u_\theta)}{r \partial r} - \frac{\partial u_r}{r \partial \theta} \right] \mathbf{e}_\varphi.\end{aligned}\quad (\text{A.3})$$

A.2.4. Laplacian of any scalar function f in Cartesian, cylindrical, and spherical coordinates

$$\begin{aligned}\nabla^2 f &= \frac{\partial^2 f}{\partial x^2} + \frac{\partial^2 f}{\partial y^2} + \frac{\partial^2 f}{\partial z^2} \\ \nabla^2 f &= \frac{\partial}{r \partial r} \left(r \frac{\partial f}{\partial r} \right) + \frac{\partial^2 f}{r^2 \partial \theta^2} + \frac{\partial^2 f}{\partial z^2} \\ \nabla^2 f &= \frac{\partial}{r^2 \partial r} \left(r^2 \frac{\partial f}{\partial r} \right) + \frac{1}{r \sin \theta} \frac{\partial}{\partial \theta} \left(\sin \theta \frac{\partial f}{r \partial \theta} \right) + \frac{1}{r^2 \sin^2 \theta} \frac{\partial^2 f}{\partial \varphi^2}\end{aligned}\quad (\text{A.4})$$

A.3. Cartesian system of vector functions and basic relations

A.3.1. Strain and displacement relations

$$\begin{aligned}\varepsilon_{xx} &= u_{x,x}, \varepsilon_{yy} = u_{y,y}, \varepsilon_{zz} = u_{z,z} \\ \varepsilon_{yz} &= 0.5(u_{y,z} + u_{z,y}) \\ \varepsilon_{xz} &= 0.5(u_{x,z} + u_{z,x}) \\ \varepsilon_{xy} &= 0.5(u_{x,y} + u_{y,x}).\end{aligned}\quad (\text{A.5})$$

A.3.2. Cartesian system of vector functions

First, we introduce the following Cartesian system of vector functions \mathbf{L} , \mathbf{M} , and \mathbf{N} :

$$\begin{aligned}\mathbf{L}(x, y; \alpha, \beta) &= \mathbf{e}_z S(x, y; \alpha, \beta) \\ \mathbf{M}(x, y; \alpha, \beta) &= \nabla S \equiv (\mathbf{e}_x \partial_x + \mathbf{e}_y \partial_y) S(x, y; \alpha, \beta) \\ \mathbf{N}(x, y; \alpha, \beta) &= \nabla \times (\mathbf{e}_z S) \equiv (\mathbf{e}_x \partial_y - \mathbf{e}_y \partial_x) S(x, y; \alpha, \beta)\end{aligned}\quad (\text{A.6})$$

where ∂_x and ∂_y are the derivatives with respect to variables x and y , and the scalar function S is defined as

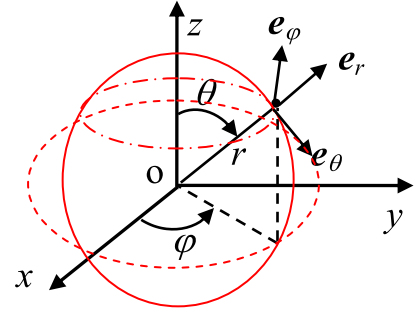


Figure A3. Spherical coordinates (r, θ, φ) , with $0 \leq r < \infty$, $0 \leq \theta \leq \pi$, $0 \leq \varphi < 2\pi$.

$$S(x, y; \alpha, \beta) = e^{-i(\alpha x + \beta y)} / (2\pi) \quad (\text{A.7})$$

and \mathbf{e}_x , \mathbf{e}_y , and \mathbf{e}_z are the unit vectors along the x -, y -, and z -axes, respectively. For applications to layered structures, the coordinates x and y are the horizontal axes, while z axis points to the problem domain; α and β are the transformation variables corresponding to the two horizontal physical variables x and y .

It can be easily shown that the scalar function S satisfied the following Helmholtz equation

$$(\partial_{xx}^2 + \partial_{yy}^2 + \lambda^2)S = 0, \quad \lambda^2 = \alpha^2 + \beta^2. \quad (\text{A.8})$$

The system of vector functions introduced in equation (A.6) satisfies the orthonormal relations below

$$\begin{aligned}\int \int_{-\infty}^{+\infty} \mathbf{L}(x, y; \alpha, \beta) \cdot \mathbf{L}^*(x, y; \alpha', \beta') dx dy &= \delta(\alpha - \alpha') \delta(\beta - \beta') \\ \int \int_{-\infty}^{+\infty} \mathbf{M}(x, y; \alpha, \beta) \cdot \mathbf{M}^*(x, y; \alpha', \beta') dx dy &= (\alpha \alpha' + \beta \beta') \delta(\alpha - \alpha') \delta(\beta - \beta') \\ \int \int_{-\infty}^{+\infty} \mathbf{N}(x, y; \alpha, \beta) \cdot \mathbf{N}^*(x, y; \alpha', \beta') dx dy &= (\alpha \alpha' + \beta \beta') \delta(\alpha - \alpha') \delta(\beta - \beta')\end{aligned}\quad (\text{A.9})$$

where the dot between two vectors indicate scalar product and the star indicates conjugate of the function or variable.

Due to these orthonormal relations, any square-integrable scalar function and vector function can be expanded in terms of this vector system. For instance, for the scalar function g and the vector function $\mathbf{f} \equiv f_x \mathbf{e}_x + f_y \mathbf{e}_y + f_z \mathbf{e}_z$, we can expand them in terms of Cartesian system of vector functions as

$$\begin{aligned}g(x, y, z) &= \int \int_{-\infty}^{+\infty} G(z) S(x, y; \alpha, \beta) d\alpha d\beta \\ \mathbf{f}(x, y, z) &= \int \int_{-\infty}^{+\infty} [F_L(z) \mathbf{L}(x, y) + F_M(z) \mathbf{M}(x, y) + F_N(z) \mathbf{N}(x, y)] d\alpha d\beta \\ &= \int \int_{-\infty}^{+\infty} \{ \mathbf{e}_x [F_M(z) \partial_x + F_N(z) \partial_y] + \mathbf{e}_y [F_M(z) \partial_y - F_N(z) \partial_x] + \mathbf{e}_z F_L(z) \} S(x, y) d\alpha d\beta.\end{aligned}\quad (\text{A.10})$$

Remark A1: If the scalar function or the vector function depend only on the their horizontal coordinates (x, y) , as for the loading prescribed on the horizontal surfaces of the structures, or the internal source located on a horizontal plane within the layered structures, the expansion coefficients G for g , and F_L , F_M , F_N for \mathbf{f} will be independent of the vertical coordinate z .

Due to the orthonormal relations (A.9), the expansion coefficients in equation (A.10) can be found as

$$\begin{aligned}G(z) &= \int \int_{-\infty}^{+\infty} g(x, y, z) S^*(x, y; \alpha, \beta) dx dy \\ F_L(z) &= \int \int_{-\infty}^{+\infty} \mathbf{f}(x, y, z) \cdot \mathbf{L}^*(x, y) dx dy \\ F_M(z) &= \lambda^{-2} \int \int_{-\infty}^{+\infty} \mathbf{f}(x, y, z) \cdot \mathbf{M}^*(x, y) dx dy \\ F_N(z) &= \lambda^{-2} \int \int_{-\infty}^{+\infty} \mathbf{f}(x, y, z) \cdot \mathbf{N}^*(x, y) dx dy.\end{aligned}\quad (\text{A.11})$$

It is noted that: (1) the expansion coefficients are functions of z as well as the transformation variables (α, β) , and (2) the solutions based on this system of vector functions contain the 2D (x, z) -plane and (y, z) -plane deformations as special cases.

A.4. Cylindrical system of vector functions and basic relations

A.4.1. Strain and displacement relations in cylindrical coordinates

$$\begin{aligned}\varepsilon_{rr} &= u_{r,r}, \varepsilon_{\theta\theta} = r^{-1}u_{\theta,\theta} + r^{-1}u_r, \varepsilon_{zz} = u_{z,z} \\ \varepsilon_{\theta z} &= 0.5(u_{\theta,z} + r^{-1}u_{z,\theta}) \\ \varepsilon_{rz} &= 0.5(u_{z,r} + u_{r,z}) \\ \varepsilon_{r\theta} &= 0.5(r^{-1}u_{r,\theta} + u_{\theta,r} - r^{-1}u_\theta).\end{aligned}\quad (\text{A.12})$$

A.4.2. Cylindrical system of vector functions

It is defined as

$$\mathbf{L}(r, \theta; \lambda, m) = \mathbf{e}_z S(r, \theta; \lambda, m)$$

$$\mathbf{M}(r, \theta; \lambda, m) = \nabla S \equiv (\mathbf{e}_r \partial_r + \mathbf{e}_\theta r^{-1} \partial_\theta) S(r, \theta; \lambda, m)$$

$$\mathbf{N}(r, \theta; \lambda, m) = \nabla \times (\mathbf{e}_z S) \equiv (\mathbf{e}_r r^{-1} \partial_\theta - \mathbf{e}_\theta \partial_r) S(r, \theta; \lambda, m)$$

with

$$S(r, \theta; \lambda, m) = J_m(\lambda r) e^{im\theta} / \sqrt{2\pi} \quad (\text{A.14})$$

where $J_m(\lambda r)$ is the Bessel function of order m with $m = 0$ corresponding to the axial symmetric deformation. Similarly, S satisfies the Helmholtz equation in the cylindrical coordinates

$$\frac{\partial^2 S}{\partial r^2} + \frac{\partial S}{r \partial r} + \frac{\partial^2 S}{r^2 \partial \theta^2} + \lambda^2 S = 0. \quad (\text{A.15})$$

Orthonormal relations among these vectors are:

$$\begin{aligned}\int_0^{2\pi} \int_0^{+\infty} \mathbf{L}(r, \theta; \lambda, m) \cdot \mathbf{L}^*(x, y; \lambda', m') r dr d\theta &= \frac{\delta(\lambda - \lambda')}{\sqrt{\lambda \lambda'}} \delta_{mm'} \\ \int_0^{2\pi} \int_0^{+\infty} \mathbf{M}(r, \theta; \lambda, m) \cdot \mathbf{M}^*(x, y; \lambda', m') r dr d\theta &= \delta(\lambda - \lambda') \sqrt{\lambda \lambda'} \delta_{mm'} \\ \int_0^{2\pi} \int_0^{+\infty} \mathbf{N}(r, \theta; \lambda, m) \cdot \mathbf{N}^*(x, y; \lambda', m') r dr d\theta &= \delta(\lambda - \lambda') \sqrt{\lambda \lambda'} \delta_{mm'}.\end{aligned}\quad (\text{A.16})$$

Expansion of any square-integrable scalar function g and vector function $\mathbf{f} \equiv f_r \mathbf{e}_r + f_\theta \mathbf{e}_\theta + f_z \mathbf{e}_z$ in terms of it as

$$\begin{aligned}g(r, \theta, z) &= \sum_m \int_0^{+\infty} G(z) S(r, \theta; \lambda, m) \lambda d\lambda \\ \mathbf{f}(r, \theta, z) &= \sum_m \int_0^{+\infty} [F_L(z) \mathbf{L}(r, \theta) + F_M(z) \mathbf{M}(r, \theta) + F_N(z) \mathbf{N}(r, \theta)] \lambda d\lambda \\ &= \sum_m \int_0^{+\infty} \{e_r [F_M(z) \partial_r + F_N(z) r^{-1} \partial_\theta] \\ &\quad + e_\theta [F_M(z) r^{-1} \partial_\theta - F_N(z) \partial_r] + e_z F_L(z)\} S(r, \theta) \lambda d\lambda.\end{aligned}\quad (\text{A.17})$$

The expansion coefficients of the scalar function g and the vector function \mathbf{f} are

$$\begin{aligned}G(z) &= \int_0^{2\pi} \int_0^{+\infty} g(r, \theta, z) S^*(r, \theta; \lambda, m) r dr d\theta \\ F_L(z) &= \int_0^{2\pi} \int_0^{+\infty} \mathbf{f}(r, \theta, z) \cdot \mathbf{L}^*(r, \theta) r dr d\theta \\ F_M(z) &= \lambda^{-2} \int_0^{2\pi} \int_0^{+\infty} \mathbf{f}(r, \theta, z) \cdot \mathbf{M}^*(r, \theta) r dr d\theta \\ F_N(z) &= \lambda^{-2} \int_0^{2\pi} \int_0^{+\infty} \mathbf{f}(r, \theta, z) \cdot \mathbf{N}^*(r, \theta) r dr d\theta.\end{aligned}\quad (\text{A.18})$$

It is noted that the expansion coefficients are functions of z and (λ, m) .

Remark A2. The solutions based on the cylindrical system of vector functions contain the axisymmetric deformation as

their special case. It is corresponding to the case where $m = 0$.

A.5. Spherical system of vector functions (or vector spherical harmonics) and basic relations

A.5.1. Strain and displacement relations in spherical coordinates.

$$\begin{aligned}\varepsilon_{rr} &= u_{r,r}, \varepsilon_{\theta\theta} = r^{-1}u_{\theta,\theta} + r^{-1}u_r, \varepsilon_{\varphi\varphi} = r^{-1}\sin^{-1}\theta u_{\varphi,\varphi} + r^{-1}u_r + r^{-1}u_\theta \cot \theta \\ \varepsilon_{r\theta} &= 0.5(u_{\theta,r} + r^{-1}u_{r,\theta} - r^{-1}u_\theta) \\ \varepsilon_{r\varphi} &= 0.5(u_{\varphi,r} + r^{-1}\sin^{-1}\theta u_{r,\varphi} - r^{-1}u_\varphi) \\ \varepsilon_{\theta\varphi} &= 0.5(r^{-1}u_{\varphi,\theta} + r^{-1}\sin^{-1}\theta u_{\theta,\varphi} - r^{-1}u_\varphi \cot \theta).\end{aligned}\quad (\text{A.19})$$

A.5.2. Spherical system of vector functions. We point out that Appendices B and C in Dahlen and Tromp (1998) contain detailed discussion on spherical harmonic functions and their various properties.

It is defined as

$$\mathbf{L}(\theta, \varphi; n, m) = \mathbf{e}_r S(\theta, \varphi; n, m)$$

$$\mathbf{M}(\theta, \varphi; n, m) = r \nabla S \equiv \left(\mathbf{e}_\theta \partial_\theta + \mathbf{e}_\varphi \frac{\partial_\varphi}{\sin \theta} \right) S(\theta, \varphi; n, m)$$

$$\mathbf{N}(\theta, \varphi; n, m) = r \nabla \times (\mathbf{e}_r S) \equiv \left(\mathbf{e}_\theta \frac{\partial_\varphi}{\sin \theta} - \mathbf{e}_\varphi \partial_\theta \right) S(\theta, \varphi; n, m)$$

(A.20)

where \mathbf{e}_r , \mathbf{e}_θ , and \mathbf{e}_φ are the unit vectors, respectively, along r -, θ - and φ -directions, and the scalar function S is the normalized surface spherical function defined by

$$\begin{aligned}S(\theta, \varphi; n, m) &= \sqrt{\frac{(2n+1)(n-m)!}{4\pi(n+m)!}} P_n^m(\cos \theta) e^{im\varphi} \\ |m| &\leq n; \quad n = 0, 1, 2, \dots\end{aligned}\quad (\text{A.21})$$

The associated Legendre function P_n^m in equation (5.2) is defined as

$$P_n^m(x) = (-1)^m (1-x^2)^{m/2} \frac{d^m}{dx^m} P_n(x) \quad (m \geq 0) \quad (\text{A.22})$$

where P_n is the Legendre function of n th degree.

It should be noted that equation (A.22) is for positive m . When this index is negative, the associated function is defined in terms of its positive one as

$$P_n^{-m}(\cos \theta) = (-1)^m \frac{(n-m)!}{(n+m)!} P_n^m(\cos \theta) \quad (m \geq 0). \quad (\text{A.23})$$

In so doing, we can define

$$S(\theta, \varphi; n, -m) = (-1)^m S^*(\theta, \varphi; n, m) \quad (\text{A.24})$$

where the superscript star denotes complex conjugate, giving as

$$\begin{aligned}S^*(\theta, \varphi; n, m) &= \sqrt{\frac{(2n+1)(n-m)!}{4\pi(n+m)!}} P_n^m(\cos \theta) e^{-im\varphi} \\ |m| &\leq n; \quad n = 0, 1, 2, \dots\end{aligned}\quad (\text{A.25})$$

It is noted that function S satisfies the following Helmholtz equation

$$\left(\frac{\partial_\theta(\sin \theta \partial_\theta)}{\sin \theta} + \frac{\partial_\varphi^2}{\sin^2 \theta} + \lambda^2 \right) S = 0 \quad (\text{A.26})$$

where $\lambda^2 = n(n+1)$. It should be noted that $N = n(n+1)$ is also used in the text when analyzing the deformation in spherical earth.

Equation (A.26) can be also written as

$$\frac{\partial^2 S}{\partial \theta^2} + \cot \theta \frac{\partial S}{\partial \theta} + \frac{1}{\sin^2 \theta} \frac{\partial^2 S}{\partial \varphi^2} + \lambda^2 S = 0. \quad (\text{A.27})$$

The spherical system of vector functions (A.20) is complete and orthogonal in the following sense.

$$\begin{aligned} \int_0^{2\pi} d\varphi \int_0^\pi \mathbf{L}(\theta, \varphi; n, m) \cdot \mathbf{L}^*(\theta, \varphi; n', m') \sin \theta d\theta &= \delta_{nn'} \delta_{mm'} \\ \int_0^{2\pi} d\varphi \int_0^\pi \mathbf{M}(\theta, \varphi; n, m) \cdot \mathbf{M}^*(\theta, \varphi; n', m') \sin \theta d\theta &= \lambda^2 \delta_{nn'} \delta_{mm'} \\ \int_0^{2\pi} d\varphi \int_0^\pi \mathbf{N}(\theta, \varphi; n, m) \cdot \mathbf{N}^*(\theta, \varphi; n', m') \sin \theta d\theta &= \lambda^2 \delta_{nn'} \delta_{mm'} \end{aligned} \quad (\text{A.28})$$

where dot means scalar product.

Expansion of any square-integrable scalar function g and vector function $\mathbf{f} \equiv F_r \mathbf{e}_r + F_\theta \mathbf{e}_\theta + F_\varphi \mathbf{e}_\varphi$ in terms of it is

$$\begin{aligned} g(r, \theta, \varphi) &= \sum_{n=0}^{\infty} \sum_{m=-n}^n G(r) S(\theta, \varphi; n, m) \\ \mathbf{f}(r, \theta, \varphi) &= \sum_{n=0}^{\infty} \sum_{m=-n}^n [F_L(r) \mathbf{L}(\theta, \varphi) + F_M(r) \mathbf{M}(\theta, \varphi) + F_N(r) \mathbf{N}(\theta, \varphi)] \\ &= \sum_{n=0}^{\infty} \sum_{m=-n}^n \left[\mathbf{e}_\theta \left\{ F_M(r) \partial_\theta + F_N(r) \frac{\partial_\varphi}{\sin \theta} \right\} \right. \\ &\quad \left. + \mathbf{e}_\varphi \left\{ F_M(r) \frac{\partial_\varphi}{\sin \theta} - F_N(r) \partial_\theta \right\} + \mathbf{e}_r F_L(r) \right] S(\theta, \varphi). \end{aligned} \quad (\text{A.29})$$

The expansion coefficients can be found, for instance, for the scalar function g and the vector function \mathbf{f} , as

$$\begin{aligned} G(r) &= \int_0^{2\pi} d\varphi \int_0^\pi \sin \theta d\theta [g(r, \theta, \varphi) S^*(\theta, \varphi; n, m)] \\ F_L(r) &= \int_0^{2\pi} d\varphi \int_0^\pi \sin \theta d\theta [\mathbf{f}(r, \theta, \varphi) \cdot \mathbf{L}^*(\theta, \varphi)] \\ F_M(r) &= \frac{1}{\lambda^2} \int_0^{2\pi} d\varphi \int_0^\pi \sin \theta d\theta [\mathbf{f}(r, \theta, \varphi) \cdot \mathbf{M}^*(\theta, \varphi)] \\ F_N(r) &= \frac{1}{\lambda^2} \int_0^{2\pi} d\varphi \int_0^\pi \sin \theta d\theta [\mathbf{f}(r, \theta, \varphi) \cdot \mathbf{N}^*(\theta, \varphi)] \end{aligned} \quad (\text{A.30})$$

Remark A3. (1) The expansion coefficients are functions of (n, m) as well as r ; (2) Equation (A.20) is not needed for the solution depending only upon r corresponding to the special case of $n = 0$ (and $m = 0$). This is the uniform deformation case; (3) For the spherically axisymmetric deformation we have $m = 0$; (4) For the deformation associated with $n = 1$, there is a rigid-body motion involved (i.e. Farrell 1972).

Remark A4. For the scalar g and vector \mathbf{f} in terms of the three systems of vector functions (equations (A.10), (A.17), and (A.29), respectively, for the Cartesian, cylindrical, and spherical systems), the following important divergence and Laplacian relations exist. In terms of either Cartesian or cylindrical system of vector functions, we have

$$\begin{aligned} \nabla^2 g &= (G'' - \lambda^2 G) S \\ \nabla \cdot \mathbf{f} &= (F_L' - \lambda^2 F_M) S \end{aligned} \quad (\text{A.31})$$

where the prime indicates derivative with respect to the vertical coordinate z . In terms of the spherical system of vector functions, we have

$$\begin{aligned} \nabla^2 g &= \frac{1}{r^2} \left[\frac{d}{dr} \left(r^2 \frac{d}{dr} \right) - \lambda^2 \right] GS \\ \nabla \cdot \mathbf{f} &= \left[\frac{1}{r^2} \frac{d}{dr} (r^2 F_L) - \frac{\lambda^2}{r} F_M \right] S \end{aligned} \quad (\text{A.32})$$

ORCID iDs

Ernian Pan  <https://orcid.org/0000-0001-6640-7805>

References

- Aagaard B T, Knepley M G and Williams C A 2013 A domain decomposition approach to implementing fault slip in finite-element models of quasi-static and dynamic crustal deformation *J. Geophys. Res. Solid Earth* **118** 3059–79
- Aagaard B T, Knepley M G and Williams C A 2017 PyLith v2.2.0, Davis CA *Comput. Infrastruct. Geodyn.* (<https://doi.org/10.5281/zenodo.438705>)
- Abbott B P *et al* 2016 Observation of gravitational waves from a binary black hole merger *Phys. Rev. Lett.* **116** 061102
- Abramowitz M and Stegun I A 1970 *Handbook of Mathematical Functions with Formulas, Graphs, and Mathematical Tables* (New York: Dover)
- Achenbach J D 1973 *Wave Propagation in Elastic Solids* (North Holland: Amsterdam)
- Adler E L, Slaboszewicz J K, Farnell G W and Jen C K 1990 PC software for SAW propagation in anisotropic multilayers *IEEE Trans. Ultrason. Ferroelectr. Freq. Control* **37** 215–23
- Agnew D 1996 *SPOTL: Some Programs for Ocean-Tide Loading (SIO Reference Series vol 96–8)* (La Jolla, CA: Scripps Institution of Oceanography)
- Agnew D 1997 NLOADF: a program for computing ocean-tide loading *J. Geophys. Res.* **102** 5109–10
- Ai Z Y and Cheng Y C 2014 Extended precise integration method for consolidation of transversely isotropic poroelastic layered media *Comput. Math. Appl.* **68** 1806–18
- Aki K and Richards P G 1980 *Quantitative Seismology Theory and Methods* vol 1 (San Francisco: Freeman)
- Al-Attar D and Woodhouse J H 2008 Calculation of seismic displacement fields in selfgravitating earth models: applications of minors vectors and symplectic structure *Geophys. J. Int.* **175** 1176–208
- Amadei B and Pan E 1992 Gravitational stresses in anisotropic rock masses with inclined strata *Int. J. Rock Mech. Min. Sci. Geomech. Abstr.* **29** 225–36
- Anderson D L 1961 Elastic wave propagation in layered anisotropic media *J. Geophys. Res.* **66** 2953–63
- Apfel R J and Luco J E 1983 On the Green's functions for a layered half-space: part II *Bull. Seismol. Soc. Am.* **73** 931–51
- Argus D F, Fu Y and Landerer F W 2014a Seasonal variation in total water storage in California inferred from GPS observations of vertical land motion *Geophys. Res. Lett.* **41** 1971–80
- Argus D F, Peltier W R, Drummond R and Moore A W 2014b The Antarctica component of postglacial rebound model ICE6G_C(VM5a) based upon GPS positioning, exposure age dating of ice thicknesses, and relative sea level histories *Geophys. J. Int.* **198** 537–63
- Bacon D J, Barnett D M and Scattergood R O 1979 Anisotropic continuum theory of lattice defects *Prog. Mater. Sci.* **23** 51–262
- Banerjee P K and Mamoan S M 1990 A fundamental solution due to a periodic point force in the interior of an elastic half-space *Earthq. Eng. Struct. Dyn.* **19** 91–105
- Barbot S and Fialko Y 2010a Fourier-domain Green's function for an elastic semi-infinite solid under gravity, with applications to earthquake and volcano deformation *Geophys. J. Int.* **182** 568–82
- Barbot S and Fialko Y 2010b A unified continuum representation of post-seismic relaxation mechanisms: semi-analytic models of afterslip, poroelastic rebound and viscoelastic flow *Geophys. J. Int.* **182** 1124–40
- Batov A V, Gudkova T V and Zharkov V N 2016 Calculation of load Love numbers and static stresses for the interior structure

- model of Mars with an elastic mantle Trapeznikov Institute of Control Sciences RAS, Moscow, Russia
- Becker J M and Bevis M 2004 Love's problem *Geophys. J. Int.* **156** 171–8
- Bellman R, Kalaba R E and Lockett J A 1966 *Numerical Inversion of the Laplace Transform: Applications to Biology, Economics, Engineering, and Physics* vol 4 (Amsterdam: Elsevier)
- Ben-Menahem A and Singh S J 1968 Eigenvector expansions of Green's dyads with applications to geophysical theory *Geophys. J. R. Astron. Soc.* **16** 417–52
- Ben-Menahem A and Gillon A 1970 Crustal deformation by earthquakes and explosions *Bull. Seism. Soc. Am.* **60** 193–215
- Ben-Menahem A and Singh S J 1981 *Seismic Waves and Sources* (New York: Springer)
- Ben-Menahem A, Singh S J and Solomon F 1969 Static deformation of a spherical earth model by internal dislocations *Bull. Seismol. Soc. Am.* **59** 813–53
- Ben-Menahem A, Singh S J and Solomon F 1970 Deformation of a homogeneous Earth model by finite dislocations *Rev. Geophys. Space Phys.* **8** 591–632
- Berry D S 1960 An elastic treatment of ground movement due to mining—I. Isotropic ground *J. Mech. Phys. Solids* **8** 280–92
- Berry D S and Sales T W 1961 An elastic treatment of ground movement due to mining—II. Transversely isotropic ground *J. Mech. Phys. Solids* **9** 52–62
- Berry D S and Sales T W 1962 An elastic treatment of ground movement due to mining—III. Three dimensional problem, transversely isotropic ground *J. Mech. Phys. Solids* **10** 73–83
- Bevis M, Alsdorf D, Kendrick E, Fortes L P, Forsberg B, Smalley R Jr and Becker J 2005 Seasonal fluctuations in the mass of the Amazon River system and Earth's elastic response *Geophys. Res. Lett.* **32** L16308
- Bevis M, Pan E, Zhou H, Han F and Zhu R 2015 Surface deformation due to loading of a layered elastic half-space: constructing the solution for a general polygonal load *Acta Geophys.* **63** 957–77
- Bhattacharya S N 1976 Extension of the Thomson–Haskell method to non-homogeneous spherical layers *Geophys. J. R. Astron. Soc.* **47** 411–44
- Bhattacharya S N 1978 Rayleigh waves from a point source in a spherical medium with homogeneous layers *Bull. Seism. Soc. Am.* **68** 231–8
- Bhattacharya S N 2005 Synthetic seismograms in a spherical Earth using exact flattening transformation *Geophys. Res. Lett.* **32** L21303
- Biot M A 1956 General solutions of the equations of elasticity and consolidation for a porous material *J. Appl. Mech.* **78** 91–6
- Bona A and Slawinski M A 2015 *Wavefronts and Rays as Characteristics and Asymptotics* 2nd edn (Singapore: World Scientific)
- Bonafede M 1990 Axi-symmetric deformation of a thermo-poro-elastic half-space: inflation of a magma chamber *Geophys. J. Int.* **103** 289–99
- Bonafede M and Rivalta E 1999a The tensile dislocation problem in a layered elastic medium *Geophys. J. Int.* **136** 341–56
- Bonafede M and Rivalta E 1999b On tensile cracks close to and across the interface between two welded elastic half-spaces *Geophys. J. Int.* **138** 410–34
- Bonafede M and Ferrari C 2009 Analytical models of deformation and residual gravity changes due to a Mogi source in a viscoelastic medium *Tectonophysics* **471** 4–13
- Bondarenko V P and Litoshenko N V 1997 Stress-strain state of a spherical layer with circular dislocation loop *Int. Appl. Mech.* **33** 525–31
- Booker J R 1974 Time dependent strain following faulting of a porous medium *J. Geophys. Res.* **79** 2037–44
- Bouchon M 1993 A numerical simulation of the acoustic and elastic wavefields radiated by a source on a fluid-filled borehole embedded in a layered medium *Geophysics* **58** 475–81
- Bouchon M 2003 A review of the discrete wavenumber method *Pure Appl. Geophys.* **160** 445–65
- Boschi E 1973 Reciprocity theorem and elastic dislocation theory for an Earth Model with an initial static stress field *J. Geophys. Res.* **78** 8584–90
- Bosl W J and Nur A 2002 Aftershocks and pore fluid diffusion following the 1992 Landers earthquake *J. Geophys. Res.* **107** 2366
- Boussinesq J 1885 *Application des Potentials a l'etude de l'equilibre et du Mouvement des Solides Elastiques* (Paris: Gauthier-Villars)
- Braga A M B 1990 Wave propagation in anisotropic layered composites *PhD Thesis* Stanford University
- Brekhovskikh L M 1980 *Waves in Layered Media* 2nd edn translated R T Beyer (New York: Academic)
- Bufler H 1971 Theory of elasticity of a multilayered medium *J. Elast.* **1** 125–43
- Burmister D M 1945 The general theory of stresses and displacements in layered soil systems *J. Appl. Phys.* **16** 84–94
- Burridge R and Knopoff L 1964 Body force equivalents for seismic dislocations *Bull. Seismol. Soc. Am.* **54** 1875–88
- Busby H R and Dydo J R 1995 Elasticity solutions for constant and linearly varying loads applied to a rectangular surface patch on the elastic half-space *J. Elast.* **38** 153–63
- Butkovskiy A G 1982 *Green's Functions and Transfer Functions Handbook* (New York: Wiley)
- Cai Y and Pan E 2018 Surface loading over a transversely isotropic and multilayered system with imperfect interfaces—revisit enhanced by the dual-boundary strategy *Int. J. Geomech.* **18** 04018032
- Cambiotti G and Sabadini R 2010 The compressional and compositional stratifications in Maxwell earth models: the gravitational overtuning and the long-period tangential flux *Geophys. J. Int.* **180** 475–500
- Cambiotti G, Barletta V R, Bordoni A and Sabadini R 2009 A comparative analysis of the solutions for a Maxwell Earth: the role of the advection and buoyancy force *Geophys. J. Int.* **176** 995–1006
- Cambiotti G, Zhou X, Sparraccino F, Sabadini R and Sun W 2017 Joint estimate of the rupture area and slip distribution of the 2009 L'Aquila earthquake by a Bayesian inversion of GPS data *Geophys. J. Int.* **209** 992–1003
- Cannell D M 2001 *George Green: Mathematician and Physicist 1793–1841: the Background to his Life and Work* (Philadelphia, PA: Society for Industrial and Applied Mathematics)
- Caputo M 1961 Deformation of a layered earth by an axially symmetric surface mass distribution *J. Geophys. Res.* **66** 1479–83
- Caputo M 1962 Tables for the deformation of an earth model by surface mass distributions *J. Geophys. Res.* **67** 1611–6
- Carcione J M 1990 Wave propagation in anisotropic linear viscoelastic media: theory and simulated wavefields *Geophys. J. Int.* **101** 739–50
- Carcione J M, Kosloff D and Kosloff R 1988 Wave propagation simulation in a linear viscoelastic medium *Geophys. J. Int.* **95** 597–611
- Celebi E and Schmid G 2005 Investigation of ground vibrations induced by moving loads *Eng. Struct.* **27** 1981–98
- Cerruti V 1888 Sulla deformazione di un corpo elastic isotropo per alcune speciali condizioni ai limit *Rend. R. Accad. Lincei Roma* **4** 785–92
- Challis L and Sheard F 2003 The green of green functions *Phys. Today* **56** 41–6
- Chan K S, Karasudhi P and Lee S L 1974 Force at a point in the interior of a layered elastic half space *Int. J. Solids Struct.* **10** 1179–99
- Chapman C H 1978 A new method for computing synthetic seismograms *Geophys. J. R. Astron. Soc.* **54** 481–518
- Chapman C H 2003 Yet another elastic plane-wave, layer-matrix algorithm *Geophys. J. Int.* **154** 212–23
- Chapman C H 2004 *Fundamentals of Seismic Wave Propagation* (Cambridge: Cambridge University Press)

- Chen E Y G, Pan E, Norfolk T S and Wang Q 2011b Surface loading of a multilayered viscoelastic pavement: moving dynamic load *Road Mater. Pavement Des.* **12** 849–74
- Chen J Y, Pan E and Heyliger P 2015 Static deformation of a spherically anisotropic and multilayered magneto-electro-elastic hollow sphere *Int. J. Solids Struct.* **60–1** 66–74
- Chen J Y, Pan E and Bevis M 2018b Accurate computation of the elastic load love numbers to high spectral degree for a finely-layered, transversely isotropic and self-gravitating Earth *Geophys. J. Int.* **212** 827–38
- Chen W T and Chen X F 2002 Modal solutions in stratified multi-layered fluid-solid half-space *Sci. China Ser. D* **45** 358–65
- Chen W Q 2000 Vibration theory of non-homogeneous, spherically isotropic piezoelectric bodies *J. Sound Vib.* **236** 833–60
- Chen W Q 2001 Free vibration analysis of laminated piezoelectric hollow spheres *J. Acoust. Soc. Am.* **109** 41–50
- Chen W Q and Ding H J 2001 Free vibration of multi-layered spherically isotropic hollow spheres *Int. J. Mech. Sci.* **43** 667–80
- Chen W Q and Ding H J 2001b A state-space-based stress analysis of a multilayered spherical shell with spherical isotropy *J. Appl. Mech.* **68** 109–14
- Chen W Q, Ding H J and Xu R Q 2001b Three-dimensional static analysis of multilayered piezoelectric hollow spheres via the state space method *Int. J. Solids Struct.* **38** 4921–36
- Chen W Q, Pao Y H, Guo Y Q and Jiang J Q 2011a On generalization of the phase relations in the method of reverberation-ray matrix *From Waves in Complex Systems to Dynamics of Generalized Continua* ed K Hutter *et al* (Singapore: World Scientific) ch 2, pp 49–74
- Chen W Q, Wang L Z and Lu Y 2002 Free vibrations of functionally graded piezoceramic hollow spheres with radial polarization *J. Sound Vib.* **251** 103–14
- Chen X 1993 A systematic and efficient method of computing normal modes for multi-layered half-space *Geophys. J. Int.* **115** 391–409
- Chen X B, Diebold L and Dautreleau Y 2001 New Green-function method to predict wave-induced ship motions and loads *23rd Symp. on Naval Hydrodynamics* pp 66–81
- Chen X F 1999 Seismogram synthesis in multilayered half-space, Part I. Theoretical formulations *Earthq. Res. China* **13** 149–74
- Chen X F, Quan Y L and Harris J M 1996 Seismogram synthesis for radially multilayered media using the generalized reflection-transmission coefficients method: theory and application to acoustic logging *Geophysics* **61** 1150–9
- Chen X F and Zhang H M 2001 An efficient method for computing Green's functions for a layered half-space at large epicentral distances *Bull. Seismol. Soc. Am.* **91** 858–69
- Chen Y G, Pan E and Green R 2009 Surface loading of a multilayered viscoelastic pavement: semianalytical solution *J. Eng. Mech.* **135** 517–28
- Chen Z, Jeffrey R G and Pandurangan V 2018a The far-field deformation caused by a hydraulic fracture in an inhomogeneous elastic half-space *Int. J. Solids Struct.* **130–1** 220–31
- Cheng A H D 2016 *Poroelasticity* (Basel: Springer)
- Cheng A H D and Detournay E 1998 On singular integral equations and fundamental solutions of poroelasticity *Int. J. Solids Struct.* **35** 4521–55
- Cheng A H D and Cheng D T 2005 Heritage and early history of the boundary element method *Eng. Anal. Bound. Elem.* **29** 268–302
- Cheng H, Zhang B, Huang L, Zhang H and Shi Y 2019 Calculating coseismic deformation and stress changes in a heterogeneous ellipsoid earth model *Geophys. J. Int.* **216** 851–8
- Chew W C 1990 *Waves and Fields in Inhomogeneous Media* (New York: The Institute of Electrical and Electronics Engineers)
- Chimenti D E 1997 Guided waves in plates and their use in material characterization *Appl. Mech. Rev.* **50** 247–84
- Chinnery M A 1975 The static deformation of an Earth with a fluid core: a physical approach *Geophys. J. R. Astron. Soc.* **42** 461–75
- Christensen R M 1982 *Theory of Viscoelasticity. An Introduction* 2nd edn (New York: Academic)
- Christensen U R 1987 Some geodynamical effects of anisotropic viscosity *Geophys. J. R. Astron. Soc.* **91** 711–36
- Chu H J and Pan E 2014 Elastic fields due to dislocation arrays in anisotropic bimetals *Int. J. Solids Struct.* **51** 1954–61
- Chu H J, Pan E, Wang J and Beyerlein I J 2011 Three-dimensional elastic displacements induced by a dislocation of polygonal shape in anisotropic elastic crystals *Int. J. Solids Struct.* **48** 1164–70
- Chu H J, Pan E, Wang J and Beyerlein I J 2012a Elastic displacement and stress fields induced by a dislocation of polygonal shape in an anisotropic elastic half-space *ASME J. Appl. Mech.* **79** 021011
- Chu H J, Pan E, Han X, Wang J and Beyerlein I J 2012b Elastic fields of dislocation loops in three-dimensional anisotropic bimetals *J. Mech. Phys. Solids* **60** 418–31
- Chu H J, Wang H M, Zhao Y F and Pan E 2013 Dislocation and traction loads over an elliptical region in anisotropic magneto-electroelastic bimetals *Smart Mater. Struct.* **22** 125020
- Cohen A M 2007 *Numerical Methods for Laplace Transform Inversion* vol 5 (Berlin: Springer)
- Cole R 2016 The beauty of Laplace's equation, mathematical key to ... everything (www.wired.com/2016/06/laplaces-equation-everywhere/)
- Comninou M A and Dunders J 1975 The angular dislocation in a halfspace *J. Elast.* **5** 203–16
- Cordier P, Demouchy S, Beausir B, Taupin V, Barou F and Fressengeas C 2014 Disclinations provide the missing mechanism for deforming olivine-rich rocks in the mantle *Nature* **507** 51–6
- Cormier V F 2007 Theory and observations—forward modeling/ synthetic body wave seismograms *Treatise on Geophysics* vol 1, ed G Schubert (Amsterdam: Elsevier) pp 157–89
- Crossley D J and Gubbins D 1975 Static deformation of the Earth's liquid core *Geophys. Res. Lett.* **2** 1–4
- Crouch S L 1976 Solution of plane elasticity problems by the displacement discontinuity method. I. Finite body solution *Int. J. Num. Meth. Eng.* **10** 301–43
- Crouch S L and Starfield A M 1983 *Boundary Element Methods in Solid Mechanics* (London: Allen & Unwin)
- Dahlen F A 1972 Elastic dislocation theory for a self-gravitating elastic configuration with an initial static stress field *Geophys. J. R. Astron. Soc.* **28** 357–83
- Dahlen F A and Tromp J 1998 *Theoretical Global Seismology* (Princeton, NJ: Princeton University Press)
- D'Agostino G, Spada G and Sabadini R 1997 Postglacial rebound and lateral viscosity variations: a semi-analytical approach based on a spherical model with Maxwell rheology *Geophys. J. Int.* **129** F9–13
- D'Amore L, Laccetti G and Murli A 1999a An implementation of a Fourier series method for the numerical inversion of the Laplace transform *ACM Trans. Math. Softw.* **25** 279–305
- D'Amore L, Laccetti G and Murli A 1999b Algorithm 796: a Fortran software package for the numerical inversion of the Laplace transform based on a Fourier series method *ACM Trans. Math. Softw.* **25** 306–15
- Datta S 2000 Nanoscale device modeling: the Green's function method *Superlattices Microstruct.* **28** 253–78
- Davies B and Martin B 1979 Numerical inversion of the Laplace transform: a survey and comparison of methods *J. Comput. Phys.* **33** 1–32
- Dehant V, Defraigne P and Van Hoolst T 2000 Computation of Mar's transfer functions for nutations, tides and surface loading *Phys. Earth Planet. Inter.* **117** 385–95

- De Hoog F R, Knight J H and Stokes A N 1982 An improved method for numerical inversion of Laplace transforms *SIAM J. Sci. Comput.* **3** 357–66
- Detournay E and Cheng A H D 1993 Fundamentals of poroelasticity *Comprehensive Rock Engineering: Principles, Practice and Projects (Analysis and Design Method vol 2)* ed C Fairhurst (Oxford: Pergamon) ch 5, pp 113–71
- deWit R 1973a Theory of disclinations: II. Continuous and discrete disclinations in anisotropic elasticity *J. Res. Natl Bur. Stand. Phys. Chem. A* **77** 49–100
- deWit R 1973b Theory of disclinations: III. Continuous and discrete disclinations in isotropic elasticity *J. Res. Natl Bur. Stand. Phys. Chem. A* **77** 359–68
- deWit R 1973c Theory of disclinations: IV. Straight disclinations *J. Res. Natl Bur. Stand. Phys. Chem. A* **77** 607–58
- Ding H J, Chen W Q and Zhang L 2006 *Elasticity of Transversely Isotropic Materials* (Netherlands: Springer)
- Dominguez J and Abascal R 1984 On fundamental solutions for the boundary integral equations in static and dynamic elasticity *Eng. Anal.* **1** 128–34
- Dong J, Sun W, Zhou X and Wang R 2014 Effects of the layer structure, self-gravity and curvature on coseismic deformations *Geophys. J. Int.* **199** 1442–51
- Dong J, Sun W, Zhou X and Wang R 2016 An analytical approach to estimate curvature effect on coseismic deformations *Geophys. J. Int.* **206** 1327–39
- Doniach S and Sondheimer E H 1999 *Green's Functions for Solid State Physicists* (London: Imperial College Press)
- Dorning J 1981 A review of local Green's function coarse-mesh and nodal methods for the numerical solution of fluid flow problems *Advances in Mathematical Methods for the Solution of Nuclear Engineering Problems vol 1* (Karlsruhe: Fachinformationszentrum Energie, Physik, Mathematik GmbH) pp 437–60
- Dubner H and Abate J 1968 Numerical inversion of Laplace transforms by relating them to the finite Fourier cosine transform *J. ACM* **15** 115–23
- Duffy D G 1993 On the numerical inversion of Laplace transforms: comparison of three new methods on characteristic problems from applications *ACM Trans Math. Softw.* **19** 333–59
- Duffy D G 2015 *Green's Functions with Applications* (London: Chapman and Hall)
- Dunkin J W 1965 Computation of modal solutions in layered, elastic media at high frequencies *Bull. Seism. Soc. Am.* **55** 335–58
- Durbin F 1974 Numerical inversion of Laplace transforms: an efficient improvement to Dubner and Abate's method *Comput. J.* **17** 371–6
- Durham W B and Goetze C 1977 Plastic flow of oriented single crystals of olivine: 1. Mechanical data *J. Geophys. Res.* **82** 5737–53
- Durham W B, Goetze C and Blake B 1977 Plastic flow of oriented single crystals of olivine: 2. Observations and interpretations of the dislocation structures *J. Geophys. Res.* **82** 5755–70
- Dyson F 1993 *Homage to George Green: How Physics Looked in the Nineteen-Forties, pages 232–247. Appendix VIb in Cannell D M 2001 George Green: Mathematician and Physicist 1793–1841: the Background to his Life and Work* (Philadelphia, PA: Society for Industrial and Applied Mathematics)
- Dziewonski A M and Anderson D L 1981 Preliminary reference Earth model *Phys. Earth Planetary Inter.* **25** 297–356
- Eringen A C and Suhubi E S 1974 *Elastodynamics vol 2* (New York: Academic)
- Eshelby J D 1957 The determination of the elastic field of an ellipsoidal inclusion, and related problems *Proc. R. Soc. A* **241** 376–96
- Eshelby J D 1961 Elastic inclusions and inhomogeneities *Progress in Solid Mechanics vol 2*, ed I N Sneddon and R Hill (North-Holland: Amsterdam) pp 89–140
- Ewing W M, Jardetzky W S and Press F 1957 *Elastic Waves in Layered Media* (New York: McGraw-Hill)
- Fabrikant V I 1989 *Applications of Potential Theory in Mechanics: a Selection of New Results* (Dordrecht: Kluwer)
- Fabrikant V I 1991 *Mixed Boundary Value Problems of Potential Theory and Their Applications in Engineering* (Dordrecht: Kluwer)
- Fang M and Hager B H 1995 The singularity mystery associated with a radially continuous Maxwell viscoelastic structure *Geophys. J. Int.* **123** 849–65
- Farrell W E 1972 Deformation of the Earth by surface loads *Rev. Geophys. Space Phys.* **10** 761–97
- Feng X and Zhang H M 2018 Exact closed-form solutions for Lamb's problem *Geophys. J. Int.* **214** 444–59
- Fialko Y 2004 Evidence of fluid-filled upper crust from observations of postseismic deformation due to the 1992 M_w 7.3 Landers earthquake *J. Geophys. Res.* **109** B08401
- Folch A, Fernández J, Rundle J B and Martí J 2000 Ground deformation in a viscoelastic medium composed of a layer overlying a half-space: a comparison between point and extended sources *Geophys. J. Int.* **140** 37–50
- Folland G B 1976 *Introduction to Partial Differential Equations* (Princeton NJ: Princeton University Press)
- Freedon W and Gerhards C 2013 *Geomathematically Oriented Potential Theory* (Boca Raton, FL: CRC Press)
- Freund L B and Barnett D M 1976 A two-dimensional analysis of surface deformation due to dip-slip faulting *Bull. Seism. Soc. Am.* **66** 667–75
- Friederich W and Dalkolmo J 1995 Complete synthetic seismograms for a spherically symmetric earth by a numerical computation of the Green's function in the frequency domain *Geophys. J. Int.* **122** 537–50
- Fryer G and Frazer L N 1984 Seismic waves in stratified anisotropic media *Geophys. J. R. Astron. Soc.* **78** 691–710
- Fryer G and Frazer L N 1987 Seismic waves in stratified anisotropic media—II. Elastodynamic eigensolutions for some anisotropic systems *Geophys. J. R. Astron. Soc.* **91** 73–101
- Fu G and Sun W 2004 Effects of spatial distribution of fault slip on calculating co-seismic displacements—case studies of the Chi-Chi earthquake ($m = 7.6$) and the Kunlun earthquake ($m = 7.8$) *Geophys. Res. Lett.* **31** L21601
- Fu G and Sun W 2006 Global co-seismic displacements caused by the 2004 Sumatra–Andaman earthquake *Earth Planets Space* **58** 149–52
- Fu G and Sun W 2007 Effects of lateral inhomogeneity in a spherical Earth on gravity Earth tides *J. Geophys. Res.* **112** B06409
- Fu G and Sun W 2008 Surface coseismic gravity changes caused by dislocations in a 3D heterogeneous earth *Geophys. J. Int.* **172** 479–503
- Fu G, Sun W, Fukuda Y and Gao S 2010 Coseismic displacements caused by point dislocations in a three-dimensional heterogeneous, spherical earth model *Geophys. J. Int.* **183** 706–26
- Fu Y, Freymueller J T and Jensen T 2012 Seasonal hydrological loading in southern Alaska observed by GPS and GRACE *Geophys. Res. Lett.* **39** L15310
- Fukahata Y and Matsu'ura M 2005 General expressions for internal deformation fields due to a dislocation source in a multilayered elastic half-space *Geophys. J. Int.* **161** 507–21
- Fukahata Y and Matsu'ura M 2006 Quasi-static internal deformation due to a dislocation source in a multilayered elastic/viscoelastic half-space and an equivalence theorem *Geophys. J. Int.* **166** 418–34
- Gao Y and Hu H 2010 Seismoelectromagnetic waves radiated by a double couple source in a saturated porous medium *Geophys. J. Int.* **181** 873–96
- Gao Y F and Larson B C 2015 Displacement fields and self-energies of circular and polygonal dislocation loops in homogeneous and layered anisotropic solids *J. Mech. Phys. Solids* **83** 104–28

- Gao Y, Huang F and Hu H 2017 Comparison of full and quasi-static seismoelectric analytically based modeling *J. Geophys. Res. Solid Earth* **122** 8066–106
- Gao Y, Chen Y, Hu H and Zhang J 2013a Early electromagnetic waves from earthquake rupturing: I. Theoretical formulations *Geophys. J. Int.* **192** 1288–307
- Gao Y, Chen Y, Hu H and Zhang J 2013b Early electromagnetic waves from earthquake rupturing: II. Validation and numerical experiments *Geophys. J. Int.* **192** 1308–23
- Gao Q, Lin J H, Zhong W X, Howson W P and Williams F W 2006 A precise numerical method for Rayleigh waves in a stratified half space *Int. J. Numer. Methods Eng.* **76** 771–86
- Garambois S and Dietrich M 2002 Full waveform numerical simulations of seismoelectromagnetic wave conversions in fluidsaturated stratified porous media *J. Geophys. Res.* **107** 2148
- Gerhards C 2018 Spherical potential theory: tools and application *Handbook of Mathematical Geodesy* ed W Freedon and M Z Nashed (Switzerland: Springer) pp 821–53
- Ghoniem N M and Han X 2005 Dislocation motion in anisotropic multilayer materials *Phil. Mag.* **85** 2809–30
- Gilbert F and Backus G E 1966 Propagator matrices in elastic wave and vibration problems *Geophysics* **31** 326–32
- Gilbert F and Backus G 1968 Elastic-gravitational vibrations of a radially stratified sphere *Dynamics of Stratified Solids* ed G Herrmann (New York: American Society of Mechanical Engineers) pp 82–95
- Gitlein O, Timmen L and Muller J 2013 Modeling of atmospheric gravity effects for high-precision observations *Int. J. Geosci.* **4** 663–71
- Gomez D D, Bevis M, Pan E and Smalley R 2017 The influence of gravity on the displacement field produced by fault slip *Geophys. Res. Lett.* **44** 9321–9
- Graff K F 1975 *Wave Motion in Elastic Solids* (Oxford: Oxford University Press)
- Grapenthin R 2014 CrusDe: A plug-in based simulation framework for composable crustal Deformation studies using Green's functions *Comput. Geosci.* **62** 168–77
- Green G 1828 *An Essay on the Application of Mathematical Analysis to the Theories of Electricity and Magnetism* (Nottingham: T. Wheelhouse)
- Greenberg M D 2015 *Application of Green's Functions in Science and Engineering* Dover edn (Englewood Cliffs, NJ: Prentice-Hall)
- Guo J Y, Li Y B, Huang Y, Deng H T, Xu S Q and Ning J S 2004 Green's function of the deformation of the Earth as a result of atmospheric loading *Geophys. J. Int.* **159** 53–68
- Guzina B B and Pak R Y S 2001 On the analysis of wave motions in a multi-layered solid *Q. J. Mech. Appl. Math.* **54** 13–31
- Haartsen M W and Pride S R 1997 Electro seismic waves from point sources in layered media *J. Geophys. Res.* **102** 24745–69
- Han D and Wahr J 1995 The viscoelastic relaxation of a realistically stratified earth, and a further analysis of postglacial rebound *Geophys. J. Int.* **120** 287–311
- Han D and Wahr J 1997 An analysis of anisotropic mantle viscosity, and its possible effects on post-glacial rebound *Phys. Earth Planet. Inter.* **102** 33–50
- Hansen L N, Zimmerman M E and Kohlstedt D L 2012 Laboratory measurements of the viscous anisotropy of olivine aggregates *Nature* **492** 415–9
- Hansen L N, Warren J M, Zimmerman M E and Kohlstedt D L 2016a Viscous anisotropy of textured olivine aggregates: Part 1. Measurement of the magnitude and evolution of anisotropy *Earth Planet. Sci. Lett.* **445** 92–103
- Hansen L N, Conrad C P, Boneh Y, Skemer P, Warren J M and Kohlstedt D L 2016b Viscous anisotropy of textured olivine aggregates: 2. Micromechanical model *J. Geophys. Res. Solid Earth* **212** 7137–60
- Harkrider D G 1970 Surface waves in multilayered elastic media. Part II. Higher mode spectra and spectral ratios from point sources in plane layered Earth models *Bull. Seismol. Soc. Am.* **60** 1937–87
- Haskell W T 1953 The dispersion of surface waves on multilayered media *Bull. Seismol. Soc. Am.* **43** 17–34
- Hashima A, Fukahata Y, Hashimoto C and Matsu'ura M 2014 Quasi-static strain and stress fields due to a moment tensor in elastic-viscoelastic layered half-space *Pure Appl. Geophys.* **171** 1669–93
- He Y M, Wang W M and Yao Z Y 2003 Static deformation due to shear and tensile faults in a layered half-space *Bull. Seismol. Soc. Am.* **93** 2253–63
- Helms L L 2009 *Potential Theory* (London: Springer)
- Heyliger P and Wu Y C 1999 Electroelastic fields in layered piezoelectric spheres *Int. J. Eng. Sci.* **37** 143–61
- Heyliger P R and Pan E 2016 Free vibration of layered magnetoelastic spheres *J. Acoust. Soc. Am.* **140** 988–99
- Heyliger P, Ramirez G and Saravanos D 1994 Coupled discrete-layer finite elements for laminated piezoelectric plates *Commun. Numer. Methods Eng.* **10** 971–81
- Hills D A, Kelly P A, Dai D N and Korsunsky A M 1996 *Solution of Crack Problems. The Distributed Dislocation Technique* (Netherlands: Springer)
- Hirth J P 1985 A brief history of dislocation theory *Metal. Transact.* **16A** 2085–90
- Hirth J P and Lothe J 1982 *Theory of Dislocations* 2nd edn (New York: Wiley)
- Hisada Y 1994 An efficient method for computing Green's functions for a layered half-space with sources and receivers at close depths *Bull. Seim. Soc. Am.* **84** 1456–72
- Hisada Y 1995 An efficient method for computing Green's functions for a layered half-space with sources and receivers at close depths (Part 2) *Bull. Seim. Soc. Am.* **85** 1080–93
- Honda J 1986 Strong anisotropic flow in a finely layered asthenosphere *Geophys. Res. Lett.* **13** 1454–7
- Honig G and Hirdes U 1984 A method for the numerical inversion of Laplace transforms *J. Comput. Appl. Math.* **10** 113–32
- Hu H and Gao Y 2011 Electromagnetic field generated by a finite fault due to electrokinetic effect *J. Geophys. Res.* **116** B08302
- Hu Y, Burgmann R, Freymueller J T, Banerjee P and Wang K 2014 Contributions of poroelastic rebound and a weak volcanic arc to the postseismic deformation of the 2011 Tohoku earthquake *Earth Planets Space* **66** 106
- Hull D and Bacon D J 2011 *Introduction to Dislocations* 5th edn (Portsmouth, NH: Heinemann)
- Jensen F B, Kuperman W A, Porter M B and Schmidt H 2011 *Computational Ocean Acoustics (Modern Acoustics and Signal Processing)* 2nd edn (New York: Springer)
- Jeyakumaran M, Rudnicki J W and Keer L M 1992 Modeling slip zones with triangular dislocation elements *Bull. Seism. Soc. Am.* **82** 2153–69
- Johnson L R 1974 Green's function for Lamb's problem *Geophys. J. R. Astron. Soc.* **37** 99–131
- Jonsson S, Segall P, Pedersen R and Bjornsson G 2003 Post-earthquake ground movements correlated to pore-pressure transients *Nature* **424** 179–83
- Jounianux L and Zyerman F 2016 A review on electrokinetically induced seismo-electrics, electro-seismics, and seismo-magnetics for Earth sciences *Solid Earth* **7** 249–84
- Jovanovich D B, Hussein M I and Chinnery M A 1974a Elastic dislocations in a layered half-space—I. Basic theory and numerical methods *Geophys. J. R. Astron. Soc.* **39** 205–17
- Jovanovich D B, Hussein M I and Chinnery M A 1974b Elastic dislocations in a layered half-space—II. The point source *Geophys. J. R. Astron. Soc.* **39** 219–39
- Kachanov M, Shafiro B and Tsukrov I 2003 *Handbook of Elasticity Solutions* (Boston, MA: Kluwer)
- Kagan Y Y 1987a Point sources of elastic deformation: elementary sources: static displacements *Geophys. J. R. Astron. Soc.* **90** 1–34

- Kagan Y Y 1987b Point sources of elastic deformation: elementary sources, dynamic displacements *Geophys. J. R. Astron. Soc.* **91** 891–912
- Kausel E 2006 *Fundamental Solutions in Elastodynamics: a Compendium* (Cambridge: Cambridge University Press)
- Kausel E and Peek R 1982 Dynamic loads in the interior of a layered stratum: An explicit solution *Bull. Seism. Soc. Am.* **72** 1459–81
- Kellogg O D 1953 *Foundations of Potential Theory* (New York: Dover)
- Kelly P A, O'Connor J J and Hills D A 1995 The stress field due to a dislocation in layered media *J. Phys. D: Appl. Phys.* **28** 530–4
- Kennett B L N 1974 Reflections, rays and reverberations *Bull. Seism. Soc. Am.* **89** 733–41
- Kennett B L N 1983 *Seismic Wave Propagation in Stratified Media* (Cambridge: Cambridge University Press)
- Kennett B L N and Kerry N J 1979 Seismic waves in a stratified half space *Geophys. J. R. Astron. Soc.* **57** 557–83
- Khan S A, Wahr J, Stearns L A, Hamilton G S, van Dam T, Larson K M and Francis O 2007 Elastic uplift in southeast Greenland due to rapid ice mass loss *Geophys. Res. Lett.* **34** L21701
- Khanna A and Kotousov A 2015 The stress field due to an interfacial edge dislocation in a multi-layered medium *Int. J. Solids Struct.* **72** 1–10
- Khojasteh A, Rahimian M, Eskandari M and Pak R Y S 2011 Three-dimensional dynamic Green's functions for a multilayered transversely isotropic half-space *Int. J. Solids Struct.* **48** 1349–61
- Klemann V, Wu P and Wolf D 2003 Compressible viscoelasticity: stability of solutions for homogeneous plane-Earth models *Geophys. J. Int.* **153** 569–85
- Kolesnikova A L and Romanov A E 2010 Representations of elastic fields of circular dislocation and disclination loops in terms of spherical harmonics and their application to various problems of the theory of defects *Int. J. Solids Struct.* **47** 58–70
- Kolesnikova A L, Gutkin M Y, Krasnitskii S A and Romanov A E 2013 Circular prismatic dislocation loops in elastic bodies with spherical free surfaces *Int. J. Solids Struct.* **50** 1839–57
- Krásná H, Böhm J and Schuh H 2013 Tidal Love and Shida numbers estimated by geodetic VLBI *J. Geodyn.* **70** 21–7
- Kuhlman K L 2013 Review of inverse Laplace transform algorithms for Laplace-space numerical approaches *Numer. Algorithms* **63** 339–55
- Kundu T and Mal A K 1985 Elastic waves in a multilayered solid due to a dislocation source *Wave Motion* **7** 459–71
- Kustowski B, Ekstrom G and Dziewonski A M 2008 Anisotropic shear-wave velocity structure of the Earth's mantle: a global model *J. Geophys. Res.* **113** B6
- Kuo J T 1969 Static response of a multilayered medium under inclined surface loads *J. Geophys. Res.* **74** 3195–207
- Kuo C H 2014 Elastic field due to an edge dislocation in a multilayered composite *Int. J. Solids Struct.* **51** 1421–33
- Lamb H 1882 On the vibrations of an elastic sphere *Proc. Math. Soc.* **13** 189–212
- Lamb H 1904 On the propagation of tremors over the surface of an elastic solid *Phil. Trans. R. Soc. A* **203** 1–42
- Langer L, Gharti H N and Tromp J 2019 Impact of topography and three-dimensional heterogeneity on coseismic deformation *Geophys. J. Int.* **217** 866–78
- Lebedev S and van der Hilst R D 2008 Global upper-mantle tomography with the automated multimode inversion of surface and S-wave forms *Geophys. J. Int.* **173** 505–18
- Lee E H 1955 Stress analysis in visco-elastic bodies *Q. Appl. Math.* **13** 183–90
- Lee E H 1962 *Viscoelasticity Handbook of Engineering Mechanics* ed W Flugge (New York: McGraw-Hill) ch 53, pp 22–53
- Lee Y G, Zou W N and Pan E 2015 Eshelby's problem of polygonal inclusions with polynomial eigenstrains in an anisotropic magneto-electro-elastic full plane *Proc. R. Soc. A* **471** 20140827
- Lev E and Hager B H 2008a Prediction of anisotropy from flow models: a comparison of three methods *Geochem. Geophys. Geosyst.* **9** Q07014
- Lev E and Hager B H 2008b Rayleigh–Taylor instabilities with anisotropic lithospheric viscosity *Geophys. J. Int.* **173** 806–14
- Li J and Berger E J 2001 A Boussinesq–Cerruti solution set for constant and linear distribution of normal and tangential load over triangular area *J. Elast.* **63** 137–51
- Li Y S and Pan E 2016 Responses of an anisotropic magneto-electroelastic and layered half-space to internal forces and dislocations *Int. J. Solids Struct.* **94–5** 206–21
- Li S and Wang G 2018 *Introduction to Micromechanics and Nanomechanics* (Singapore: World Scientific)
- Liao J J and Wang C D 1998 Elastic solutions for a transversely isotropic half-space subjected to a point load *Int. J. Num. Anal. Methods Geomech.* **22** 425–47
- Liu H and Pan E 2018 Time-harmonic loading over transversely isotropic and layered half-spaces with imperfect interfaces *Soil Dyn. Earthq. Eng.* **107** 35–47
- Liu G R and Xi Z C 2001 *Elastic Waves in Anisotropic Laminates* (London: Taylor and Francis)
- Liu J X, Liu X L and Zhao Y B 2001 Green's functions for anisotropic magneto-electroelastic solids with an elliptical cavity or a crack *Int. J. Eng. Sci.* **39** 1405–18
- Liu H, Pan E and Cai Y 2018 General surface loading over layered transversely isotropic pavements with imperfect interfaces *Adv. Eng. Softw.* **115** 268–82
- Liu Y J, Mukherjee S, Nishimura N, Schanz M, Ye W, Sutradhar A, Pan E, Dumont N A, Frangi A and Saez A 2011 Recent advances and emerging applications of the boundary element method *ASME Appl. Mech. Rev.* **64** 030802–38
- Long M D and Becker T W 2010 Mantle dynamics and seismic anisotropy *Earth Planet. Sci. Lett.* **297** 341–54
- Longman I M 1962 A Green's function for determining the deformation of the Earth under surface loads: 1. Theory *J. Geophys. Res.* **67** 845–50
- Longman I M 1963 A Green's function for determining the deformation of the Earth under surface loads: 2. Computations and numerical results *J. Geophys. Res.* **68** 485–96
- Love A E H 1911 *Some Problems of Geodynamics* (Cambridge: Cambridge University Press)
- Love A E H 1944 *A Treatise of the Mathematical Theory of Elasticity* (New York: Dover)
- Lowe M 1992 Plate Waves for the NDT of diffusion bonded titanium *PhD Thesis* Department of Mechanical Engineering, Imperial College, London
- Lowe M and Pavlakovic B 2013 *Disperse User Manual* (Online document)
- Lubarda V A 2013 Circular loads on the surface of a half-space: displacement and stress discontinuities under the load *Int. J. Solids Struct.* **50** 1–14
- Lubis A M, Hashima A and Sato T 2013 Analysis of afterslip distribution following the 2007 September 12 southern Sumatra earthquake using poroelastic and viscoelastic media *Geophys. J. Int.* **192** 18–37
- Lucas S K 1995 Evaluating infinite integrals involving products of Bessel functions of arbitrary order *J. Comput. App. Math.* **64** 269–82
- Luco J E and Apsel R J 1983 On the Green's functions for a layered half-space: part I *Bull. Seismol. Soc. Am.* **73** 909–29
- Lure A I 1964 *Three Dimensional Problems of the Theory of Elasticity* (New York: Inter-science)

- Ma X Q and Kusznir N J 1992 3D subsurface displacement and strain fields for faults and fault arrays in a layered elastic half space *Geophys. J. Int.* **111** 542–58
- Ma X Q and Kusznir N J 1994 Effects of rigidity layering, gravity and stress relaxation on 3D subsurface fault displacement fields *Geophys. J. Int.* **118** 201–20
- Ma C C and Lee J M 2009 Theoretical analysis of generalized loadings and image forces in a planar magneto-electroelastic layered half-plane *J. Mech. Phys. Solids* **57** 598–620
- Ma Y, Wang R and Zhou H 2012 A note on the equivalence of three major propagator algorithms for computational stability and efficiency *Earthq. Sci.* **25** 55–64
- Maerten L, Gillespie P and Pollard D D 2002 Effect of local stress perturbation on secondary fault development *J. Struct. Geol.* **24** 145–53
- Maerten F, Maerten L and Pollard D D 2014 iBem3D, a three-dimensional iterative boundary element method using angular dislocations for modeling geologic structures *Comput. Geosci.* **72** 1–17
- Maerten F, Resor P, Pollard D D and Maerten L 2005 Inverting for slip on three-dimensional fault surfaces using angular dislocations *Bull. Seismol. Soc. Am.* **95** 1654–65
- Mal A K 1988 Wave propagation in layered composite laminates under periodic surface loads *Wave Motion* **10** 257–66
- Marmo F and Rosati L 2016 A general approach to the Boussinesq's problem for polynomial pressures acting over polygonal domains *J. Elast.* **122** 75–112
- Marmo F, Sessa S and Rosati L 2016 Analytical solution of the Cerruti problem under linearly distributed horizontal loads over polygonal domains *J. Elast.* **124** 27–56
- Marmo F, Sessa S, Vaiana N, De Gregorio D and Rosati L 2018 Complete solution of three-dimensional problems in transversely isotropic media *Contin. Mech. Thermodyn.* (<https://doi.org/10.1007/s00161-018-0733-8>)
- Marone F and Romanowicz B 2007 The depth distribution of azimuthal anisotropy in the continental upper mantle *Nature* **447** 198–201
- Martens H R, Simons M, Owen S and Rivera L 2016 Observations of ocean tidal load response in South America from subdaily GPS positions *Geophys. J. Int.* **205** 1637–64
- Martinec Z and Wolf D 1999 Gravitational viscoelastic relaxation of eccentrically nested spheres *Geophys. J. Int.* **138** 45–66
- Maruyama T 1964 Static elastic dislocations in an infinite and semi-infinite medium *Bull. Earthq. Res. Inst.* **42** 289–368
- Maruyama T 1966 On two-dimensional elastic dislocations in an infinite and semi-infinite medium *Bull. Earthq. Res. Inst.* **44** 811–71
- Marzeion B, Jarosch A H and Hofer M 2012 Past and future sea-level change from the surface mass balance of glaciers *Cryosphere* **6** 1295–322
- Matsu'ura M and Sato R 1975 Static deformations due to the fault spreading over several layers in a multi-layered medium. Part II: strain and tilt *J. Phys. Earth* **23** 1–29
- Matsu'ura M, Tanimoto T and Iwasaki T 1981 Quasi-static displacements due to faulting in a layered half-space with an intervening viscoelastic layer *J. Phys. Earth* **29** 23–54
- Meng C 2017 Benchmarking Defmod, an open source FEM code for modeling episodic fault rupture *Comput. Geosci.* **100** 10–26
- Meng C and Wang H 2018 A finite element and finite difference mixed approach for modeling fault rupture and ground motion *Comput. Geosci.* **113** 54–69
- McClung H B 1989 The elastic sphere under nonsymmetric loading *J. Elast.* **21** 1–26
- McClung H B 1991 Asymmetric vibrations of an elastic sphere *J. Elast.* **25** 75–94
- McNamara A K, van Keken P E and Karato S 2002 Development of anisotropic structure in the Earth's lower mantle by solid-state convection *Nature* **416** 310–3
- Meade B J 2007 Algorithms for the calculation of exact displacements, strains and stresses for triangular dislocation elements in a uniform elastic half space *Comput. Geosci.* **33** 1064–75
- Melini D, Gegout P, King M, Marzeion B and Spada G 2015 On the rebound: modeling Earth's ever-changing shape *Earth Space Sci. News* **96** (<https://doi.org/10.1029/2015EO033387>)
- Melnikov Y A and Melnikov M Y 2012 *Green's Functions: Construction and Applications (De Gruyter Studies in Mathematics)* (Berlin: Walter de Gruyter)
- Merriam J B 1992 Atmospheric pressure and gravity *Geophys. J. Int.* **109** 488–500
- Metivier L, Greff-Lefftz M and Diament M 2005 A new approach to computing accurate gravity time variations for a realistic earth model with lateral heterogeneities *Geophys. J. Int.* **162** 570–4
- Metivier L, Greff-Lefftz M and Diament M 2006 Mantle lateral variations and elastogravitational deformations-I. Numerical modeling *Geophys. J. Int.* **167** 1060–76
- Metivier L, Greff-Lefftz M and Diament M 2007 Mantle lateral variations and elastogravitational deformations-II. Possible effects of a superplume on body tides *Geophys. J. Int.* **168** 897–903
- Mikolaj M, Meurers B and Guntner A 2016 Modelling of global mass effects in hydrology, atmosphere and oceans on surface gravity *Comput. Geosci.* **93** 12–20
- Miller S A, Colletini C, Chiaraluce L, Cocco M, Barchi M and Kaus B J P 2004 Aftershocks driven by a high-pressure CO₂ source at depth *Nature* **427** 724–27
- Mindlin R D 1936 Force at a point in the interior of a semi-infinite solid *J. Appl. Phys.* **7** 195–202
- Mitrovica J X and Peltier W R 1991 A complete formalism for the inversion of post-glacial rebound data: resolving power analysis *Geophys. J. Int.* **104** 267–88
- Molavi Tabrizi A and Pan E 2015 Time-dependent displacement and stress fields due to shear and tensile faults in a transversely isotropic viscoelastic half-space *Geophys. J. Int.* **202** 163–74
- Molavi Tabrizi A, Pan E, Martel S J, Xia K, Griffith W A and Sangghaleh A 2014 Stress fields induced by a non-uniform displacement discontinuity in an elastic half plane *Eng. Fract. Mech.* **132** 177–88
- Molodensky S M 1977 About connection of Love number with loading coefficients *Izv. Akad. Sci. USSR* **3** 3–7
- Mondal P and Korenaga J 2018a The Rayleigh–Taylor instability in a self-gravitating two-layer viscous sphere *Geophys. J. Int.* **212** 1859–67
- Mondal P and Korenaga J 2018b A propagator matrix method for the Rayleigh–Taylor instability of multiple layers: a case study on crustal delamination in the early Earth *Geophys. J. Int.* **212** 1890–901
- Morse P M and Feshbach H 1953 *Methods of Theoretical Physics. Part I and Part II (International Series in Pure and Applied Physics)* (New York: McGraw-Hall)
- Moshtagh E, Pan E and Eskandari-Ghadi M 2017 Wave propagation in a multilayered magneto-electro-elastic half-space induced by external/internal circular time-harmonic mechanical loading *Int. J. Solids Struct.* **128** 243–61
- Moshtagh E, Pan E and Eskandari-Ghadi M 2018 Shear excitation of a multilayered magneto-electro-elastic half-space considering a vast frequency content *Int. J. Eng. Sci.* **123** 214–35
- Mura T 1987 *Micromechanics of Defects in Solids* (Dordrecht: Martinus Nijhoff)
- Nabarro F R N 1967 *Theory of Crystal Dislocations* (Oxford: Clarendon)
- Naeni M R, Campagna R, Eskandari-Ghadi M and Ardalan A A 2015 Performance comparison of numerical inversion methods for Laplace and Hankel integral transforms in engineering problems *Appl. Math. Comput.* **250** 759–75

- Nakiboglu S M and Lambeck K 1982 A study of the Earth's response to surface loading with application to Lake Bonneville *Geophys. J. Int.* **70** 577–620
- Nayfeh A H 1995 *Wave Propagation in Layered Anisotropic Media with Applications to Composites (Series in Applied Mathematics and Mechanics vol 39)* (New York: North-Holland)
- Nikkhoo M and Walter T R 2015 Triangular dislocation: an analytical, artefact-free solution *Geophys. Int. J.* **201** 1119–41
- Norris A N and Shuvalov A L 2012 Elastodynamics of radially inhomogeneous spherically anisotropic elastic materials in the Stroh formalism *Proc. R. Soc. A* **468** 467–84
- Nur A and Booker J R 1972 Aftershocks caused by pore fluid flow? *Science* **175** 885–87
- Ohno I 1976 Free vibration of a rectangular parallelepiped crystal and its application to determination of elastic constants of orthorhombic crystals *J. Phys. Earth* **24** 355–79
- Ohno I, Yamamoto S, Anderson O L and Noda J 1986 Determination of elastic constants of trigonal crystals by the rectangular parallelepiped resonance method *J. Phys. Chem. Solids* **47** 1103–8
- Okada Y 1985 Surface deformation due to shear and tensile faults in a half-space *Bull. Seism. Soc. Am.* **75** 1135–54
- Okada Y 1992 Internal deformation due to shear and tensile faults in a half-space *Bull. Seism. Soc. Am.* **82** 1018–40
- Okubo S 1988 Asymptotic solutions to the static deformation of the Earth—I. Spheroidal mode *Geophys. J. Int.* **92** 39–51
- Okubo S 1993 Reciprocity theorem to compute the static deformation due to a point dislocation buried in a spherically symmetric earth *Geophys. J. Int.* **115** 921–8
- O'Toole T B and Woodhouse J H 2011 Numerically stable computation of complete synthetic seismograms including the static displacement in plane layered media *Geophys. J. Intern.* **187** 1516–36
- Pak R Y S and Guzina B B 2002 Three-dimensional Green's functions for a multilayered half-space in displacement potentials *ASCE J. Eng. Mech.* **128** 449–61
- Pan E 1989a Static response of a transversely isotropic and layered half-space to general surface loads *Phys. Earth Planet. Inter.* **54** 353–63
- Pan E 1989b Static response of a transversely isotropic and layered half-space to general dislocation sources *Phys. Earth Planet. Inter.* **58** 103–17
- Pan E 1990 Thermoelastic deformation of a transversely isotropic and layered half-space by surface loads and internal sources *Phys. Earth Planet. Inter.* **60** 254–64
- Pan E 1991 Dislocation in an infinite poroelastic medium *Acta Mech.* **87** 105–15
- Pan E 1997 Static Green's functions in multilayered half-spaces *Appl. Math. Modelling* **21** 509–21
- Pan E 1999 Green's functions in layered poroelastic half-spaces *Int. J. Numer. Anal. Methods Geomech.* **23** 1631–53
- Pan E 2004a Eshelby problem of polygonal inclusions in anisotropic piezoelectric full- and half-planes *J. Mech. Phys. Solids* **52** 567–89
- Pan E 2004b Eshelby problem of polygonal inclusions in anisotropic piezoelectric bimaterials *Proc. R. Soc. A* **460** 537–60
- Pan E and Chen W Q 2015 *Static Green's Functions in Anisotropic Media* (Cambridge: Cambridge University Press)
- Pan E and Ding Z 1986 Reciprocity theorem and some relations between Love numbers and surface loading coefficients *Acta Geophys. Sin.* **29** 54–60 (in Chinese with English abstract)
- Pan E and Han F 2004 Green's functions for transversely isotropic piezoelectric multilayered half-spaces *J. Eng. Math.* **49** 271–88
- Pan E, Yang B, Cai G and Yuan F G 2001 Stress analysis around holes in composite laminates using boundary element method *Eng. Anal. Bound. Elem.* **25** 31–40
- Pan E, Zhang Y, Chung P W and Denda M 2008 Strain energy on the surface of an anisotropic half-space substrate: effect of quantum-dot shape and depth *Comput. Model. Eng. Sci.* **24** 157–67
- Pan E, Yuan J H, Chen W Q and Griffith W A 2014 Elastic deformation due to polygonal dislocations in a transversely isotropic half-space *Bull. Seismol. Soc. Am.* **104** 2698–716
- Pan E, Molavi Tabrizi A, Sangghaleh A and Griffith W A 2015a Displacement and stress fields due to finite faults and opening-mode fractures in an anisotropic elastic half-space *Geophys. J. Int.* **203** 1193–206
- Pan E, Chen J Y, Bevis M, Bordononi A, Barletta V R and Molavi Tabrizi A 2015b An analytical solution for the elastic response to surface loads imposed on a layered, transversely isotropic, and self-gravitating Earth *Geophys. J. Int.* **203** 2150–81
- Pan E, Bevis M, Han F, Zhou H and Zhu R 2007 Surface deformation due to loading of a layered elastic half-space: a rapid numerical kernel based on a circular loading element *Geophys. J. Int.* **88** 90–100
- Pan E, Liu H and Zhang Z Q 2018 Vertical and torsional vibrations of a rigid circular disc on a transversely isotropic and layered half-space with imperfect interfaces *Soil Dyn. Earthq. Eng.* **113** 442–53
- Pao Y H, Chen W Q and Su X Y 2007 The reverberation-ray matrix and transfer matrix analyses of unidirectional wave motion *Wave Motion* **44** 419–38
- Peirce A P and Siebrits E 2001a The scaled flexibility matrix method for the efficient solution of boundary value problems in 2D and 3D layered elastic media *Comput. Methods Appl. Mech. Eng.* **190** 5935–56
- Peirce A P and Siebrits E 2001b Uniform asymptotic approximations for accurate modeling of cracks in layered elastic media *Int. J. Fract.* **110** 205–39
- Peirce A P, Gu H and Siebrits E 2009 Uniform asymptotic Green's functions for efficient modelling of cracks in elastic layers with relative shear deformation controlled by linear springs *Int. J. Numer. Anal. Methods Geomech.* **33** 285–308
- Peltier W R 1974 The impulse response of a Maxwell Earth *Rev. Geophys. Space Phys.* **12** 649–69
- Peltier W R 1985 The LAGEOS constraint on deep mantle viscosity: results from a new normal mode method for the inversion of viscoelastic relaxation spectra *J. Geophys. Res.* **90** 9411–21
- Peltier W R 2004 Global glacial isostasy and the surface of the ice-age Earth: the ICE-5G (VM2) model and GRACE *Ann. Rev. Earth Planet. Sci.* **32** 111–49
- Peltier W R, Argus D F and Drummond R 2015 Space geodesy constrains ice-age terminal deglaciation: the global ICE6G_C(VM5a) model *J. Geophys. Res. Solid Earth* **120** 450–87
- Peltzer G, Rosen P, Rogez F and Hudnut K 1998 Poroelastic rebound along the Landers 1992 earthquake surface rupture *J. Geophys. Res.* **103** 30131–45
- Petrov L and Boy J P 2004 Study of the atmospheric pressure loading signal in very long baseline interferometry observations *J. Geophys. Res.* **109** B03405
- Pfeffer W T *et al* 2014 The Randolph Glacier inventory: a globally complete inventory of glaciers *J. Glaciol.* **60** 537–52
- Piombo A, Tallarico A and Dragoni M 2007 Displacement, strain and stress fields due to shear and tensile dislocations in a viscoelastic halfspace *Geophys. J. Int.* **170** 1399–417
- Plag H P and Juttner H U 1995 Rayleigh–Taylor instabilities of a self-gravitating Earth *J. Geodyn.* **20** 267–88
- Plag H P and Van Dam T 2002 Solid Earth deformation and gravity changes due to surface loading: Status and scientific problems *IERS Workshop on Combination Research and Global Geophysical Fluids* 22p

- Pollitz F F 1992 Postseismic relaxation theory on the spherical Earth *Bull. Seism. Soc. Am.* **82** 422–53
- Pollitz F F 1996 Coseismic deformation from earthquake faulting on a layered spherical Earth *Geophys. J. Int.* **125** 1–14
- Pollitz F F 1997a Gravity anomaly from faulting on a layered spherical earth with application to central Japan *Phys. Earth Planet. Inter.* **99** 259–71
- Pollitz F F 1997b Gravitational viscoelastic postseismic relaxation on a layered spherical Earth *J. Geophys. Res. Solid Earth* **102** 17921–41
- Pollitz F F, Burgmann R and Banerjee P 2006 Postseismic relaxation following the great 2004 Sumatra–Andaman earthquake on a compressible self-gravitating Earth *Geophys. J. Int.* **167** 397–420
- Pollitz F F *et al* 2011 Coseismic slip distribution of the February 27, 2010 Mw 8.8 Maule, Chile earthquake *Geophys. Res. Lett.* **38** L09309
- Polonsky I A, Romanov A E, Gryaznov V G and Kaprelov A M 1991 Screw dislocation in an elastic sphere *Czech. J. Phys.* **41** 1249–55
- Pride S R 1994 Governing equations for the coupled electromagnetics and acoustics of porous-media *Phys. Rev.* **B50** 15678–96
- Purcell A, Dehecq A, Tregoning P, Potter E K, McClusky S C and Lambeck K 2011 Relationship between glacial isostatic adjustment and gravity perturbations observed by GRACE *Geophys. Res. Lett.* **38** L18305
- Purcell A, Tregoning P and Dehecq A 2016 An assessment of the ICE6G_C(VM5a) glacial isostatic adjustment model *J. Geophys. Res. Solid Earth* **121** 3939–50
- Qiao S, Shang X C and Pan E 2016a Elastic guided waves in a coated spherical shell *Nondestruct. Test. Eval.* **31** 165–90
- Qiao S, Shang X C and Pan E 2016b Characteristics of elastic waves in FGM spherical shells, an analytical solution *Wave Motion* **62** 114–28
- Qin Q H 2007 *Green's Function and Boundary Elements of Multifield Materials* (New York: Elsevier)
- Qureshi T and Bhattacharya S N 2008 Solutions in exponential functions for Rayleigh wave equations of motion with gravity in a radially heterogeneous spherical Earth *Geophys. J. Int.* **172** 49–55
- Radok J R M 1957 Visco-elastic stress analysis *Q. Appl. Math.* **15** 198–202
- Rangelov T V and Manolis G D 2010 Time-harmonic elastodynamic Green's function for the half-plane modeled by a restricted inhomogeneity of quadratic type *J. Mech. Mat. Struct.* **5** 909–24
- Ratnanather J T, Kim J H, Zhang S, Davis A M J and Lucas S K 2014 Algorithm 935: IIPBF, a MATLAB toolbox for infinite integral of products of Bessel functions *ACM Trans. Math. Softw.* **40** 14
- Ren H, Huang Q and Chen X 2010 A new numerical technique for simulating the coupled seismic and electromagnetic waves in layered porous media *Earthq. Sci.* **23** 167–76
- Ren H, Chen X and Huang Q 2012 Numerical simulation of coseismic electromagnetic fields associated with seismic waves due to finite faulting in porous media *Geophys. J. Int.* **188** 925–44
- Ren H, Huang Q and Chen X 2016a Existence of evanescent electromagnetic waves resulting from seismoelectric conversion at a solid-porous interface *Geophys. J. Int.* **204** 147–66
- Ren H, Huang Q and Chen X 2016b Numerical simulation of seismo-electromagnetic fields associated with a fault in a porous medium *Geophys. J. Int.* **206** 205–20
- Revil A, Pezard P A and Glover P W J 1999a Streaming potential in porous media: 1. Theory of the zeta potential *J. Geophys. Res.* **104** 20021–31
- Revil A, Schwaeger H, Cathles L M and Manhardt P D 1999b Streaming potential in porous media: 2. Theory and application to geothermal systems *J. Geophys. Res.* **104** 20033–48
- Rice J R and Cleary M P 1976 Some basic stress diffusion solutions for fluid-saturated elastic porous media with compressible constituents *Rev. Geophys. Space Phys.* **14** 227–41
- Rice J R and Simons D A 1976 The stabilization of spreading shear faults by coupled deformation-diffusion effects in fluid-infiltrated porous materials *J. Geophys. Res.* **81** 5322–34
- Riley K F, Hobson M P and Bence S J 2002 *Mathematical Methods for Physics and Engineering* 2nd edn (Cambridge: Cambridge University Press)
- Roach G F 1982 *Green's Functions* 2nd edn (Cambridge: Cambridge University Press)
- Rokhlin S I and Wang L 2002 Stable recursive algorithm for elastic wave propagation in layered anisotropic media: stiffness matrix method *J. Acoust. Soc. Am.* **112** 822–32
- Romanov A E and Vladimirov V I 1992 *Disclinations in Crystalline Solids (Dislocations in Solids vol 9)* ed F R N Nabarro (Amsterdam: North-Holland) ch 47, pp 191–402
- Roth F 1990 Subsurface deformations in a layered elastic half-space *Geophys. J. Int.* **103** 147–55
- Rudnicki J W 1987 Plane strain dislocations in linear elastic diffusive solids *J. Appl. Mech.* **54** 545–52
- Rudnicki J W 2001 Coupled deformation-diffusion effects in the mechanics of faulting and failure of geomaterials *Appl. Mech. Rev.* **54** 483–502
- Rudnicki J W and Koutsibelas D A 1991 Steady propagation of plane strain shear cracks on an impermeable plane in an elastic diffusive solid *Int. J. Solids Struct.* **27** 205–25
- Rundle J B 1978 Viscoelastic crustal deformation by finite quasi-static sources *J. Geophys. Res.* **83** 5937–45
- Rundle J B 1980 Static elastic-gravitational deformation of a layered half space by point couple sources *J. Geophys. Res.* **85** 5355–63
- Rundle J B 1981 Vertical displacements from a rectangular fault in layered elastic-gravitational media *J. Phys. Earth* **29** 173–86
- Rundle J B 1982 Viscoelastic-gravitational deformation by a rectangular thrust fault in a layered earth *J. Geophys. Res.* **87** 7787–96
- Rybicki K 1971 The elastic residual field of a very long strike-slip fault in the presence of discontinuity *Bull. Seism. Soc. Am.* **61** 79–92
- Rybicki K 1986 *Dislocations and Their Geophysical Application (Continuum Theories in Solid Earth Physics)* ed R Teisseyre (Warsaw: PWH-Polish Scientific Publishers) pp 18–175
- Sabadini R, Yuen D A and Boschi E 1982 Polar wandering and the forces responses of a rotating, multilayered, viscoelastic planet *J. Geophys. Res.* **87** 2885–903
- Saito M 1974 Some problems of static deformation of the Earth *J. Phys. Earth* **22** 123–40
- Saito M 1967 Excitation of free oscillations and surface waves by a point source in a vertically heterogeneous earth *J. Geophys. Res.* **72** 3689–99
- Sato R 1971 Crustal deformation due to dislocation in a multi-layered medium *J. Phys. Earth* **19** 31–46
- Sato R and Matsu'ura M 1973 Static deformations due to the fault spreading over several layers in a multi-layered medium. Part I: displacement *J. Phys. Earth* **21** 227–49
- Sato Y and Usami T 1962a Basic study on the oscillation of a homogeneous elastic sphere; Part I, frequency of the free oscillations *Geophys. Mag.* **31** 15–24
- Sato Y and Usami T 1962b Basic study on the oscillation of a homogeneous elastic sphere; Part II, distribution of displacement *Geophys. Mag.* **31** 25–47
- Sato Y, Usami T and Ewing M 1962 Basic study on the oscillation of a homogeneous elastic sphere. IV. Propagation of disturbances on the sphere *Geophys. Mag.* **31** 237–42

- Sato Y, Usami T, Landisman M and Ewing M 1963 Basic study on the oscillation of a sphere. Part V: propagation of torsional disturbances on a radially heterogeneous sphere case of a homogeneous mantle with a liquid core *Geophys. J. Int.* **8** 44–63
- Savio L, Lucas M C M and Murray D B 2004 Vibrations of free and embedded anisotropic elastic spheres: application to low-frequency Raman scattering of silicon nanoparticles in silica *Phys. Rev. B* **69** 113402
- Savio L and Murray D B 2009 Acoustic vibrations of anisotropic nanoparticles *Phys. Rev. B* **79** 214101
- Savio L and Murray D B 2005 Longitudinal versus transverse spheroidal vibrational modes of an elastic sphere *Phys. Rev. B* **72** 205433
- Singh S J 1972 Static deformation of a multilayered sphere by internal sources *Geophys. J. R. Astron. Soc.* **27** 1–14
- Savage J C 1980 *Dislocations in Seismology (Dislocations in Solids, Moving Dislocations vol 3)* ed F R N Nabarro (North-Holland: Amsterdam) pp 251–339
- Savage J C 1998 Displacement field for an edge dislocation in a layered half-space *J. Geophys. Res.* **103** 2439–46
- Schapery R 1962 Approximate methods of transform inversion for visco-elastic stress analysis *Proc. Fourth US National Congress on Applied Mechanics* vol 2 pp 1075–85
- Schwinger J 1993 *The Greening of Quantum Field Theory: George and I, pages 220–231. Appendix VIa in Cannell D M 2001 George Green: Mathematician and Physicist 1793–1841: the Background to his Life and Work* (Philadelphia, PA: Society for Industrial and Applied Mathematics)
- Segall P 2010 *Earthquake and Volcano Deformation* Student edn (Princeton, NJ: Princeton University Press)
- Selvadurai A P S 2007 The analytical method in geomechanics *Appl. Mech. Rev.* **60** 87–106
- Selvadurai A P S and Suvorov A P 2016 *Thermo-Poroelasticity and Geomechanics* (Cambridge: Cambridge University Press)
- Seremet V D 2003 *Handbook of Green's Functions and Matrices* (Boston, MA: WIT Press)
- Shao Z G, Fu R S and Jiang C 2010 Short-time postseismic deformation of 2001 Ms8.1 Kunlun (China) earthquake *Concurr. Comput.: Pract. Exper.* **22** 1803–12
- Shida T 1912 On the elasticity of the earth and the earth's crust vol 4 *Memoirs of the College of Science and Engineering, Yoshidahonmachi, Sakyo Ward, Kyoto Imperial University* pp 1–286
- Siebrits E and Peirce A P 2002 An efficient multi-layer planar 3D fracture growth algorithm using a fixed mesh approach *Int. J. Numer. Meth. Eng.* **53** 691–717
- Simmons J, de Wit R and Bullough R 1970 *Fundamental Aspects of Dislocation Theory (Special Publication 317 vols 1–2)* (Washington, DC: National Bureau of Standards)
- Simons D A 1977 Boundary layer analysis of propagating mode II cracks in porous elastic media *J. Mech. Phys. Solids* **25** 99–115
- Singh S J 1970 Static deformation of a multilayered half-space by internal sources *J. Geophys. Res.* **75** 3257–63
- Singh S J 1986 Static deformation of a transversely isotropic multilayered half-space by surface loads *Phys. Earth Planet. Inter.* **42** 263–73
- Singh S J and Rosenman M 1974 Quasi-static deformation of a viscoelastic half-space by a displacement dislocation *Phys. Earth Planet. Inter.* **8** 87–101
- Slichter L B and Caputo M 1960 Deformation of an Earth model by surface pressures *J. Geophys. Res.* **65** 4151–6
- Small J C and Booker J R 1984 Finite layer analysis of layered elastic materials using a flexibility approach. Part 1—strip loadings *Int. J. Numer. Methods Eng.* **20** 1025–37
- Small J C and Booker J R 1986 Finite layer analysis of layered elastic materials using a flexibility approach. Part 2—circular and rectangular loadings *Int. J. Numer. Methods Eng.* **23** 959–78
- Smith B and Sandwell D 2004 A three-dimensional semianalytical viscoelastic model for time-dependent analyses of the earthquake cycle *J. Geophys. Res.* **109** B12401
- Smylie D E and Mansinha L 1971 The elasticity theory of dislocations in real Earth models and changes in the rotation of the Earth *Geophys. J. R. Astron. Soc.* **23** 329–54
- Spada G 2008 ALMA, a Fortran program for computing the viscoelastic Love numbers of a spherically symmetric planet *Computers Geosci.* **34** 667–87
- Spada G and Boschi L 2006 Using the post-widder formula to compute the Earth's viscoelastic love numbers *Geophys. J. Int.* **166** 309–21
- Spada G, Barletta V R, Klemann V, Riva R E M, Martinec Z, Gasperini P, Lund B, Wolf D, Vermeersen L L A and Kin M A 2011 A benchmark study for glacial isostatic adjustment codes *Geophys. J. Int.* **185** 106–32
- Spencer T W 1960 The method of generalized reflection and transmission coefficients *Geophysics* **25** 625–41
- Song Y and Rudnicki J W 2017 Plane-strain shear dislocation on a leaky plane in a poroelastic solid *J. Appl. Mech.* **84** 021008
- Song Y, Hu H and Rudnicki J W 2016 Shear Properties of heterogeneous fluid-filled porous media with spherical inclusions *Int. J. Solids Struct.* **83** 154–68
- Song Q H, Li Z H and Pan E 2019 Concentrated sources on the interface of diffusive bimaterial media: the steady-state deformation *Mech. Mater.* **128** 38–58
- Stehfest H 1970 Algorithm 368: numerical inversion of Laplace transforms [D5] *Commun. ACM* **13** 47–9
- Steketee J A 1958 On Volterra's dislocation in a semi-infinite elastic medium *Can. J. Phys.* **36** 192–205
- Stoneley R 1926 The elastic yielding of the earth *Geophys. J. Int.* **1** 356–9
- Sun W 1992a Potential and gravity changes raised by dislocations in spherically symmetric earth models *PhD Thesis* The University of Tokyo
- Sun W 1992b Potential and gravity changes caused by dislocations in spherically symmetric Earth models *Bull. Earthquakes Res. Inst. Univ. Tokyo* **67** 89–238
- Sun W 2003 Asymptotic theory for calculating deformations caused by dislocations buried in a spherical Earth—Geoid change *J. Geod.* **77** 381–7
- Sun W 2004a Asymptotic solution of static displacements caused by dislocations in a spherically symmetric Earth *J. Geophys. Res.* **109** B05402
- Sun W 2004b Asymptotic theory for calculating deformations caused by dislocations buried in a spherical Earth—Gravity change *J. Geod.* **78** 76–81
- Sun W and Okubo S 1993 Surface potential and gravity changes due to internal dislocations in a spherical earth—I. Theory for a point dislocation *Geophys. J. Int.* **114** 569–92
- Sun W and Okubo S 1994 Spheroidal displacement due to point dislocations in a spherical earth—1. Theory *Acta Geophys. Sin.* **37** 225–40
- Sun W and Okubo S 1995 Spheroidal displacement due to point dislocations in a spherical earth—2. Dislocation love numbers *Acta Geophys. Sin.* **38** 89–101
- Sun W and Okubo S 1998 Surface potential and gravity changes due to internal dislocations in a spherical earth—II. Application to a finite fault *Geophys. J. Int.* **132** 79–88
- Sun W and Okubo S 2002 Effects of the Earth's curvature and radial heterogeneity in dislocation studies—for a point dislocation *Geophys. Res. Lett.* **29** 1605
- Sun W and Okubo S 2004 Co-seismic deformations detectable by satellite gravity missions—a case study of Alaska (1964, 2002) and Hokkaido (2003) earthquakes in the spectral domain *J. Geophys. Res.* **109** B04405

- Sun W and Zhou X 2012 Co-seismic deflection change of vertical caused by the 2011 Tohoku–Oki earthquake ($M_w 9.0$) *Geophys. J. Int.* **189** 937–55
- Sun W and Dong J 2013 Relation of dislocation love numbers and conventional Love numbers and corresponding Green functions for a surface rupture in a spherical Earth model *Geophys. J. Int.* **193** 717–33
- Sun W, Okubo S and Vanicek P 1996 Global displacement caused by dislocations in a realistic earth model *J. Geophys. Res.* **101** 8561–77
- Takagi Y and Okubo S 2017 Internal deformation caused by a point dislocation in a uniform elastic sphere *Geophys. J. Int.* **208** 973–91
- Takeuchi H 1950 On the Earth tide of the compressible Earth of variable density and elasticity *EOS Trans. Am. Geophys. Union Banner* **31** 651–89
- Takeuchi H and Saito M 1972 Seismic surface waves *Methods in Computational Physics* vol 11, ed B A Bolt (New York: Academic) pp 217–95
- Talbot A 1979 The accurate numerical inversion of Laplace transforms *IMA J. Appl. Math.* **23** 97–120
- Tan X C, Kou S Q and Lindqvist P A 1998 Application of the DDM and fracture mechanics model on the simulation of rock breakage by mechanical tools *Eng. Geol.* **49** 277–84
- Tanaka Y, Okuno J and Okubo S 2006 A new method for the computation of global viscoelastic post-seismic deformation in a realistic earth model (I)—Vertical displacement and gravity variation *Geophys. J. Int.* **164** 273–89
- Tang H and Sun W 2017 Asymptotic expressions of surface co-seismic strain change for a homogeneous sphere *Geophys. J. Int.* **209** 202–25
- Tang H and Sun W 2018a Closed-form expressions of seismic displacement in a homogeneous Maxwell Earth model *J. Geophys. Res. Solid Earth* **123** 6033–51
- Tang H and Sun W 2018b Asymptotic co- and post-seismic displacements in a homogeneous Maxwell sphere *Geophys. J. Int.* **214** 731–50
- Telste J G and Noblesse F 1986 Numerical evaluation of the Green function of water-wave radiations and diffraction *J. Ship Res.* **30** 69–84
- Tewary V K 1973 Green's function method for lattice statics *Adv. Phys.* **22** 757–810
- Tewary V K and Fortunko C M 1992 A computationally efficient representation for propagation of elastic waves in anisotropic solids *J. Acoust. Soc. Am.* **91** 1888–96
- Thompson W 1848 Note on the integration of the equation of equilibrium of an elastic solid *Camb. Dublin Math. J.* **1848** 76–99
- Thomson W T 1950 Transmission of elastic waves through a stratified solid medium *J. Appl. Phys.* **21** 89–93
- Ting C T C 1996 *Anisotropic Elasticity* (Oxford: Oxford University Press)
- Titovich A S and Norris A N 2012 Green's function for symmetric loading of an elastic sphere with application to contact problems *J. Mech. Mat. Struct.* **7** 701–19
- Tregoning P and van Dam T 2005 Atmospheric pressure loading corrections applied to GPS data at the observation level *Geophys. Res. Lett.* **32** L22310
- Ulitko A F 1979 *Method of Special Vector Functions in Three-dimensional Elasticity* (Kiev: Naukova Dumka) 264p (in Russian)
- Ursin B 1983 Review of elastic and electromagnetic wave propagation in horizontally layered media *Geophysics* **48** 1063–81
- van der Hijden J H M T 1987 *Propagation of Transient Elastic Waves in Stratified Anisotropic Media (Series in Applied Mathematics and Mechanics vol 32)* (New York: North-Holland)
- van Zwieten G J, Hanssen R F and Gutierrez M A 2013 Overview of a range of solution methods for elastic dislocation problems in geophysics *J. Geophys. Res. Solid Earth* **118** 1721–32
- Vattre A and Pan E 2017 Interaction between semicoherent interfaces and Volterra-type dislocations in dissimilar anisotropic materials *J. Mater. Res.* **32** 3947–57
- Vattre A and Pan E 2018 Three-dimensional interaction and movements of various dislocations in anisotropic bicrystals with semicoherent interfaces *J. Mech. Phys. Solids* **116** 185–216
- Vattre A and Pan E 2019 Semicoherent heterophase interfaces with core-spreading dislocation structures in magneto-electro-elastic multilayers under externally applied loads *J. Mech. Phys. Solids* **124** 929–56
- Vermeersen L L A and Mitrovica J X 2000 Gravitational stability of spherical self-gravitating relaxation models *Geophys. J. Int.* **142** 351–60
- Visscher W M, Migliori A, Bell T M and Reinert R A 1991 On the normal modes of free vibration of inhomogeneous and anisotropic elastic objects *J. Acoust. Soc. Am.* **90** 2154–62
- Wahr J 1981 Body tides on an elliptical, rotating, elastic and oceanless earth *Geophys. J. R. Astron. Soc.* **64** 677–703
- Wahr J, Khan S A, van Dam T, Liu L, van Angelen J H, van den Broeke M R and Meertens C M 2013 The use of GPS horizontals for loading studies, with applications to northern California and southeast Greenland *J. Geophys. Res. Solid Earth* **118** 1795–806
- Wang C D and Liao J J 2001 Elastic solutions for a transversely isotropic half-space subjected to arbitrarily-shaped loads using triangulating technique *ASCE Int. J. Geomech.* **1** 193–224
- Wang C D and Liao J J 2002a Elastic solutions of displacements for a transversely isotropic half-space subjected to three-dimensional buried parabolic rectangular loads *Int. J. Solids Struct.* **39** 4805–24
- Wang C D and Liao J J 2002b Elastic solutions for stresses in a transversely isotropic half-space subjected to three-dimensional parabolic rectangular loads *Int. J. Numer. Anal. Methods Geomech.* **26** 1449–76
- Wang C D, Pan E, Tzeng C S, Han F and Liao J J 2006a Displacements and stresses due to a uniform vertical circular load in an inhomogeneous transversely isotropic half-space *ASCE Int. J. Geomech.* **6** 1–10
- Wang C D and Tzeng C S 2009 Displacements and stresses due to nonuniform circular loadings in an inhomogeneous cross-anisotropic material *Mech. Res. Commun.* **36** 921–32
- Wang C D, Tzeng C S, Pan E and Liao J J 2003a Displacements and stresses due to a vertical point load in an inhomogeneous transversely isotropic half-space *Int. J. Rock Mech. Min. Sci.* **40** 667–85
- Wang C D, Wang W J and Ruan Z W 2013 Average increase in vertical stress due to uniform embedded rectangular loadings in cross-anisotropic materials *Mech. Res. Commun.* **53** 9–14
- Wang C D, Ye Z Q and Ruan Z W 2009 Displacement and stress distributions under a uniform inclined rectangular load on a cross-anisotropic geomaterial *Int. J. Numer. Anal. Methods Geomech.* **33** 709–48
- Wang C Y and Achenbach J D 1994 Elastodynamic fundamental solutions for anisotropic solids *Geophys. J. Int.* **118** 384–92
- Wang C Y and Achenbach J D 1995 Three-dimensional time-harmonic elastodynamic Green's functions for anisotropic solids *Proc. R. Soc. A* **449** 441–58
- Wang C Y and Achenbach J D 1996 Lamb's problem for solids of general anisotropy *Wave Motion* **24** 227–42
- Wang H F 2000 *Theory of Linear Poroelasticity with Applications to Geomechanics and Hydrogeology* (Princeton, NJ: Princeton University Press)
- Wang H M and Ding H J 2007 Radial vibration of piezoelectric/magnetostrictive composite hollow sphere *J. Sound Vib.* **307** 330–48

- Wang H S, Xiang L W, Jia L L, Jiang L M, Wang Z Y, Hu B and Gao P 2012 Load Love numbers and Green's functions for elastic Earth models PREM, iasp91, ak135, and modified models with refined crustal structure from Crust 2.0 *Comput. Geosci.* **49** 190–9
- Wang L and Rokhlin S I 2001 Stable reformulation of transfer matrix method for wave propagation in layered anisotropic media *Ultrasonics* **39** 413–24
- Wang Q and Zhan H 2015 On different numerical inverse Laplace methods for solute transport problems *Adv. Water Resour.* **75** 80–92
- Wang R 1999 A simple orthonormalization method for stable and efficient computation of Green's functions *Bull. Seism. Soc. Am.* **89** 733–41
- Wang R 2005a On the singularity problem of the elastic-gravitational dislocation theory applied to plane-Earth models *Geophys. Res. Lett.* **32** L06307
- Wang R 2005b The dislocation theory: a consistent way for including the gravity effect in (visco) elastic plane-earth models *Geophys. J. Int.* **161** 191–6
- Wang R 2007 Erratum to 'The dislocation theory: a consistent way for including the gravity effect in (visco) elastic plane-earth models' *Geophys. J. Int.* **170** 857
- Wang R, Heimann S, Zhang Y, Wang H and Dahm T 2017 Complete synthetic seismograms based on a spherical self-gravitating Earth model with an atmosphere-ocean-mantle-core structure *Geophys. J. Int.* **210** 1739–64
- Wang R and Kumpel H J 2003 Poroelasticity: efficient modeling of strongly coupled, slow deformation processes in a multilayered half-space *Geophysics* **68** 705–17
- Wang R, Lorenzo-Martín F and Roth F 2006b PSGRN/PSCMP—a new code for calculating co- and post-seismic deformation, geoid and gravity changes based on the viscoelastic-gravitational dislocation theory *Comput. Geosci.* **32** 527–41
- Wang R, Marfi F L and Roth F 2003b Computation of deformation induced by earthquakes in a multi-layered elastic crust—FORTRAN programs EDGRN/EDCMP *Comput. Geosci.* **29** 195–207
- Wang R and Wang H 2007 A fast converging and anti-aliasing algorithm for Green's functions in terms of spherical or cylindrical harmonics *Geophys. J. Int.* **170** 239–48
- Wang W, Sun W and Jiang Z 2010 Comparison of fault models of the 2008 Wenchuan earthquake (Ms8.0) and spatial distributions of co-seismic deformations *Tectonophysics* **491** 85–95
- Wang X and Pan E 2007 A moving screw dislocation interacting with an imperfect piezoelectric bimaterial interface *Phys. Status Solidi. b* **244** 1940–56
- Wang Z and Hu H 2016 Moment tensors of a dislocation in a porous medium *Pure Appl. Geophys.* **173** 2033–45
- Wang Z, Hu H and Yang Y 2015 Reciprocity relations for the elastodynamic fields generated by multipole sources in a fluid-solid configuration *Geophys. Int. J.* **203** 883–92
- Weeks W T 1966 Numerical inversion of Laplace transforms using Laguerre functions *J. ACM* **13** 419–29
- Weertman J 2008 *Dislocation Based Fracture Mechanics* (Singapore: World Scientific)
- Williams S D P and Penna N T 2011 Non-tidal ocean loading effects on geodetic GPS heights *Geophys. Res. Lett.* **38** L09314
- Willis J R, Bullough B and Stoneham A M 1983 The effect of dislocation loop on the lattice parameter, determined by x-ray diffraction *Phil. Mag. A* **48** 95–107
- Woodhouse J H and Deuss A 2007 *Theory and Observations—Earth's Free Oscillations, in Treatise on Geophysics* vol 1 (Amsterdam: Elsevier) pp 31–65
- Wu Y C and Heyliger P R 2001 Free vibration of layered piezoelectric spherical caps *J. Sound Vib.* **245** 527–44
- Wu B and Chen X F 2016 Stable, accurate and efficient computation of normal modes for horizontal stratified models *Geophys. J. Int.* **206** 1281–300
- Wu K C and Chid Y T 1995 The elastic fields of a dislocation in an anisotropic strip *Int. J. Solids Struct.* **32** 543–52
- Wu P and Peltier W R 1982 Viscous gravitational relaxation *Geophys. J. R. Astron. Soc.* **70** 435–85
- Wu M and Wang H F 1988 Deformations and inferred stress field for ellipsoidal sources at Long Valley, California, 1975–1982 *J. Geophys. Res.* **93** 13285–96
- Wu M, Rudnicki J W, Kuo C H and Keer L M 1991 Surface deformation and energy release rates for constant stress drop slip zones in an elastic half-space *J. Geophys. Res.* **96** 16509–24
- Xia R, Wu W and Wu R 2016 Elastic field due to dislocation loops in isotropic multilayer system *J. Mater. Sci.* **51** 2942–57
- Xiao H T and Yue Z Q 2014 *Fracture Mechanics in Layered and Graded Solids: Analysis Using Boundary Element Methods* (Berlin: De Gruyter)
- Xu P C and Mal A K 1987 Calculation of the inplane Green's functions for a layered viscoelastic solid *Bull. Seism. Soc. Am.* **77** 1823–37
- Xu C and Sun W 2014 Earthquake-origin expansion of the Earth inferred from a spherical-Earth elastic dislocation theory *Geophys. J. Int.* **199** 1655–61
- Xu C and Chao B F 2017 Coseismic changes of gravitational potential energy induced by global earthquakes based on spherical-Earth elastic dislocation theory *J. Geophys. Res. Solid Earth* **122** 4053–63
- Xu C, Sun W and Chao B F 2014 Formulation of co-seismic changes in Earth rotation and low-degree gravity field based on the spherical-Earth dislocation theory *J. Geophys. Res. Solid Earth* **119** 9031–41
- Yacoub T 1999 Three-dimensional analysis of lenticular ore bodies using displacement discontinuity elements *PhD Dissertation* University of Toronto 164p
- Yagi K and Yunes N 2013 I-Love-Q relations in neutron stars and their applications to astrophysics, gravitational waves, and fundamental physics *Phys. Rev. D* **88** 023009
- Yagi K and Yunes N 2014 I-Love-Q: unexpected universal relations for neutron stars and quark stars *Science* **341** 365–8
- Yagi K and Yunes N 2017 Approximate universal relations for neutron stars and quark stars *Phys. Rep.* **681** 1–72
- Yakhno V G and Cerdik Yaslan H 2011 Equations of anisotropic elastodynamics as a symmetric hyperbolic system: deriving the time-dependent fundamental solution *J. Comput. Appl. Math.* **235** 4802–15
- Yan R, Woith H and Wang R 2014 Groundwater level changes induced by the 2011 Tohoku earthquake in China mainland *Geophys. J. Int.* **199** 533–48
- Yang J Y, Zhou X, Yi S and Sun W 2015 Determining dislocation love numbers using GRACE satellite mission gravity Data *Geophys. J. Int.* **203** 257–69
- Yip K L S and Leung P T 2017 Tidal Love numbers and moment-Love relations of polytropic stars *Mon. Not. R. Astron. Soc.* **472** 4965–81
- Yoffe E H 1960 The angular dislocation *Phil. Mag.* **5** 161–75
- Yoffe E H 1961 A dislocation at a free surface *Phil. Mag.* **6** 1147–55
- Yuan H and Pan Z 2016 Discussion on the time-harmonic elastodynamic half-space Green's function obtained by superposition *Math. Prob. Eng.* **2016** 2717810
- Yuan J H, Chen W Q and Pan E 2013a Line-integral representations of the displacement and stress fields due to an arbitrary Volterra dislocation loop in a transversely isotropic elastic full space *Int. J. Solids Struct.* **50** 160–75
- Yuan J H, Pan E and Chen W Q 2013b Line-integral representations for the elastic displacements, stresses and interaction energy of

- arbitrary dislocation loops in transversely isotropic bimetals *Int. J. Solids Struct.* **50** 3472–89
- Yuan L, Chao B F, Ding X and Zhong P 2013 The tidal displacement field at Earth's surface determined using global GPS observations *J. Geophys. Res. Solid Earth* **118** 2618–32
- Yuan J H, Huang Y, Chen W Q, Pan E and Kang G Z 2019 Theory of dislocation loops in multilayered anisotropic solids with magneto-electro-elastic couplings *J. Mech. Phys. Solids* **125** 440–71
- Yue Z Q 1995 On generalized Kelvin solutions in multilayered elastic media *J. Elast.* **40** 1–44
- Yue Z Q 1996 On elastostatics of multilayered solids subjected to general surface traction *Q. J. Mech. Appl. Math.* **49** 471–99
- Yue Z Q 2015 Yue's solution of classical elasticity in n-layered solids: part 1, mathematical formulation; Part 2, mathematical verification *Frontiers Struct. Civil Eng.* **9** 215–49
- Yue Z Q, Xiao H T, Tham L G, Lee C F and Yin J H 2005 Stresses and displacements of a transversely isotropic elastic halfspace due to rectangular loadings *Eng. Anal. Bound. Elem.* **29** 647–71
- Yue Y M, Xu K Y, Chen Q D and Pan E 2015 Eshelby problem of an arbitrarily polygonal inclusion in anisotropic piezoelectric media with quadratic eigenstrains *Acta Mech.* **226** 2365–78
- Zemanian A H 1987 *Distribution Theory and Transform Analysis* (New York: Dover)
- Zhang C Z 1992 Love numbers of the moon and of the terrestrial planets *Earth Moon Planets* **56** 193–207
- Zhang C and Gross D 1998 *On Wave Propagation in Elastic Solids with Cracks* (Southampton: Computational Mechanics Publications)
- Zhang Z and Pan E 2019a Vertical and torsional vibrations of an embedded rigid circular disc in a transversely isotropic multilayered half-space *Eng. Anal. Bound. Elem.* **99** 157–68
- Zhang Z and Pan E 2019b Coupled horizontal and rocking vibrations of a rigid circular disc on a transversely isotropic and layered half-space with imperfect interfaces *Int. J. Solids Struct.* **165** 176–91
- Zhao Y F, Shang X C and Pan E 2013 Analytical solutions of uniform extended dislocations and tractions over a circular area in anisotropic magnetoelastic bimaterials *Acta Mech. Sin.* **29** 73–84
- Zhao Y F, Shang X C and Pan E 2014 Analytical solutions of 3D anisotropic magneto-electro-elastic bi-materials under extended non-uniform dislocations and tractions over a circular area *Int. J. Eng. Sci.* **85** 105–24
- Zhao Y F, Zhao M H and Pan E 2015 Displacement discontinuity analysis of a nonlinear interfacial crack in three-dimensional magneto-electro-elastic bi-materials *Eng. Anal. Bound. Elem.* **61** 254–64
- Zhong W X, Lin J H and Gao Q 2004 The precise computation for wave propagation in stratified materials *Int. J. Num. Methods Eng.* **60** 11–25
- Zhong X, Dabrowski M and Jamtveit B 2019 Analytical solution for the stress field in elastic half-space with a spherical pressurized cavity or inclusion containing eigenstrain *Geophys. J. Int.* **216** 1100–15
- Zhou X, Sun W, Zhao B, Fu G, Dong J and Nie Z 2012 Geodetic observations detecting coseismic displacements and gravity changes caused by the $M_w = 9.0$ Tohoku–Oki earthquake *J. Geophys. Res.* **117** B05408
- Zhou X, Cambiotti G, Sun W and Sabadini R 2014 The coseismic slip distribution of a shallow subduction fault constrained by prior information: the example of 2011 Tohoku (M_w 9.0) megathrust earthquake *Geophys. J. Int.* **199** 981–95
- Zhou J, Pan E and Bevis M 2019 A point dislocation in a layered, transversely isotropic and self-gravitating Earth part I: analytical dislocation love numbers *Geophys. J. Int.* **217** 1681–705
- Zhu L and Rivera L A 2002 A note on the dynamic and static displacements from a point source in multilayered media *Geophys. J. Int.* **148** 619–27
- Zhu F, Wang B, Qian Z H and Pan E 2018 Accurate characterization of 3D dispersion curves and mode shapes of waves propagating in generally anisotropic viscoelastic/elastic plates *Int. J. Solids Struct.* **128** 243–61
- Zou W N and Pan E 2012 Eshelby's problem in an anisotropic multiferroic bimaterial plane *Int. J. Solids Struct.* **49** 1685–700



Ernian Pan is a Professor of Civil Engineering at the University of Akron since 2008. He obtained his PhD in joint Geophysics/Civil Engineering from Cooperative Institute for Research in Environmental Sciences (CIRES), the University of Colorado, Boulder (CU-Boulder). He is a Fellow of the American Society of Mechanical Engineering (ASME) and the American Society of Civil Engineering (ASCE). He started his research on Green's functions (GFs) for geophysics when he was at Peking University pursuing his master degree on global responses of spherically stratified Earth to body forces and surface loads. At CIRES, he benefitted from two seminal papers, one by W. E. Farrell (1972) titled "Deformation of the Earth by surface loads", and the other by W. R. Peltier (1974) titled "The impulse response of a Maxwell Earth". His recent works on GFs for geophysics have been greatly influenced by his local colleagues M. Bevis (global GFs) and A. Griffith (regional GFs) at Ohio State University.